Palestine Polytechnic University

Deanship of Graduate Studies and Scientific Research

Master of Civil Engineering

Flexural Performance of RC Beams Strengthened Using GFRP Bars

Done by:
Ahmad Mohammad Thweib

Supervisor:
Ph.D. Belal ALmassry

Thesis submitted in partial fulfillment of requirements of the degree
Master of Civil Engineering

July, 2023

The undersigned hereby certify that they have read, examined and recommended to the Deanship of Graduate Studies and Scientific Research at Palestine Polytechnic University:

Flexural Performance of RC Beams Strengthened Using GFRP Bars

Ahmad Mohammad Thweib

in partial fulfillment of the requirements for the degree of Master in Civil Engineering.

Graduate Advisory Committee:

Prof./Dr. …… University: ……

Signature:———————————— Date:————————

Prof./Dr. …… University: ……
Signature:———————————— Date:————————

Prof./Dr. …… University: ……
Signature:———————————— Date:————————

Prof./Dr. …… University: ……
Signature:———————————— Date:————————

Thesis Approved by:

Name:

Dean of Graduate Studies & Scientific Research

Palestine Polytechnic University

Signature: …….

Date: …….

Flexural Performance of RC Beams Strengthened Using GFRP Bars

Ahmad Mohammad Thweib

Abstract

Recently, new materials have emerged that play an important role in improving the structural behavior of RC elements. The bending behavior of glass fiber reinforced polymer (GFRP) in RC beams will be studied. Various specimens with longitudinal rebar made of GRP and other parameters without GFRP are presented and the specimens are analyzed by Abaqus software based on the finite element method (FEM).

A parametric study is run with the following parameters:

The diameter of the rebar, the distance between the load points, the results are compared with the experimental literature, and the relationship between load and displacement, ductility and bending strength of RC beams is shown.

تعزيز أداء الإنحناء للجسور الخرسانية المسلحة باستخدام قضبان البوليمر المقوى بالألياف الزجاجية

أحمد محمد ذويب

المستخلص

ظهرت مؤخرًا مواد جديدة تلعب دورًا مهمًا في تحسين السلوك الانشائي لعناصر الخرسانة المسلحة . سوف يتم دراسة سلوك العزم للبوليمر المقوى بالألياف الزجاجية (GFRP) في الجسور المسلحة.سيتم القيام بعرض عينات مختلفة مع حديد التسليح الطولي المصنوع من البوليمر المقوى بالألياف الزجاجية والعينات الأخرى بدون البوليمر المقوى بالألياف الزجاجية و تحليل العينات بواسطة برنامج Abaqus بناءً على طريقة العناصر المحدودة.(FEM)

يتم إجراء دراسة حدية بتغيير الالعوامل التالية:

قطر حديد التسليح ، المسافة بين نقاط التحميل ، ثم مقارنة النتائج مع التجربة العملية ، و عرض العلاقة بين الحمل والإزاحة ، الليونة وقوة الانحناء لعزم الجسور المسلحة.

Dedication

Praise be to Allah, Lord of the worlds

To the Prophet Mohammad

Blessings and Peace be upon him

To my father

To my mother

To my brother

To my sisters

To my precious ones

To all friends and colleagues

To my teachers

To everyone working in this field

To all of them

I literally dedicate this work

Acknowledgment

First of all, praise is to Allah for helping me in making this research possible. I would like to extend thanks to many people who helped me during my research work. Countless words are to be said in acknowledging the efforts of my enthusiastic supervisors – Dr. Belal ALmassry. Their tremendous academic support and continuous
encouragement cannot be shortened in few words.
Special thanks to Prof. Dr. **Abdulsamee Halahla** from the civil engineering Department.
Many thanks to the defense committee for their efforts in reviewing my thesis.
Special gratitude is to the Computer Engineering Department for providing

Special mention goes to my parents, brothers, sister, friends and colleagues.

الإقرار

أنا الموقع أدناه مقدم الرسالة التي تحمل عنوان:

Flexural Performance of RC beams Strengthened with Longitudinal GFRP

أقر بأن ما اشتملت عليه هذه الرسالة إنما هي نتاج جهدي الخاص، باستثناء ما تم الإشارة اليه حيثما ورد، وأن هذه الرسالة ككل، أو أي جزء منها لم يقدم لنيل أي درجة أو لقب علمي أو بحثي لدى أي مؤسسة تعليمية أو بحثية أخرى

Declaration

I declare that the Master Thesis entitled " Flexural Performance of RC Beams Strengthened Using GFRP Bars" is my own original work, and herby certify that unless stated, all work contained within this thesis is my own independent research and has not been submitted for the award of any other degree at any institution, except where due acknowledgement is made in the text.

Student Name: Ahmad Mohammad Thweib

Signature:———————————— Date:————————————

Table of Contents

List of Figures

List of Tables

Chapter 1: Introduction

Recently, new materials have emerged that have significantly improved the structural behavior of RC members. The flexural performance of RC beams made of Glass Fiber Reinforced Polymer (GFRP) will be studied. A number of samples with different parameters with longitudinal bars made of GRP and other without GRP are presented and the samples are analyzed with a finite element method (FEM) based program such as the Abaqus program.

A parametric study is run with the following parameters: bar diameter, yield strength of steel, flexural strengthening of RC beams using longitudinal bars made of GFRP and steel. Results are compared with the experimental literature. The relationship between load and displacement of RC beams is also shown as the relationship between ductility and bending strength

1.1 Overview

flexural behavior performance of RC beams has GFRP materials have become an important issue for engineers and have emerged as an alternative to manufacturing reinforcement. GFRP bars are non-corrosive which gives them an advantage over steel bars. Due to other differences in the physical and mechanical performance of FRP materials compered to steel, clear guidance on the engineering and construction of concrete structures reinforced with GFRP bars is essential. Numerous research projects have been carried out in the field of reinforced concrete beams with GFRP bars. Nowadays(Ruan et al., 2020)the flexural behavior and durability of hybrid-reinforced concrete beams with GFRP and steel bars are studied, and under the design service loads, the crack width and deflection at the same values of GFRP and steel bars reach the ultimate bending strength of GFRP-steel-reinforced concrete beams. Reported that beams were almost 91–97% of the value of RC steel beams. In 2019, (Krall and Polak, 2019) studied the effects of different GFRP arrangements on beam flexural performance. (Abdelkarim et al., 2019)measured the flexural strength and durability behavior of concrete beams reinforced with GFRP bars and found that increasing the FRP reinforcement ratio had a greater effect on the bearing

moment than on the resistance moment. (El-Nemr et al., 2018) evaluated the flexural strength and maintainability of concrete beams reinforced with different types of GFRP bars. The cracking behavior of the tested beams tends to confirm that the sand coating of GFRP bars improves. The concrete adhesion performance over the spiral grooved profiles. Also, a curvature limit of 0.005/d seems suitable for checking the serviceability of GFRP RC beams. (Goldston et al., 2016) the behavior of concrete beams reinforced with GFRP bars under static and impact loads is studied and the GFRP RC beams with high bending stiffness after cracking and undergo significant bending failure under static loading. Reported that (Maranan et al., 2015) evaluated the flexural capacity and serviceability of GFRP geopolymer RC beams. The Results show that the diameter of bar does not significantly affect the bending behavior of the beam, and the maintainability of the beam increases as the reinforcement ratio increases.

Many types of studies on the behavior of RC beams reinforced with GFRP bars have been done during the past decades, in addition, the finite element technique (FEM) was used, Numerical results and experimental results are compared. The results of this study showed that the use of GRP stiffeners significantly improved the ductility of RC beams without reducing their load carrying capacity.

1.2 Definition of ductility

Ductility describes the ability of a structure to withstand large deformations without significant loss of strength. However, there are different levels of ductility, many types of ductility, as material ductility, section ductility, member ductility, and structural ductility.

The ductility of a material as indicated by a standard stress-strain curve has a fundamental ductility level, which represents the maximum ductility when all points in the structure behave the same and are evenly stressed, this is highly unlikely. The ductility of the section is less than the ductility of the material because the material layers of the section are not uniformly stressed. The ductility of a component is much lower than its cross-sectional ductility, as it often yields only at certain points. Finally, structural ductility is the lowest since any structure consists of multiple elements, not all of which reach plastic capacity at

the same time. Generally, ductility of a structure is affected mostly by joint failures (Ghobarah and Said, 2002)Thus, ensuring sufficient ductility at the joints can increase overall structural ductility.

1.3 Scope of research

Today, scientific advances in the use of modern materials play an important role in improving the structural behavior of concrete members. The purpose of this study is to compare the effects of glass fiber reinforced polymer (GFRP) and longitudinal steel bars on the bending performance of reinforced concrete (RC) beams. This study focuses on the effect of glass fiber reinforced polymer (GFRP) on bending reinforcement of RC beams and is based on several parameters such as bar diameter and load position.

The numerical FE model is run in the commercial software Abaqus, the nonlinear behavior of the material is taken into account, and the numerical model is validated against previous experimental results testing the performance of RC beams reinforced with GFRP bars.

Then use the model to run a parametric study, change one parameter, and set the other. We then compare the results to study the effect of the parameters on the bending strength of RC beams. Results are compared to other hands-on experiments using scientific papers by researchers working on the same subject during the same internship. Comparing the RC beams reinforced with GRP with the experimental results was proposed.

1.4 Research objectives

The primary goal of this research is to quantify the effect of using specific GFRP bars in R.C Beams to improve flexural before failure. The following tasks are carried out in order to achieve this primary goal:

1- Look at the literature on the use of GFRP bars in RC beams. This will be expanded upon in Chapter 2.

2- Create a 3-D non-linear F.E. model of an RC beam. The model incorporates both material and geometrical nonlinearities, as well as GFRP-concrete interfacial properties. To create a generic parametric model of R.C beam with and without GFRP bars, the commercial (F.E.) software ABAQUS is used. Geometry, materials, and all required input data are sourced from the literature and used to build the model.
3- Validate the model by comparing it with published experimental data. Sensitivity and parameter studies to identify key parameters affecting beam ductility. This is shown in Chapter 4 of the thesis.
4- Correlate the results of the FE model. This is covered in Chapter 5.
5- Check the results by comparing the numerical and analytical results Results based on mechanics and plasticity fundamentals. This is shown as See Chapter 6 for details.
6- Summarize the results and make conclusions and recommendations to engineers regarding the use of GFRP and future work.

1.5 Research methodology

Numerical investigation of structures offers an attractive technique of research due to low cost, quick results and ability to study several variables in depth. Therefore, a three-dimensional non-linear F.E. a simply supported beam model is built using commercial software ABAQUS. This chapter illustrates a general description of an R.C simply supported beam modeling, while the material parameters for this model will be shown in verification and parametric study chapters. The modeling of the beam includes definition of materials, creation of parts, modeling of interfaces, selection of analysis regime, loading setup, boundary conditions and meshes as it will be discussed in the following subsections.

1.6 Research hypothesis

The following factors, which are based on earlier data from the literature review and are considered to have no effects on the findings, were taken into account when conducting this study:

- Two steel plates, one of which served as a roller and the other as a pin support, were attached to the bottom of the beam to support it. To transfer the load to the beam, two top steel plates were fastened. The four-point load test approach is used in this case.
- Steel plates are fully fixed to beams to transmit the load applied on plates to beams.
- The load on the beams was increasing statically.
- By taking into account the needed development length and passing the reinforcement through the support points, reinforcement (steel and GFRP) was judged to be completely attached to concrete with no sliding. Furthermore, all reinforcement components were represented as embedded region constraints.
- The results were investigated using static loads, which ignored the impacts of dynamic loads.

Chapter 2: Literature Review

2.1 General Background

Our ancient ancestors adopted the load bearing stone walls system in constructions. Nevertheless, this system has many disadvantages. For instance, it required too much thick walls that are 60 centimeters thick which needed a lot of time as well as effort in order to construct. Those walls also occupied too much space of the total building area due to their thickness. Additionally, it did not allow to add up extra stories to the ground story freely which does not fit with our today's life that requires vertical constriction in order to save space and money. Moreover, the dimensions of the rooms in those stone buildings could not be large.

With the development of science and technology, cement was invented and used in construction field as a new ingredient to concrete. Yet, using concrete without steel is not a practical choice since plain concrete structures have poor tensile strength. Such concrete structures have low load capacity, so that cracks will form in the tension zone. Thus, longitudinal steel bars are placed in concrete in the tensile zone since they have high tensile strength so that they increase load capacity. Another reason for choosing steel is that both steel and concrete have the same thermal expansion coefficients roughly. Such concrete in which steel is embedded so that both materials resist tensile and compression is called reinforced concrete (Bosc et al., 2001).

Reinforced concrete has been very essential particularly with the emerge of the frame system as a replacement for the ancient bearing stone wall system. A frame system mainly consists of slabs, beams, columns and foundations. In a frame system, the load is basically subjected on the slab. It then gradually transfers from the slab to the beams which after transfer the load to the columns. The load after transfers from the columns to the foundation and then transfers to the soil or rock. The aforementioned structural elements are reinforced in order to carry loads as well as resist the resulting internal forces which are usually in the form of moment and shear forces. There are mainly two types of frames that are used in construction. The first one is the rigid frame structure which is also called moment frame system. It is called rigid because it has the ability to resist the deformation. This type can resist the vertical and horizontal loads. Additionally, the rigidity of this type results from

the rigidity of beams, columns, and the connections among them. This type can be classified based on the type of the support into two subtypes which are the fix ended rigid frame structure and the pined ended frame structure. The other type of the frame systems is the braced frame system. This type is simple to analyze and construct. Another advantage of this type is that it gives more effective resistance against earthquakes and wind loads (Darwin et al., 2016).

As mentioned before, slabs, beams, columns in addition to foundations are the main elements in the frame system. The slab is a horizontal structural reinforced element which is directly subjected to the load and it transfers the load to the beam. It can be categorized into two types based on the direction of loading, one-way slab and two-way slab. In the one-way slabs, the load is mainly transferred in one direction which is the shorter direction. Whereas it is transferred to two directions which approximately have the same dimensions in the two-way slabs. Slabs can be further classified into different types based on the method according to which they are designed. To begin with, flat slabs which are supported directly by columns. Next, solid slabs which are supported by beams and can be one-way or two-way slabs. Finally, ribbed slabs that are supported by beams and they can be also one-way or two-way (Darwin et al., 2016).

Another element of the frame system is beams. The beam is a horizontal reinforced structural element designed to carry lateral load and transfer it to the column. It is reinforced by longitudinal bars in addition to cross section in order to majorly resist the bending moment. Beams are also reinforced by stirrups in order to resist the shear forces. Sometimes, they are reinforced by additional longitudinal bars and stirrups in order to resist torsion. The capacity and strength of a reinforced concrete beam can be found and determined by considering the equilibrium of tensile and compressive forces. A reinforced concrete beam can be categorized based on shape of cross section into: T- section beam, L-section beam, and rectangular beam which is the most common form. T-section and L-section beams are referred to as flanged beams. L- Section beams are usually external beams while T- section beams are internal beams. Reinforced concrete beams can be also divided into several types in relation to the support which they receive. That is, a simply-supported beam which has one span, continuous beam which has more than one span, and cantilever which is supported from one side. In addition, they may be classified to singly

and doubly reinforced concrete beams. A singly reinforced concrete beam is a beam that has main reinforcement in the tension zone. On the other hand, a doubly reinforced concrete beam is the one that has main reinforcement in both the tension and compression zones. The capacity of doubly reinforced concrete beams is higher than that of singly reinforced concrete beams.

A Column is a vertical reinforced structural element which transfers the load from the beam to the foundation. Columns are reinforced with vertical longitudinal bars for many reasons first of which is to resist the load which is transferred through columns from beams or slabs and thus reduce the area of the concrete section. Second, these bars help resist moment which produced by eccentricity. Next, they help resist the buckling in slenderness column. Finally, using vertical bars makes columns more dramatically resistant to stresses caused from concrete shrinkage and prevents sudden failure. It is further reinforced with horizontal reinforcement or spiral in order to protect the column from buckling, deflection, to prevent the movement of vertical rebar during concrete pouring, to resist shear forces and to bear part of the horizontal tension caused by vertical compression. A column can be classified into a short column and a long column. It can be also classified based on its own shape to circular section and rectangular section.

A foundation is a horizontal reinforced structural element which is directly supported by soil to which it transfers the load. Foundations provide resistance to winds and earthquakes and help prevent over turning. They can be classified into two types based on their depth. First type is a deep foundation which looks like piles. The second is a shallow foundation which is divided into many types the most common of which are the isolated footing carrying a single column, the combined footing carrying two columns, and the mat foundation that carries many columns. This type is used when the bearing capacity of soil is very weak or the total area of the foundations is more than (50-60)% of the total area of the whole construction. Another type of shallow foundations is the wall footing which carries a bearing walls or shear walls.

2.2 Strengthening of RC beams

There are many reasons why strengthening RC beams is necessary. Sometimes, people change the purpose of their buildings, for example, from houses to stores, factories or workshops, so having the buildings well-strengthened makes such process possible, easier

and safer. It is effective in the case of the corrosion of steel reinforcement and structural deterioration due to ageing and environmental exposures. It is needed when there are design and implementation errors. So there are different methods have been applied and developed (Mondal, 2019) (Khan, Rafeeqi & Ayub, 2013).

Strengthening of RC structural elements is a critical process within the field of structural engineering. The purpose of strengthening is to increase the capacity of a building structural element. Structural elements need to be strengthened due to several reasons the most important of which are overloading, under-designed structural elements and the lack of quality control (Jumaat and Alam, 2007).

2.3 Fiber Reinforced polymer (FRP) Material in Civil Engineering

In this chapter, the history of fiber reinforced polymer (FRP) materials as strengthening materials in civil engineering will be presented. It will further show the kinds of FRP bars and present in detail information related to their properties and compare them with conventional steel bars. It will also present the advantages and disadvantages of using FRP bars in addition to summarizing and presenting previous conducted research on GFRP.

2.3.1 History of Fiber Reinforced Polymer (FRP) Reinforcement

In the last century, scientists found out that synthetic resins (plastics) are better than natural materials. However, plastics by themselves cannot provide the required strength for some engineering necessities of accelerating technological progress. In 1930’s, the primary glass fiber mixed with modern synthetic resins was found out by Owens Corning (Muhammad, 2019). The idea of combining different materials together to create composite material is a new one. Yet, it dates back to the time when straw was used as a reinforcement in a mud by the ancient Egyptians in order to create a reliable and durable composite material. An FRP is a new and improved model of the previous idea (Salh, 2014.). FRP bars were neither considered a useful solution nor commercially available until late 1970s though they had been already known (American Concrete Institute, 2015).

FRP industry started during World War II. This led to greater usage and improvement FRPs. The industry was flourishing in producing cars and planes fully employing this FRP material of high strength and light weight (Muhammad, 2019).

In the 1980s, non-metallic materials were highly demanded to improve particular advanced technologies. They were especially demanded in buildings accommodating MRI medical apparatus and they were considered acceptable materials for this type of construction. In the mid-1990s, the number of applications of FRP reinforcement in Japan exceeded 100 in both residential and commercial projects (Machida & Uomoto, 1997). China became the country with the highest number of GRP reinforced structures in the 2000s, from nine underground works to bridge decks (American Concrete Institute, 2015). In 1986, applying GRP reinforcement began in Europe, a pre-stressed highway bridge was constructed and reinforced GRP (American Concrete Institute, 2015).

2.3.2 Fiber Reinforced Polymer (FRP) Bar

Fiber Reinforced Polymer (FRP) bars are reinforcing materials that are composed of contiguous fibers in a polymer resin matrix. Such combination provides the physical and mechanical properties required for some applications.

Continuous contiguous fibers are used for producing FRP bars as they have high strength and stiffness besides light weight. The fibers provide the required strength. Carbon, aramid, glass in addition to basalt are the common types of fibers used in making FRP bars.

The function of the polymeric matrix is to keep the fibers together and prevent surface damage during production, use, and throughout the service life of the bars. Besides, the matrix in relation to the strength of the bars is transferring stresses to the fibers. The fibers and the resin matrix must have good compatibility in terms of chemical and thermal properties. Some resins are polyester, epoxy, and vinyl esters (Muhammad, 2019).

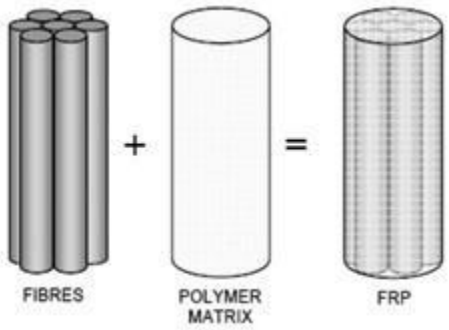

Figure 1: component of an FRP fiber(Said, n.d.)

2.4 Manufacturing Process

"FRP bars are manufactured using a process called pultrusion" (Kocaoz et al., 2005). The process involves making bundles of long parallel fiber of needed diameters which are then passed 10 via container of liquid resin. They are then passed via a die and the fibers are then compressed and changed into different bar sizes. The bars can then undergo various surface treatments such as indentation, sandblasting or twisted yarn wrapped around the bar to increase the bonding properties of the final product. The process of pultrusion makes new properties that the fibers and the resin plastic do not have while preserving their distinct chemical properties(Alsalihi, 2014.). There are three forms of FRPs:

1. Stirrups and longitudinal bars for internal reinforcement.
2. Structural elements on its own where it is entirely made of FRP.
3. Wrapping sheet for strengthening beams and columns.

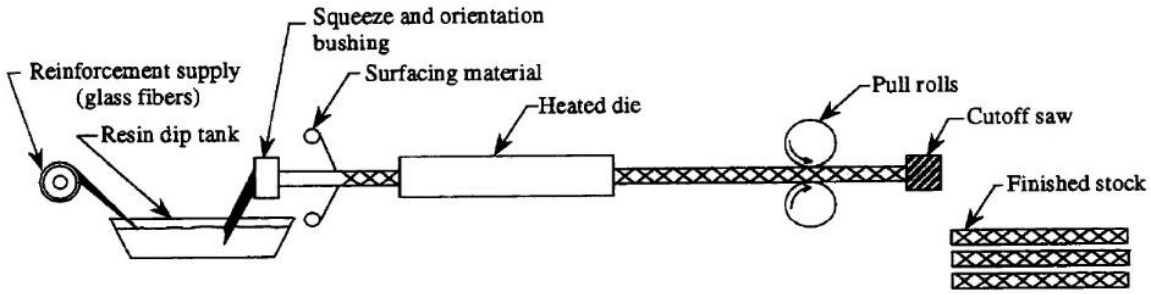

Figure 2: pultrusion process(Muhammad, 2019)

2.5 Types of Fiber Reinforced Polymer (FRP) Bar

There are many types of FRP bars used for reinforcing structural concrete element.

2.5.1 Carbon fiber reinforced polymer (CFRP) bar

This type never absorbs moisture and is capable of enduring heat more than AFRP. CFRP has a very low coefficient of heat; an advantage that it can be used for constructions in places exposed to extreme temperatures. They are often suitable for certain concrete structures due to their high tensile strength compared to other FRPs.

2.5.2 Aramid fiber reinforced polymer (AFRP) bar

This fiber is made from a type of polymer called aromatic polyamide. It was first known in the 1960s as Kevlar (Bhatnagar and Asija, 2016). Aramid fiber has low melting point, high moisture absorbability, very low compressive strength and high initial cost. They are lighter than other FRPs and have high energy absorption capacity due to their higher coefficient of deformation and damping.

2.5.3. Basalt fiber reinforced polymer (BFRP) bar

This kind of fiber is a modern manufactured FRP, yet it is not as known as other bars. Basalt fiber is used as the outer reinforcing plate and as internal reinforcement. They have high performance in terms of chemical resistance and are not harmful to the environment. It does not burn and does not react with water (Muhammad, 2019).

2.5.4 Glass fiber reinforced polymer (GFRP) bar

It is highly recommended for use in construction due to its good insulation properties, low cost and high resistance to some chemicals. More information will be presented later in this study.

Figure 3 Samples of FRP bar

2.6 Advantage and disadvantage of FRB bars

Fiber Reinforced Polymer (FRP) bars like any material is considered to have advantages and disadvantages.

2.6.1 Advantages

FRP bars have the following:

1. Lightweight (0.2 – 0.25 of the weight of steel bar).
2. Higher tensile strength than steel bars.
3. Resistance to electrical and thermal conductivity (limited to GFRP bar only).
4. Non-corrosive properties.
5. More durability in corrosive environment than steel bars.
6. Durability of high levels of fatigue.
7. Capability of reducing the thickness of concrete cover.
8. Better damage tolerance than steel bar covered with epoxy.
9. High resistance to chemical attack and chloride ions.
10. More cost efficiency than steel bar coated with epoxy covered or galvanized steel bar.

2.6.2 Disadvantages

The common disadvantages of FRP bars are mentioned as follows;

1. Brittle failure as it never yield before rupture.
2. When exposed to ultraviolet radiation, polymeric resins and fibers may be damaged.
3. The potential for fire damage depends on the type of matrix and the thickness of the concrete cover.
4. Higher thermal expansion coefficient.
5. Low elastic modulus based on the fiber type.
6. Lower creep - rupture limit when compared to steel.
7. FRP is anisotropic while steel is isotropic.

2.7 Properties of Fiber Reinforced Polymer

Fiber Reinforced Polymer (FRP) bars are made from materials each of which have its own unique properties. These are combined in order to compose a superior new product, reinforcing bar (Muhammad, 2019). The physical, mechanical and long-term behaviors of FRP bars are presented below.

2.7.1 Mechanical properties

These properties help determine the range of efficiency of a material and the expected durability.

2.7.1.1 Compressive Behavior

It is not recommended to use FRP reinforcement bars in order to resist compression stresses. There are many studies shiwed that the compressive stress of FRP hardly exists whereas its tensile stress is higher. According to the American Concrete Institute, the compressive elastic modulus is nearly 85%, 80% and 100%, of CFRP, GFRP and AFRP respectively (American Concrete Institute, 2015). The reason for the lower compressive elastic modulus is that the compression test leads to failure due to end brooming besides micro-buckling of the internal fiber (Muhammad, 2019).

2.7.1.2 Tensile Behavior

An important property of FRP bars is tensile strength. These bars never yield before rupture. That is, they have linear behavior until failure without experiencing yielding (Muhammad, 2019). Figure 4 shows the relationship between stress and strain of the various types of fiber reinforcement polymer bars and steel bars (Fico, 2008.).

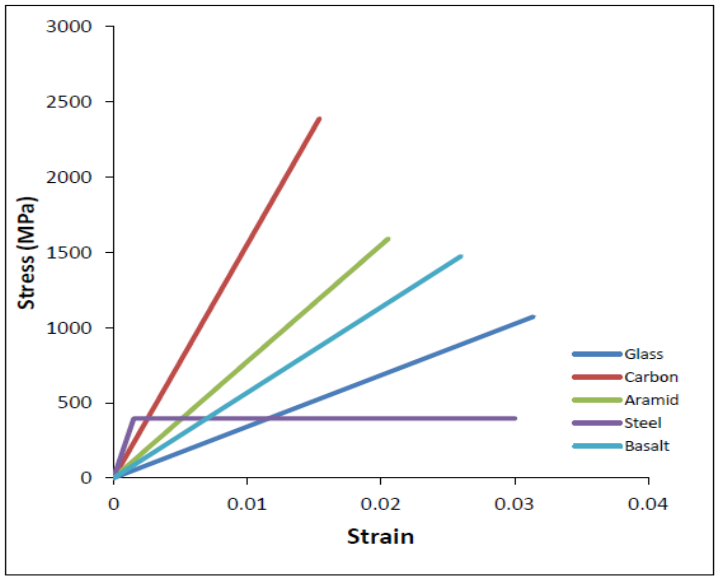

Figure 4 stress-strain curve of Typical Reinforcing bars (Fico, n.d.)

Both the stiffness and tensile strength of FRP bars depend on several factors. As strength of fiber is higher than resin, the fiber-volume ratio to the total volume of an FRP bar the most contributes to the tensile properties of the bar. Thus, strength and stiffness of an FRP bar vary based on fiber-volume ratio in addition to the type of the fiber and its orientation. These characteristics also help determine curing rate, quality control and the manufacturing technique (American Concrete Institute, 2015).

The tensile properties of an FRP bar must be provided by the manufacturer. In addition, the guaranteed tensile strength (fu) must be stated clearly. The GTS (fu) can be calculated by subtracting thrice the standard deviation from mean strength ($fu = fu, ave - 3\sigma$) and rupture strain ($\varepsilon u, ave^{*}$) is computed by ($\varepsilon u, * = \varepsilon u, - 3\sigma$). Furthermore, guaranteed elastic modulus can be known as the mean modulus Ef ($Ef = Ef, ave$) (American Concrete Institute, 2015).

Since FRP bars have brittle nature and undergo sudden and sharp failures without experiencing deflection, the cross section does not shrink along the bar (Salh, 2014.). As a result, FRP bars have higher tensile strength compared to steel.

Table 1 Tensile properties of steel and FRP bars (American Concrete Institute, 2015)

	STEEL	**AFRP**	**BFRP**	**CFRP**	**GFRP**
Nominal yield strength (MPa)	276 -517	—	—	—	—
Tensile Strength (MPa)	483- 690	250-2540	1200	600-3690	483-1600
Yield Strain %	0.14 -0.25	—	—	—	—
Rapture Strain %	6-12	1.9-4.4	2.5	0.5-1.7	1.2-3.1

2.7.1.3 Shear behavior

Since layers of resin are not reinforced between fiber layers, FRP bars are usually too weak to resist shear forces. The shear strength depends on the resin polymer which is weak and reinforcement across layers that is absent. In addition, the orientation of FRP bars has

influence on the shear strength. Straight bars have shear strength lower than Braided and twisted bars due to the varying orientation of the fibers present in the bars.(Muhammad, 2019).

2.7.1.4 Bond behavior

The manufacturing process, environment, and design all affect on the bond performance of FRP bars. In addition, the diameter of bar and the bond strength are in inverse proportion; that is, as the diameter increases the bonding strength decreases and vice versa.

The bond may be transferred due to a couple of factors such as the friction resistance force owing to the surface roughness of the FRP bar. It can be transferred by the chemical bond of the interface between bars and concrete. Another factor can transfer the bond is the pressure against the FRP bars which takes place as a result of the shrinkage of the hardened concrete and the swelling of the FRP bars caused by moisture absorption and temperature changes.

Several techniques such as sand coating, surface deformations, over molding a new surface on the bar, can be applied in order to enhance the bond strength between FRP reinforcement and the concrete. (Salh, 2014.). Different tests were used to determine the bonding properties as splice test and pull-out test to determine the embedment length equation (Abdelkarim et al., 2019).

2.7.2 Physical properties

Like other materials, the FRP bars have physical properties, and they will be addressed below.

2.7.2.1 Thermal expansion coefficient

In General, the metallic reinforcing materials have higher thermal expansion coefficient than FRP bars. This coefficient is liable to have inconsistent values depending on the direction of the bar; transverse or longitudinal. For transverse direction, the coefficient depends on the type of the resin. However, in the case of the longitudinal direction, it is the type of the fiber in addition to the volume –ratio of the fiber that govern the value of the coefficient. The properties of the fiber is responsible for the longitudinal CTE. The thermal coefficient expansion of longitudinal and transverse steel and FRP bars are presented in

Table 2. The negative values of CTE presented in the table refer to those materials that shrink due to the rise in temperature but expand when the temperature decreases (Muhammad, 2019). “The thermal expansion of FRPs in longitudinal direction is lower than in transverse direction, but the thermal expansion in transverse direction is higher than that of hardened concrete” (Masmoudi et al., 2005). “The strength of FRP fiber perpendicular to the fiber axis is ten times lower than the strength of a FRP fiber which is parallel to the longitudinal axis”(Salh, 2014.)

Table 2 Coefficient of thermal expansion of steel bar and FRP bars (Salh, 2014)

$CTE \times 10{-}6/°C$					
Direction	**Steel**	**AFRP**	**BFRP**	**CFRP**	**GFRP**
Longitudinal (αL)	11.7	(-6) - (-2)	21/K	-9 - 0	6 -10
Transverse (αL)	11.7	60 - 80	--	74 - 104	21 - 23

2.7.2.2 Density

The density of FRP does not exceed a 25% of the density of steel, as it approximately ranging from 1250 – 2150, as shown in the following table:

Enrollment in local colleges, 2005

Table 3 Density of steel bar and FRP bars(Salh, 2014)

Types	**Steel**	**AFRP**	**BFRP**	**CFRP**	**GFRP**
Density (kg/m³)	7900	1250 - 1400	1950	1500 - 1600	1200 - 2100

2.7.2.3 Effects of fire and high temperature

Per ACI 440.1R-03, the use of FRP bar in areas exposed to high heat and fires is not recommended. The high temperature softens the polymer and reduces its modulus.

In general, the use of GRP bars in fire-risk areas is not recommended as the polymer softens and loses its modulus at high temperatures (Wang et al., 2009). FRP components include

hydrogen, nitrogen, and carbon atoms which all have high flammability emit dangerous toxic gases (Hollaway, 2010). The shear and flexure capacity of FRP reinforced elements are affected by the concrete cover when they are exposed to fire. Additionally, high temperature caused rapid reduction in flexural and shear capacity (Saafi, 2002).

2.7.2.4 Thermal conductivity

The ability of a material to conduct heat is called thermal conductivity.

Generally, all FRP materials have very low thermal conductivity. In other word, they are very good heat insulators (Hollaway, 2010).

2.7.3 Long Term Behaviors

The time factor is a very important and influential factor for the following characteristics.

2.7.3.1 Creep Rupture

For steel bars used to reinforce concrete, creep rupture effects are not a significant consideration except at extreme temperatures. Creep rapture or static fatigue is consequence of exceeding the strength limit when the FRP bars exposed to tension forces continually via a significant time period. This leads concrete to experience catastrophic failure (Muhammad, 2019). Under dangerous environmental conditions such as exposure to ultra violet radiation, dry and humid cycles, high temperatures, freeze and thaw cycles, or high alkalinity, FRP bars fail under static load over time (Salh, 2014.).

Glass fibers perform worse than aramid fibers when it comes to creep rupture. Carbon fibers have better creep rupture strength compared to other fibers, all dependent on environmental factors such as humidity and temperature (American Concrete Institute, 2015).

2.7.3.2 Fatigue

Varying amounts of data on FRP life and fatigue have been accumulated over the past three decades, but they are limited to the field industry. There are too few studies on RC elements. FRP is said to be less prone to fatigue among FRP. At about 1 million cycles, fatigue strength increases by 30-50% compared to the initial static strength. AFRP bars in concrete tend to lose 27-46% of their tensile strength at about 2 million cycles(American Concrete Institute, 2015).

Fatigue performance is extremely dependent on the environmental conditions such as alkalinity, acidity and moisture of the concrete mass covering the bars. In contrast to steel, the fatigue limit cannot be clearly determined. It is significant to note that resin or fiber interface degradation can be detrimental in alkaline and humid environments. Generally, fatigue behavior of FRP largely depends on the bonding between the fiber and the resin matrix (Rahmatian, 2014).

2.7.3.3 Durability

There are many factors that affect the durability of FRP reinforced concrete elements, the most important of which are water, high temperature, acidic or alkaline solutions, in addition to saline solutions and exposure to ultraviolet radiation. The most important parameters of FRP bars that must be considered through the construction of reinforced concrete structures are bond and tensile properties. Stiffness and strength of FRP depend on type of material and exposure condition (American Concrete Institute, 2015).

2.8 Glass Fiber Reinforced Polymer (GFRP)

A type of FRP bars contains a huge quantity of continuous tiny glass fibers held together in a polymeric resin matrix (Muhammad, 2019). Due to its non-corrosive nature when compared to steel bar, GFRP has been recommended for a variety of structural applications. Other noteworthy advantages include chemical attack resistance, high stiffness and strength to weight ratio, good fatigue properties, control over damping characteristics, thermal expansion and electromagnetic wave resistance (Abdalla, 2002). In addition to having good physical and mechanical properties, FRP bars are considered to be more cost-effective than steel bars especially when corrosion poses concerns (Worner and Palermo, 2015).

The most common types of fiber used in producing GFRP bar are S-glass (high strength and modulus) and E-glass (electric/conventional type). The resins used depend on the rigidity, strength, cost, and long term stability. The fibers are responsible for the bar's strength and stiffness, while the polymeric resin holds the fiber in place to allow stress transfer between them. To achieve the highest probable tensile strength, the fiber orientation should be the same as the longitudinal direction of the bar, though other manufacturers use various fiber orientations (Worner, 2015).

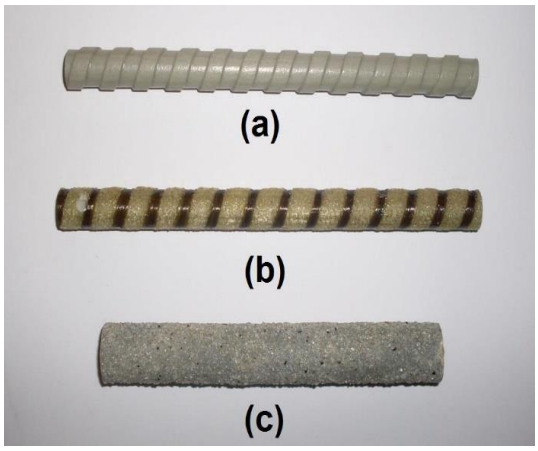

Figure 5 Types of bar surface (Fico, n.d.)

Table 4 and table 5 present the full names of the glass fibers and the chemical composition of the different types of GFRP respectively.

Table 4 Types of glass fibre (Fico, n.d.)

Type	Full name
E - GFRP	Standard conventional glass type
S - GFRP	High strength and high modulus glass
C- GFRP	Chemical resistant glass
A - GFRP	Alkali resistant glass
ECR GFRP	Chemically resistant conventional glass

Table 5 Chemical composition of different types of GFRP (ACI 440.1R-15, 2015)

Component	A - GFRP	C - GFRP	E- GFRP	ECR - GFRP	S- GFRP
SiO_2	54	60	60-65	54-62	62
CaO	20-24	14	14	21	5.9
Al_2O_3	14-15	25	2.6	12-13	-

MgO	-	3	1-3	4.5	1-4
B_2O_3	6-9	<1	2-7	<1	<0.5
K_2O	<1	<1	8	0.6	-
Na_2O	-	-	-	-	12-17
ZrO_2	-	-	-	-	17

As shown in the previous table, silicon is a predominate element participates in the all types of glass fiber. Silicon gives the fiber strength, yet it has disadvantages because it participates in chemical reactions in the presence of hydroxyl ions. This reaction degrades the fiber reinforcement leading to the degeneration of the internal structure of the reinforcing bars.

(Kocaoz et al., 2005) tested GFRP bars with four various coatings and tensile strengths. In this study, they discovered that the coating of the bar had had an effect on its tensile strength.

As the GFRP diameter increases, tensile strength decreases due to shear lag effect, so tensile strength varies depending on diameter of bars. The elastic modulus does not affected by the Bar size, however it is affected by the volume of fiber present(Kocaoz et al., 2005). The GFRP bars used has certain tensile strength of 1250 MPa. The steep initial slope of the steel bar curve due to the high elastic modulus of the steel. But it was shown that GFRP bars have better bearing capacity than steel bars do (Worner, 2015.).

2.9 Application of GFRP in Civil Engineering

Indeed, there are many applications of GFRP composites in the engineering field. However, it is the applications related to the civil engineering field that will be discussed hereafter.

2.9.1 Bridges

It is very expensive to repair and maintain bridges. Bridges are exposed to environmental and stress factors. For instance, the deicing chlorides that reduce the service life of the

structure after steel bars are exposed to them. GFRP bars are designed in a way which enables them sustain overweight traffic loads as well as natural catastrophes such as earthquakes. GFRP bars are used in bridges since they help reduce the costs of maintenance (TUF-BAR, 2018).

In fact, GFRB bars were first used in constructing bridges was in 1996 in the United States, Mckinleyville Brooke County. It was used due to its advantage of durability under fatigue and static loads when used as internal reinforcement in concrete structures (Shekar et al., 2003).

Figure 6 Bridge Deck in Morristown – Vermont, USA (Fico, n.d.)

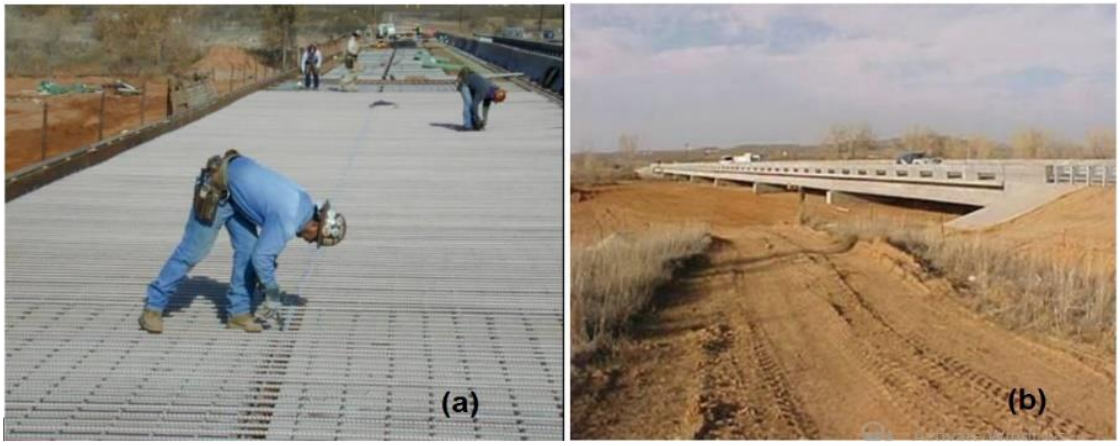

Figure 7 Sierrita de la Cruz Creek Bridge, Potter County, Texas (a) Under construction (b) In service (Salh, n.d.)

Figure 8: GFRP Bridge Deck, Cookshire-Eaton, Quebec (a) Under construction (b) In service (Muhammad, 2019)

2.9.2 Parking garages

In general, vehicles catch salts, water and gas emissions from the environment on their bodies, so they cause parking garages to undergo corrosion. GFRP is able to resist such factors. Thus, it is a perfect material to be used in constructing parking garages (TUF-BAR, 2018).

La Chanceliere, a parking garage in Quebec, Canada, broke down because of corrosion. It was consisted of two-way slab system where the internal steel bar is dramatically corroded (Figure 9a). It was asked for attempts of retrofitting through using GFRP bars as reinforcement in the slabs. At first, two designs were made; one with steel bars and another with GFRP bars. The cost of the steel design was lower than the GFRP design. However, cost analysis proved that cost effectiveness can be reached with the GFRP design, thus the GFRP design was still used (Ahmed et al., 2017).

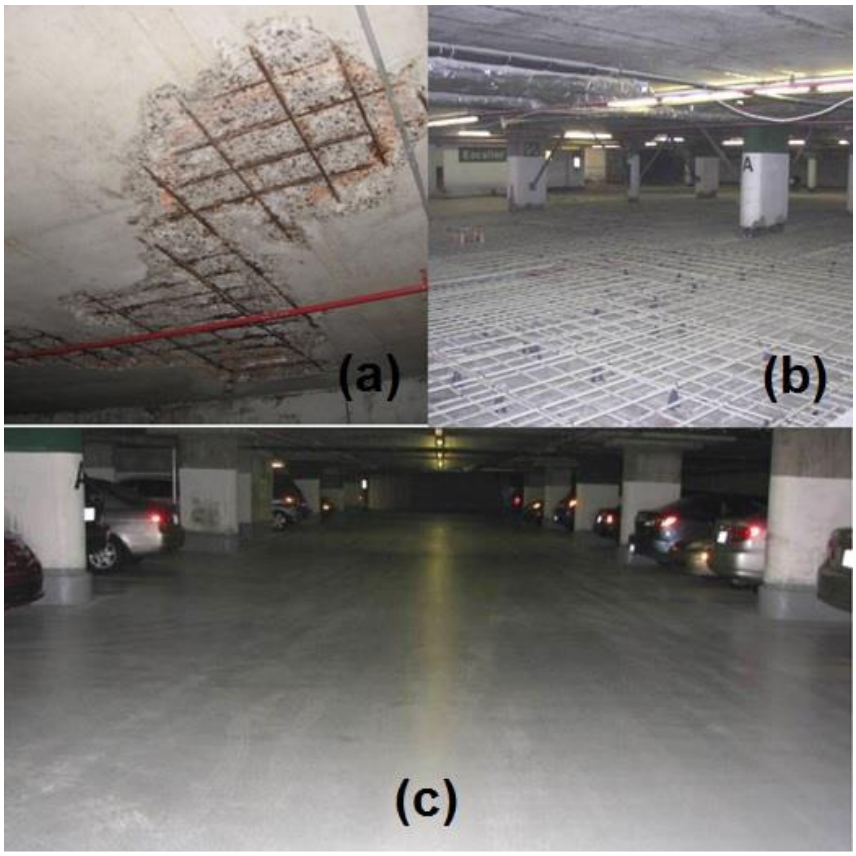

Figure 9 La Chanceliere Parking Garage in Quebec, Canada (a) Corroded steel in Slab, (b) Placement of GFRP reinforcement, (c) Parking Garage in Service (Ahmed et al., 2017)

2.9.3 Rail.

There has been always a need for a significant increase in the facilities of public transportation due to increasing population growth. Adopting GFRP designs is the ideal choice to be used in railways in contrast to magnetic and conducive materials that may be dangerous if used around electric trains. (Muhammad, 2019).

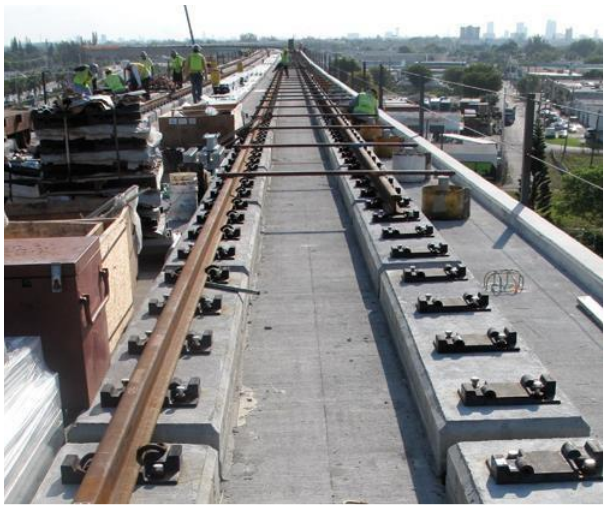

Figure 10 GFRP as railway plinths (Composites World, 2011)

2.9.4 Airport runways.

The size and weight of airplanes are increasing over time. When it comes to airport runways, achieving a service durability should be taken into consideration. The GFRP bars used to strengthen the runway help withstand the landing impact of aircraft weighing more than half a million pounds. When building the concrete base for airport runways, rigid adherence to standards for flexibility and strength is required. Runways are strengthened with GFRP bars, which make them strong, resilient, and long-lasting. Traditional steel shouldn't be used for runways. Over a century, GFRP bars can maintain the runway's structural integrity. (TUF-BAR, 2018).

2.9.5 Medical and Information Technology

GFRP is a non-magnetic, non-metallic and non-conductive material, making GFRP a preferred and recommended material to be used in medical and IT facilities. These facilities contain equipment that emits magnetic waves or requires massive electric currents. Additionally, the GFRP bar's tensile strength is two times higher than that of steel bars. (TUF-BAR, 2018).

Figure 11 MRI room in Lincoln General Hospital, NE, USA (Aslan FRP, 2022a).

Figure 12 Trauma Centre in York Hospital (Aslan FRP, 2022b).

2.9.6 Seawalls

Seawalls are vertical structures created to prevent the impact of floods on the environment. Seawalls, floating marine docks, water breaks, artificial reefs and other marine constructions such as buildings near the sea are commonly reinforced with steel bars, making them sensitive to salt and chloride that can damage the structures. GFRP bars are highly resistant to corrosion and exhibits higher strength making it recommended materials for marine constructions (TUF-BAR, 2018).

Figure 13 Seawall restoration in Palm Beach Florida, USA (Aslan FRP, 2018)

Figure 14 : Seawall of Lyles residence in California, USA (Aslan FRP, 2018)

2.9.7 Unique structures

There are many special constructions in the world which work as a landmark generally due to their unique character and appearance. Several of the unique buildings constructed using glass fiber reinforced polymer (GFRP) bar can be seen in the figures below (Aslan FRP, 2018).

Figure 15 Pyramid shaped winery in British Columbia (Aslan FRP, 2018)

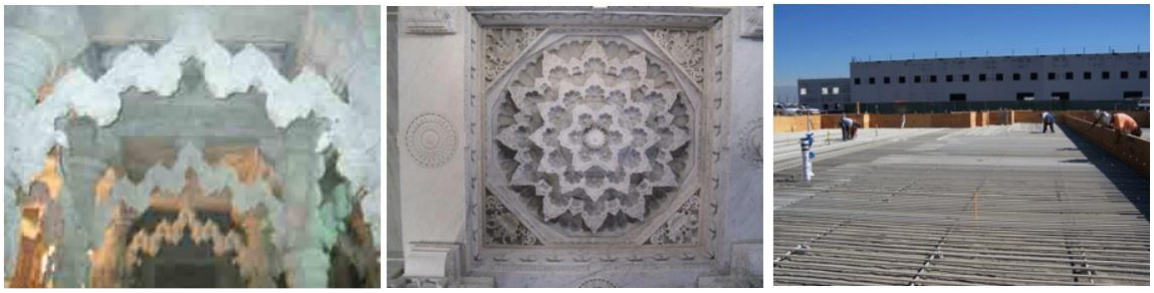

Figure 16 Hindu temple design with service life of 1000 years (Aslan FRP, 2018)

2.9.8 Precast

Similarly, RC elements are exposed to corrosion, just like precast concrete. Using GFRP bars to reinforce in precast concrete increases the service life up to more than one century. GFRP bars are non-metallic, making precast concrete structures corrosion-free and preventing discoloration due to rust stains. In addition, it makes it lighter (TUF-BAR, 2018).

Figure 17 Culvert bridge in City of Rolla, Phelps County, Missouri (Nanni, 2000)

2.10 Previous Experimental Studies

(Shanour et al., 2014) reinforced the beams using locally made GFRP and steel reinforced beams then tested them by subjecting them to four point loads. The most important parameters on which they have focused are the impact of changing compressive strength, the reinforcement ratio and the type of material used whether it is steel or GFRP. It was concluded that the middle span deflection and width of crack were decreasing as the reinforcement ratio was increased. Furthermore, as the reinforcement ratio increased, the ultimate capacity of the beam increased significantly.

(Ashour, 2006)'s experiment was conducted on 12 GFRP reinforced beams subjected to four point loads. The result was that flexural and shear failure were obtained, the flexural resulting from tensile rupture of the GFRP bar and the shear failure is experienced in the shear span of the beam caused by a great diagonal crack.

(Brown, 2015) attempted to determine how glass fiber reinforced polymer (GFRP) bars behave when it is used in reinforced concrete compression elements. The compressive loads were applied on beams until failure and compared the results which showed that GFRP is a possible technique, the capacity of GFRP and steel are approximately equal when reinforced the columns with the same area of either of them, and using GFRP as stirrups develops the bending capacity of the longitudinal bars.

(Balendran, 2004) performed a test on beams with sand coated GFRP and mild steel as reinforcement in flexure and compared the results which showed that the ultimate tensile

strength of steel was one fifth (20%) of the GFRP and the modulus of elasticity of steel was found to be four times higher than that of the GFRP. However, the deflection in the GFRP reinforced beams was larger than steel reinforced beams. In general, low elastic modulus is considered to be a significant technical disadvantage as GFRP reinforced concrete elements may be exposed to greater deformation than reinforced concrete elements, but based on the experiments of (Benmokrane et al., 1995), the deflection of GFRP is three times larger than steel's at the same load value.

(Micelli and Nanni, 2004) suggested a trial protocol to test the result of accelerated ageing on fiber reinforced polymer bars. Resin properties have a great influence on the durability of the FRP bars, and when the resin does not sufficiently protect the fiber, the GFRP bar is susceptible to alkali attack.

(Chidan, 2017) carried out an experiment on beams which is subjected to four point test. The beams where in groups, each group has a different reinforcement ratio. The results showed that as the reinforcement ratio increases, the ultimate capacity of the beams increases. In addition, it presented how valid the ACI standard is in the design of beam.

(Saikia, 2005) performed an experimental work to verify the behavior of hybrid (GFRP and steel) bars used as longitudinal reinforcement bars on normal strength concrete beams. Most of the tests performed, whether experimental or analytic, show GFRP to be a better alternative in terms of bending behavior. However, according to (Modi, 2017), the findings of the experiments that compared GFRP and steel in reinforced beams show that the steel to be better material in flexural behavior when the area of reinforcement required for steel is 1.94 times that of GFRP in reinforced beam having same moment capacity.

(Kheni et al., 2016.) Carried out an experimental and analytical study to study the behavior of the GFRP RC element compared with steel RC element. The main parameters were compressive strength of Concrete and different reinforcement size. The analytical research was carried out using finite element modelling software to simulate each of the beams. The ultimate capacity of GFRP reinforced beam was find out higher than steel reinforced beam through comparison between the two results. In addition combining steel and GFRP bars together was recommended in order to improve the ultimate capacity.

(Shin et al., 2009) performed a four point bend test on beams reinforced with steel and GFRP bars, the parameters studied were reinforcement ratio and compressive strength of

concrete. The results recorded were displacement, crack width and strain of the two types of beams, the larger strains and displacement were recorded for the GFRP reinforced beams. And it was discovered that the crack width and the crack spacing were not affected by the compressive strength of concrete. In addition it was concluded that GFRP over reinforced beams are safer for designing especially when deformability is taken into account.

(Barris et al., 2012) experiment were performed on GFRP reinforced concrete beams to conclude their short-term behavior during bending with varying given reinforcement ratio and varying the effective depth to height ratio. Several predictive models were looked at and tried to compare them with experimental results. It were concluded that the behavior of beam remained linear until cracking due to lack of plasticity of GFRP bars, however the failure is experienced at larger displacements. ACI 440.1R prediction for flexural load at service load levels were good agreement with the experimental result but that was not the case in higher load levels. In addition the experimental crack width corresponded exactly to the minimum value suggested by ACI 440.1R. This indicates a good bond between the GFRP bar and concrete. All beam failed due to concrete crushing and the expected ultimate capacity of the beam according to the ACI standard was less than the experimental ultimate capacity.

Chapter 3: Failure modes in simple beam and GFRP design guidelines

3.1 Introduction

This chapter describes the failure modes that occur in simple beams and the conditions that determine their occurrence. In addition, explains the design guidelines according to ACI 440.1R-15.

3.2 Flexure failure

Flexure failure occurs when a stress crack propagates and the principal stresses in the beam approach the tensile strength of the concrete. Even if the beam is well reinforced, when the load exceeds the bearing capacity of the beam, the rebar will yield, causing concrete failure known as flexural failure. Reinforcement bar yields when the stress exceeds the flexure capacity of reinforcement bar in beam, as a result the tension cracks propagate upward and become visible when the beam deflects. As the ultimate bending capacity is exceeded, flexural failure happens and is experienced in the region of the maximum moment. Flexural failure is less dangerous than other mode of failures because occurs gradually and is followed due to the obvious cracks which increases as the beam deflects more. Figure 3.1 shows a flexural failure showing how a vertical crack develops in the center of the beam and stresses are redistributed (Darwin et al., 2016).

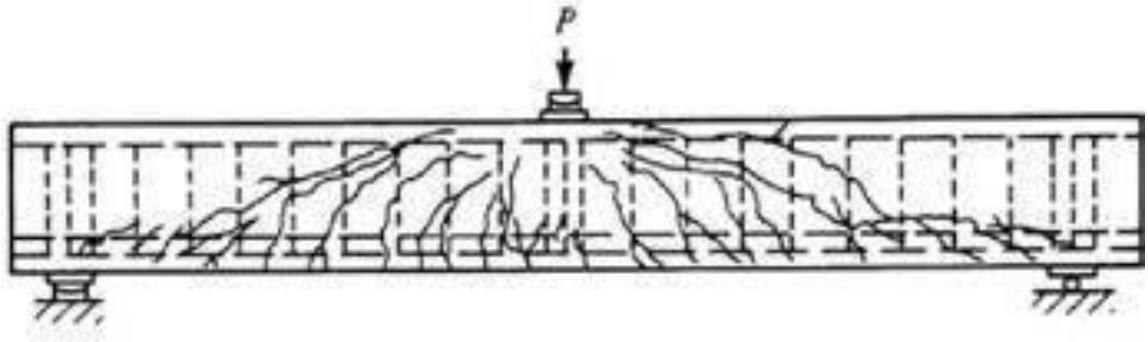

Figure 18 Illustration of flexural failure (Shanour et al., 2014)

3.2.1 Flexure tension failure

Flexure tension failure happens when the section of the beam is under-reinforced which means the reinforcement ratio is less than the balanced reinforcement ratio as required by the code ACI 318-14. It begins by yielding of steel reinforcement before damage of concrete at compression side.

The great deflection and the development of cracks at the beam in the tension side which is reach to the compression side are the warning for this type, these cracks appears at middle third of the span and mainly are vertical, in other word this type is ductile failure and it is required failure type in design method because it does not occurs suddenly.

3.2.2 Flexure compression failure

The flexure compression failure occurs when the reinforcement ratio is more than balanced reinforcement ratio which is called over-reinforced section of the beam as requirement of the code ACI 318-14. The flexure compression failure is brittle failure and very dangerous because it is sudden without any warning. It initiates by damage the concrete before the yielding of the tension steel reinforcement.

3.2.3 Balanced failure

In this type the concrete crush happen in the same time with the steel yields. This type happens when the reinforcement ratio is equal to the balanced reinforcement ratio as requirement of the code ACI 318-14.

3.3 shear failure

This type is a brittle failure, Shear failure more dangerous than flexure failure because it happens suddenly without any warning, The main parameter for determining the type of shear failure is the clear span to effective depth ratio, stirrups are used to prevent the occurrence of this type, this type can be categorized as follow:

3.3.1 Diagonal Tension Failure

It also called shear failure, one of the most important in reinforcement concrete is the shear failure because of its occurrence is devastating and dangerous. This is the most undesirable type of failure because it occurs unexpectedly and progresses rapidly. Throughout the years, its reasons and occurrences should be investigated through experimental tests in order to better understand the phenomenon. The main parameters influence the shear are geometry, bar properties and load mode. Cracks are the main cause of diagonal tensile failures that happen because of large shear forces nearby the support area. As shown in Figure 3.2, the diagonal crack starts when the flexural cracks mid-span ends and it occurs toward the concrete at support and reinforcement bar. When the crack spreads into the high shear region close to the support, beam suddenly fails (Darwin et al., 2016).

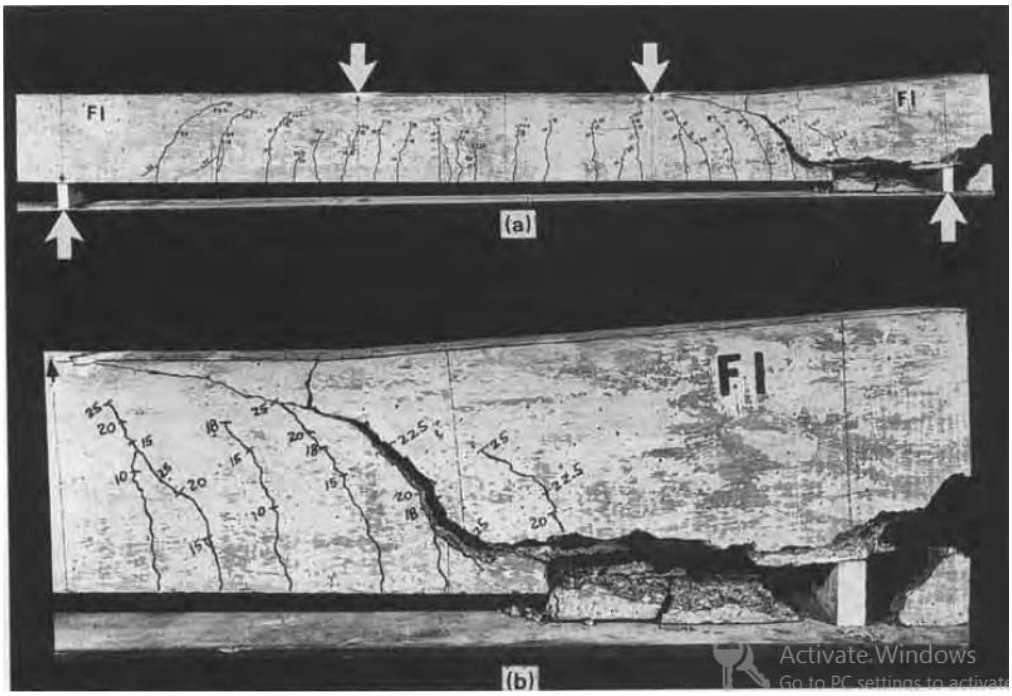

Figure 19 Diagonal tension failure of concrete beam
(a) whole beam view (b) near support view

3.3.2 Shear Compression Failure

Shear Compression Failure happens when shear forces cause a diagonal crack to spread and reach the compression zone in the form of a secondary crack without warning, as occurs in diagonal tensile failure. Concrete is also crushed to above the tip of the inclined crack near the compression flange, as shown in Figure. This failure is generally attributed to short beams (Darwin et al., 2016)

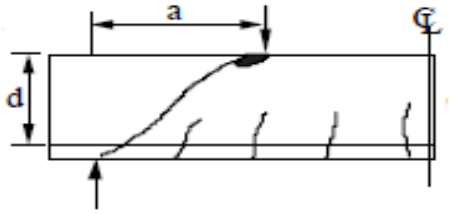

Figure 20 Illustration of shear compression failure (Shanour et al., 2014)

3.3.3 Splitting Shear Failure

This type is expected when the shear span to depth ratio is less than one. This type of beam is named deep beam in which loads are directly transferred to supports, and shear strength is much higher than that in ordinary flexural beams. Sometimes, failure in compression of the region nearby the supports may happen instead of splitting shear failure (Darwin et al., 2016).

3.3.4 Anchorage failure

In this type, the splitting of concrete is along the longitudinal reinforcement due to small diagonal cracks. It happens when the main reinforcement is not adequately anchored beyond the crack(Darwin et al., 2016).

3.4 Design Philosophy

Design guidelines for FRP RC structures have been developed in Japan (JSCE, 1997), Canada (ISIS, 2001; CSA-S806, 2002), USA (ACI 440.1R-01, 2001; ACI 440.1R-03, 2003; ACI 440.1R-06, 2006), and Europe (Byars et al., 2006).

The table below shows historical development of the existing publications for guiding the design with FRP (International Federation for Structural Concrete, 2007).

Table 6 Historical Development of the Existing Publications for Guiding the Design with FRP (Salh,2014)

1970s	**1996**	**1997**
Using fiber reinforcement in concrete	The European Committee for Concrete (Eurocrete) issued a set of design guidelines for FRP RC	The Japan Society of Civil Engineers (JSCE) published a number of design recommendations for FRP RC
1999	**2000**	**2001**
The Swedish National code for FRP RC was published	The Canadian Standard Association (CSA) issued a number of design recommendations for FRP RC bridges (CAN/CSA S6-00)	The ISIS Canada published a guide on the use of internal FRP reinforcement The American Concrete Institute (ACI 440) issued the 1st edition of design recommendations for internal FRP reinforcement (440-1R)
2002	**2003**	**2006**
The CSA published a number of design guidelines for FRP RC buildings (CAN/CSA S806-02) CUR Building & Infrastructure issued a set of design recommendations for FRP RC (The Netherlands)	ACI Committee 440 published the second version of recommendations 440	The National Research Council (CNR) published the Italian design guidelines for internal FRP reinforcement (CNR-DT 203/2006) ACI Committee 440 published the third edition of guidelines 440.1R

FRP reinforcement concrete structures are currently governed by the guidelines which are given in the form of modifications to existing steel reinforcement concrete codes of practice which uses the limit state design approach. Those modifications consist of basic principles, majorly impacted by the mechanical characteristics of FRP reinforcement, and empirical formulas according to experimental investigations on FRP reinforcement concrete elements.

As FRP composite materials are of high strength and lower stiffness, the amount of reinforcement must be determined through another approach when considering FRP reinforcement in regard to steel. The strength to stiffness ratio in FRP reinforcement is greater than that of steel by nearly %5. This definitely influences the distribution of stresses along the section (Salh, 2014.).

The neutral axis depth for FRP RC sections might be extremely close to the compressive side in a balanced section, Thus, in such a section, the compressive zone is exposed to a greater strain gradient and a greater area of the cross section is exposed to tensile stresses. Further, larger deflections and lower shear strength might take place in cross sections similar to that of steel (Pilakoutas et al., 2002).

3.4.1 Review of Current Guidelines Design Philosophy

Current design codes for structural concrete reinforced with FRP offer information for using common FRP materials like glass (GFRP), carbon (CFRP) and aramid (AFRP). Yet, there has not been design recommendations available on the use of basalt so far (BFRP).

Japan:

Japan Society of Civil Engineers (JSCE) design guidelines are based on the modification of the Japanese steel RC code of practice, and can be applied for the design of concrete reinforced or pre-stressed with FRP rebar. The JSCE design philosophy showed that material as well as member safety factors were slightly higher than the factors used for steel reinforcement. Still, there is no information regarding the predominant mode of flexural failure that might take place as a result of applying the recommended partial safety factors although the flexural design includes both modes of flexural failures, (Machida and Uomoto, 1999).

Europe:

The European design guideline by the Eurocrete project (Byars et al., 2003) based on the modification of British (BS8110-1997) and European RC codes of practice (*Structural use of concrete*, 1997) . The guidelines provide a set of partial safety factors for the material strength and stiffness. These factors take into account the short as well as long term structural behavior of FRP reinforcement. It is worth mentioning that the values got by this guideline are relatively higher those values adopted by other guidelines. The guidelines do not differentiate between the two modes of flexural failure which are concrete rupture failure and FRP bar rupture failure. Besides, they do not present clear hints concerning the predominant failure type which might follow the application of these partial safety factors.

Canada:

The Canadian Standards Association (CSA) design guidelines CAN/CSA-S806-02(Standard, 2002) are the most recently published guidelines on the design and construction of building components with FRP. The guidelines further provide information about characterization tests for internal FRP reinforcement. They were officially approved in 2004 as a national standard of Canada and they were intended to be used along with the national building code of Canada CSA A23.3 2004 (Dupuis et al., 2014).

The document prescribes that the factored resistance of a member, its cross section, and its connection shall be taken as the resistance calculated in accordance with the requirements and assumptions of this standard, multiplied by the appropriate material resistance factors. The factored member resistance shall be calculated using the factored resistance of the component materials with the application of an additional member resistance factor as appropriate (Dupuis et al., 2014).

For the predominant type of failure, the CSA S806-02 asserts that all FRP reinforced concrete sections shall be designed in a way that makes the failure of the section initiate by crushing of the concrete in the compression zone (Cheung, 2001). A design guide including design provision for FRP RC structures has been also published by the Canadian Network of Centers of Excellence on Intelligent Sensing for Innovative Structures (ISIS, 2001). These guidelines also present information regarding the mechanical properties of commercially accessible FRP reinforcements. This guideline stems from the modifications to existing steel RC codes of practice adopting flexural failure as the predominant mode of failure that can be sustained because of either concrete crushing (compressive failure) or rupture of the layer of FRP reinforcement (tensile failure).

USA:

ACI Committee on Fiber Reinforced Polymer Reinforcement, Printed documents

1. ACI 440.1R-6, Guide for the Design and Construction of Structural Concrete Reinforced with FRP Bars 2006.
2. ACI 440.5-08, Specification for Carbon and Glass Fibre Reinforced Polymer Reinforcing Bars.

3. ACI 440.2R-08, Guide for the Design and Construction of Externally Bonded FRP Systems for Strengthening Concrete Structures
4. ACI 440.4R, Pressurising Concrete Structures with FRP Tendons.
5. ACI 440R-96, State-of-the-Art Report on Fibre Reinforced Plastic (FRP) Reinforcement for Concrete Structures
6. ACI 440.1R-03, Guide and Construction of Concrete Reinforced with FRP Bars.

3.4.2 Limit State Flexure Design of FRP RC structures According to ACI code.

The design approach for concrete beams reinforced with FRP is almost identical to the design methodology of traditional steel reinforcements taking into consideration the differences in the mechanical characteristics of the FRP bars. The design of steel reinforced concrete structures is based on the linear elastic and perfectly plastic behavior of steel bars providing sufficient ductility to the whole construction. On the other hand, FRP bars do not undergo plastic deformation which requires some modifications (Salh, 2014).

The American Concrete Institute (ACI) design guidelines for FRP reinforced structural concrete (ACI 440.1R-06, 2006) are based on the modification of the (ACI 318-02, 2002) steel code of practice. The ACI 440 design guide stems from the fact that FRP behavior is brittle. Nevertheless, either FRP rupture or concrete crushing in the design of FRP reinforced concrete beam is acceptable if the strength and serviceability standards are met. The design guide remarks that in order to recompense the lack of ductility in FRP reinforced concrete beams, the factor of safety has to be higher than the one used in steel reinforced concrete design. (GangaRao,1993).

According to previous studies, the fact that FRP is a brittle elastic material and acts towards failure in a linear way without indicating any yielding has been agreed upon. Therefore, concrete crushing failure is more desirable for flexural elements reinforced with FRP (Bakis et al., 2002) as the concrete shows some plasticity prior to crushing. This clarify why the same resistance factor 0.9 of steel which ensures the ductile failure of under reinforced elements cannot be used with the FRP reinforced elements. For over reinforced FRP sections in which the failure is concrete crushing, the resistance factor is given as 0.65, and it is 0.55 for under reinforced FRP section where FRP tensile rupture which is brittle failure occurs (Aiello and Ombres, 2000).

Both the design failure strain (ε_{fu}), and design strength (f_{fu}), are determined from the provided strength and provided failure strain by multiplying them by an environmental factor, (C_E), which depends on the fiber type in the bar and the type of service desired, as illustrated in Table 7.

Table 7 Environmental factor of reduction under different condition of exposure

Exposure condition	**Type of fiber**	**Environmental factor of reduction C_E**
Concrete not exposed to weather and earth	Aramid Carbon Glass	0.9 1 0.8
Concrete exposed to weather and earth	Aramid Carbon Glass	0.8 0.9 0.7

The FRP reinforcement ratio is calculated by the following equation:

$$\rho_f = A_f / bd \quad (1)$$

Where, A_f is the reinforcement area, b and d are the cross-sectional dimensions.
The balanced reinforcement ratio is calculated as following;

$$\rho_{fb} = 0.85\beta_1 \times (f'c / f_{fu}) \times E_f \varepsilon_{cu} / (Ef\varepsilon cu + f_{fu}) \quad (2)$$

Where, β_1 the factor depends on concrete strength, $f'c$ is the compressive concrete strength, E_f is the provided elasticity longitudinal modulus of the FRP, ε_{cu} is the ultimate compressive strain for concrete which is usually 0.0035 and f_{fu} is the given longitudinal tensile strength of the FRP bars.

When FRP bars in doubly reinforced FRP concrete sections are employed as compression reinforcement, according to ACI code, FRP cannot contribute to carry the compressive strength. The flexural capacity of FRP reinforced concrete beams shows neither desirable nor undesirable results of FRP bars in the compression zone (Bank, 2006).

For FRP reinforced concrete sections, the rupture of FRP bars governs the type of failure for an under reinforced section. However, as in the case of steel reinforced concrete sections, it is the crushing of concrete that governs the mode of failure of an over reinforced concrete section. The balanced reinforcement ratio shown in equation (2) guarantees that both the crushing of concrete and the rupture of FRP bars to occur simultaneously. Such distinction is of great significance similarly as FRP beam where failure modes are brittle due to the linear elastic behavior of the FRP bar. Nevertheless, the rupture of FRP bars in tension zone is brittler than the crushing of concrete in the compression zone (Bank, 2006). In other words, it is better to design the FRP reinforced concrete beams as over reinforced. Yet, it is preferred to design the steel beams as under reinforced.

The nominal moment capacity for over reinforced FRP concrete section is calculated by:

$$M_n = A_f f_f \, (d - a/2) \tag{3}$$

Where

$$a = A_f f_f / 0.85 f'c b \tag{4}$$

And

$$f_f = ((E_f \varepsilon_{cu})^2 / 4 + (0.85 \beta_1 f' c / \rho_f) E_f \varepsilon_{cu})^{0.5} - 0.5 E_f \varepsilon_{cu} \tag{5}$$

Where, f_f is the stress in the FRP rebar at concrete compressive failure, E_f is modulus of elasticity of the FRP of longitudinal bar, ε_{cu} is the maximum compressive strain in concrete, a is the depth of the stress block, d is the effective depth of the beam, b is the width of the beam and A_f is the area of FRP reinforcement and ρ_f is the reinforcement ratio. The desire of the concrete can provide some capacity for large post-peak strains even at reduced stress

levels (Bank, 2006). The moment redistribution cannot be applied due to the linear elastic behavior of FRP bars because of it does not allow the formation of plastic hinges. in contrast to the steel bars in order to calculate the moment capacity of the section when the FRP bars are used in layers, the stress in each layer must be calculated individually, where in case of layers of steel bars the resultant tensile force is assumed that in the centroid of the bar layers. This was also confirmed by the different studies that the anisotropic nature of the material does not significantly affect the flexure behavior of the section (Bakis et al., 2002).

The failure mode for under reinforced sections is the rupture of the FRP in the tension zone. Whereas it is the concrete crushing that takes place in the compression zone for over reinforced sections. Yet, the minimum area of reinforcement can be calculated by Equation 6, which has been determined by multiplying the current ACI 318-05 equation of minimum area of reinforcement for steel by 1.64 to prevent failure upon concrete cracking.

$$A_{fmin} = 4.9((f'c)^{0.5}/f_{fu}) b_w d > (330/ f_{fu}) b_w d \quad (6)$$

According to ACI 40 code for the design of FRP reinforced concrete structures, the design method is depend on the limit state design principles which are fatigue strength, creep rupture strength, and It should be checked for serviceability criteria. (GangaRao, 1993). The fundamental factors that determine the design of FRP reinforced concrete structures are the maintainability criteria, which are mainly deflection and crack width. The high tensile strength and low modulus of FRP bar mean that the reinforced elements are highly deformable. Since FRP bars are less rigid than steel bars, the structural elements are reinforced with FRP bars have greater deflection and crack widths than the structural elements are reinforced with steel bars. Due to the linear elastic brittle behavior of FRP bars, the ACI code does not allow the use of moment redistribution, as plastic hinges cannot be formed.

3.4.3 Serviceability

The FRP reinforced beams are exposed to larger deflections than steel reinforced beams since the elastic modulus of the FRP is lower than that of steel bars with the same

reinforcement ratio. As a result significant cracking will happen along the length of the beam thereby reducing its flexural stiffness and causing greater deflection. The service limit state design for FRP reinforced concrete beams take into account two important service conditions which are deflection and cracking.

3.4.4 Cracking

Despite the importance of the relationship between the stress and the strain in order to determine the bending moment strength of the FRP reinforced concrete beam, the stiffness behavior can be similarly important for different other structural requirements. This can be especially important in determining varying degrees of relevance to service criteria. The stiffness or modulus of elasticity of the FRP bars is expressively lower than the steel bars. This may cause an extreme deflection of the beam which leads to larger crack widths will happen. Because of low modulus, the FRP materials are very sensitive to the condition of large deflection so the criteria used can be a fundamental issue on the design of FRP reinforced concrete beams. Based on the study done by Nanni (GangaRao, 1993)to compare the flexure behavior of aramid FRP reinforced beams with normal steel reinforced concrete beams, many significant principles can be stated. The moment curvature analysis for AFRP reinforced and steel reinforced beams were carried out. This determined that the maximum moment and curvature of the FRP reinforced sections are the same as in the case of steel reinforced concrete beams with a slightly lower reinforcement ratio, but the flexural rigidity of the FRP section is only 38% that of the steel reinforced beam. As a result, for FRP reinforced beams, the deflection criteria may be as significant as the flexural strength (Bakis et al., 2002). The maximum crack width per ACI 440.1R-21 can be calculated by the following equation:

$$w = (2 f_f / E_f) (d_c^{\,2} + (s/2)^{\,2})^{0.5}$$

where w is maximum width of crack, f_f is the stress of the reinforcement, E_f is modulus of elasticity of the reinforcement, β is a ratio of distance between neutral axis and tension face to distance between neutral axis and centroid of reinforcement, d_c is the thickness of concrete cover, s is bar spacing and k_b is the coefficient of the degree of bonding between FRP bars and the surrounding concrete. Due to the corrosion resistance property of FRP bars under severe environmental conditions where the allowable crack width is greater than

that of steel, where The allowable values of crack width are 0.020 in (0.5 mm) and 0.028 in (0.7 mm) for exterior and interior conditions respectively. While these value in steel reinforced concrete are 0.013 in (0.3 mm) and 0.016 in (0.4 mm) for exterior and interior conditions respectively according to the ACI code.

3.4.5 Deflection

Deflection was traditionally calculated using the elastic deflection equation, which contains the effective moment of inertia (Ie) introduced by Branson for reinforced concrete. (Branson, 1963). Previous researches have shown that using Branson's equations provide a response that is too stiff for FRP reinforced concrete resulting in reduction of deflection (Yasir et al., 2019). The reason for this is due to various factors such as poor adhesion and excessive cracking, both have been hypothesized to be responsible for the loss of stress stiffening due to FRP reinforcement. The appropriacy of the Branson formula for FRP reinforced concrete beams can be therefore questioned. Originally developed for reinforced concrete, the Branson formula uses the effective moment of inertia (I_e) to calculate deflection in combination with elastic deflection equation. This relationship was experimentally resulting and shows a gradual transition from the gross moment of inertia (I_g) to the cracked moment of inertia (I_{cr}). In the general form this can be presented as:

$$I_e = (m_{cr}/m_a)^m I_g + (1-(m_{cr}/m_a)^m)\, I_{cr} > I_g \qquad (12)$$

Where, The exponent m is found to be equal to 3 for the steel reinforced beam, but an exponent of 4 was found to give better approximations of effective moment of inertia for individual sections(Theriault and Benmokrane, 1998). For ratios of total moment of inertia I_g to crack moment of inertia I_{cr} between 1.5 and 4, these value were verified by the Branson's equation. (Bischoff and Paixao, 2004). In general, the values of this ratio for FRP reinforced concrete beams are greater than 5 which, as a result, leads to a more rigid response and irrelevant predictions of calculated deflections when used with the original Branson equation simultaneously (Bischoff, 2007). The exponent m has also physical importance as it adds a smooth transition from the gross moment of inertia to the cracking moment of inertia when the load arrive at ultimate value. In other words, that transition

from the gross moment of inertia of FRP reinforced beam to the cracking moment of inertia is therefore faster. This accordingly clarifies why the faster decline in the stiffness of the beam occurs. Nonetheless, they are not fully amendable to the original Branson equation, which expects relatively slower degradation with the exponent equal to 3. Making the exponent "m" to be higher than 3 has been suggested by Dolan. When reinforcement ratio lower than 4% in GFRP reinforced beams, they can have a ratio of the un-cracked to cracked moment of inertia of 5-16, which confirms the significance of the exponent "m". the FRP bars and the surrounding concrete may not have enough bond in FRP reinforced concrete beams where the experimental deflection exceeds the moment of inertia of cracked section (I_{cr}) limitation on deflection. The Branson equation can therefore give the transition from gross moment of inertia (I_g) to the cracked moment of inertia (I_{cr}). such a modification was proposed in 1997 by (Theriault and Benmokrane, 1998) as follows:

$$I_e = \alpha\, I_{cr} + ((I_g/\beta) - \alpha\, I_{cr})\,(M_{cr}/M_a)^3 \qquad (13)$$

Where α is equal to 0.87, and β is equal to 7. In the afore-stated equation, the factor α provides the transition from the gross moment of inertia to the cracked moment of inertia. A modification on the original Branson equation was proposed by the ACI committee 440.1R-03 (Nanni, 2005) in order to reduce the tension stiffening module which relies on the ratio of gross to cracked moment of inertia to realistic levels. Such relation was given as:

$$I_e = (M_{cr}/M_a)^3 \beta_d I_g + (1 - (M_{cr}/M_a)^3)\, I_{cr} < I_g \qquad (14)$$

Where E_f and E_s are elastic modulus values for FRP and steel bars, β_d the coefficient was first assigned equal to 0.6 and set later as $\beta_d = \alpha_b (E_f/E_s + 1)$, and α_b is the bond dependent factor which presumed equal to 0.5 until more data was available and set . $\alpha_b = 0.064\,(\rho/\rho_b) + 0.13$ (Recent changes by ACI 440.1R-06 recommend using
$\alpha_b = 0.2\,(\rho/\rho_b)$ Nwys stated that the deflection prediction varies with the amount of reinforcement (Yasir et al., 2019)]. He further reported that the under-estimation of the

deflection changes reversely with the reinforcement ratio. Sunna conducted examinations on FRP reinforced concrete beams and reported similar results (Al-Sunna, 2006).
The deflection calculation based on the original or modified form seems to over-estimate the stiffness of the member hence resulting in under-predicting deflection. Yet, the predictions get better when the reinforcement ratio grows. He presented the next relation:

$$I_e = \alpha I_{cr} + (\beta I_g - \alpha I_{cr}) (M_{cr}/ M_a)^3 \quad (15)$$

Where

$$\beta = 0.1e (\rho E_f/E_s)^{1.2} \quad (16)$$

Where α the value of proposed to be between 0.85, 0.9 and 1 for GFRP, CFRP and steel reinforced concrete beams, respectively, with respect to bond characteristic of the different materials. Similar results were reported by Rafi relating to the over-prediction of the stiffness of the CFRP reinforced concrete beams (Rafi et al., 2007). Extensive research has been done by previous scholars and a plot has been established to explain the relationship between the reinforcement ratio and the discrepancy in theoretical prediction calculated by the Branson equation and actual deflection is shown in the figure below (Ascione et al., 2010).

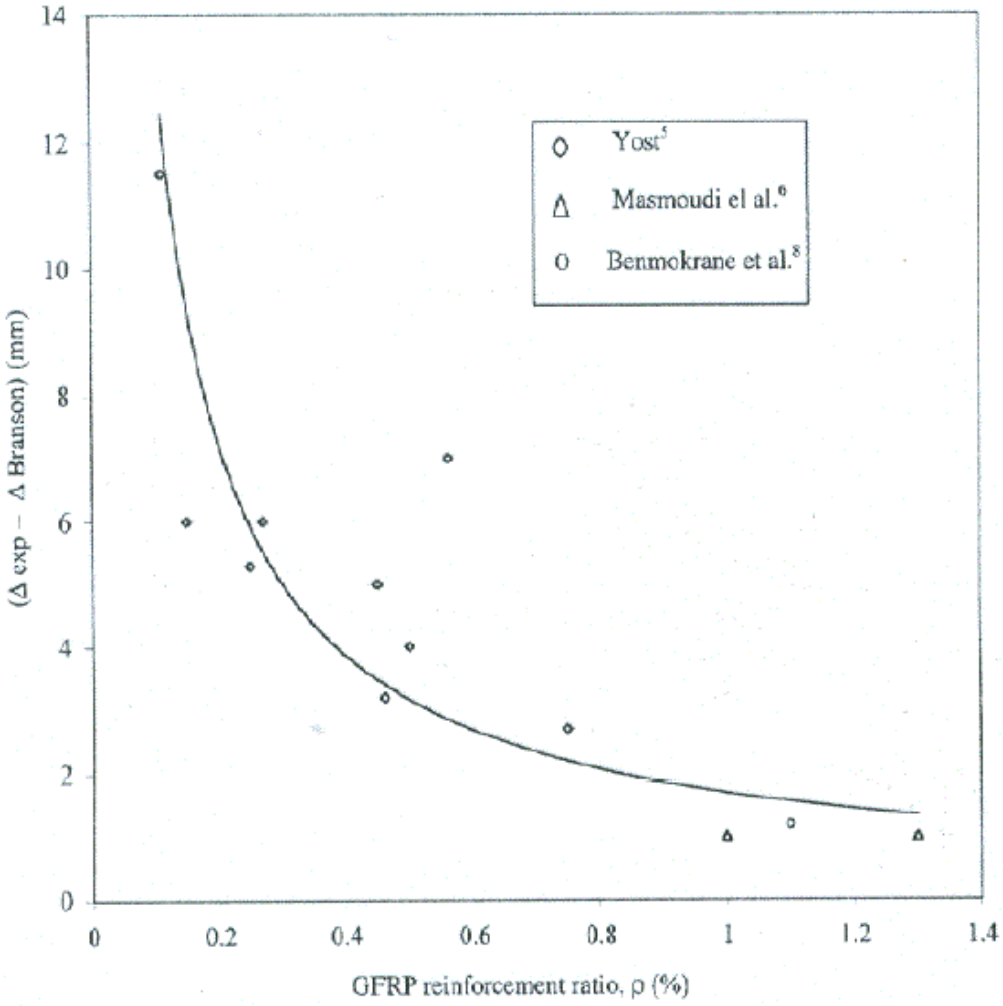

Figure 21Effect of Reinforcement Ratio on the Deflection

The plot above made by Yost, Masmoudli and Benmokrane on the GFRP reinforced concrete beams. It shows that the discrepancy between the actual and theoretical deflection is higher when the lower reinforcement ratio has been used, while it improves as the reinforcement ratio increases. It can be suggested therefore, that the behavior of FRP reinforcement concrete beams is ultimately dissimilar to that of steel reinforcement concrete beams. Consequently, tension stiffening significantly contribute to the analysis of FRP reinforced concrete sections.

In GFRP reinforced concrete beams, according to previous studies, the ratio of gross moment of inertia to cracked moment of inertia varies between 5 to 25 when the reinforcement ratio is between 2 to 3 (Bischoff and Paixao, 2004). Therefore, the applicability of the Branson equations is possible when the reinforcement ratio is less than 4%. As an attempt to handle this issue, a theoretical model based on the actual mechanics of the structure including tension stiffening was developed by Bischoff.

Bischoff's model can give the relationship of all the parameters a general form based on the essential mechanics of the structure and appropriate hypotheses. Bischoff's formula of the effective moment of inertia is given as (Bischoff, 2007):

$$I_e = \frac{I_{cr}}{1-\varkappa_{ts}\eta\left(\frac{M_{cr}}{M_a}\right)} = \mathrm{I}cr1-\eta\,(\mathrm{M}crMa)2 \le Ig \tag{17}$$

Where

$$\eta = 1-\mathrm{I}crIg \tag{18}$$

And

$$\varkappa_{ts} = \frac{M_{cr}}{M_a} \tag{19}$$

Bischoff's equation shows that the tension stiffening factor is equivalent to the estimation made for axial tension members. It also indicates that it is based on the presumption that the tension stiffening strain varies inversely with the reinforcement stress at the crack location. That is, $\varkappa_{ts} \sim f_{b,cr}/f_b$. Where, $f_{b,cr}$ is the stress in the bar at first cracking and is the stress in the bar at M_a . Thus, the tension stiffening strain is higher when FRP reinforced beams have lower reinforcement ratio.

The stiffness of an FRP reinforced concrete section is a function of the reinforcement ratio. In 2000, Toutanji and Safi addressed this factor affects the exponent "m" in the basic Branson equation. Likewise, Dolan proposed the limit of exponent "m" for FRP reinforced concrete beams as follows (Salh, 2014.):

For $(E_{FRP}/E_s)\,\rho_{FRP} < 0.3 \quad m = 6 - (10\,E_{FRP}/E_s)\,\rho_{FRP}$

For $(E_{FRP}/E_s)\,\rho_{FRP} > 0.3 \quad m = 3$

Where, E_{FRP} is the elastic modulus of GFRP bars used in the study, E_s is the elastic modulus of steel and ρ_{FRP} is the FRP longitudinal reinforcement ratio. Through analyzing the deflection of CFRP reinforced concrete beams, Maji and Oronzco developed the next modification for effective moment of inertia in 2005 (Adhikari, 2009):

$$I_e = \gamma \left[\eta \left(\frac{M_{cr}}{M_a}\right)^3 I_g + \left[1 - \frac{M_{cr}}{M_a}\right]^3 I_{cr}\right] \tag{20}$$

Where γ is the modification factor and its value is equal to the ratio of elastic modulus of FRP to the elastic modulus of steel. η is a factor that relies on the reinforcement ratio and it is as follows:

$$\eta = 100\rho - 0.2 \tag{21}$$

The deflection of FRP reinforced concrete beams depends on the reinforcement ratio and is impacted upon by its lower modulus of elasticity. In accordance with the latest ACI 440.1R-06, for an FRP reinforced concrete section, an amended form of Branson equation is utilized to determine the effective second moment of the beam. This is given as follows:

$$I_e = \left(\frac{M_{cr}}{M_a}\right)^3 \beta_d I_g + \left[1 - \left(\frac{M_{cr}}{M_a}\right)^3\right] I_{cr} \leq I_g \tag{22}$$

Where, M_{cr} is the moment of cracking and β_d is a reduction coefficient for FRP reinforced beams and is as follows:

$$\beta_d = \frac{1}{5}\left(\frac{\rho_f}{\rho_{fb}}\right) \leq 1 \tag{23}$$

Likewise, in the case of a steel reinforced concrete section, the cracked second moment of area is given as follows:

$$I_{cr} = \frac{bd^3}{3} k^3 + \eta_f A_f d^2 (1-k)^2 \tag{24}$$

Where $k = c / d$ and it is the ratio of the depth of the neutral axis to the effective depth of the section under service load and η_f is the modular ratio for the FRP reinforcement.

Meshing type

Instead of employing a global or sweep mesh, the beam components are meshed individually on a part-by-part basis. The solid parts, concrete and loading plate, are represented by an eight-nodded linear brick element (C3D8R). As illustrated in Figure 22, a 2-node linear 3-D truss element (T3D2) is utilized to model main and transfers reinforcement (T3D2), while a 4-noded shell element (S4R) is used to simulate CFRP

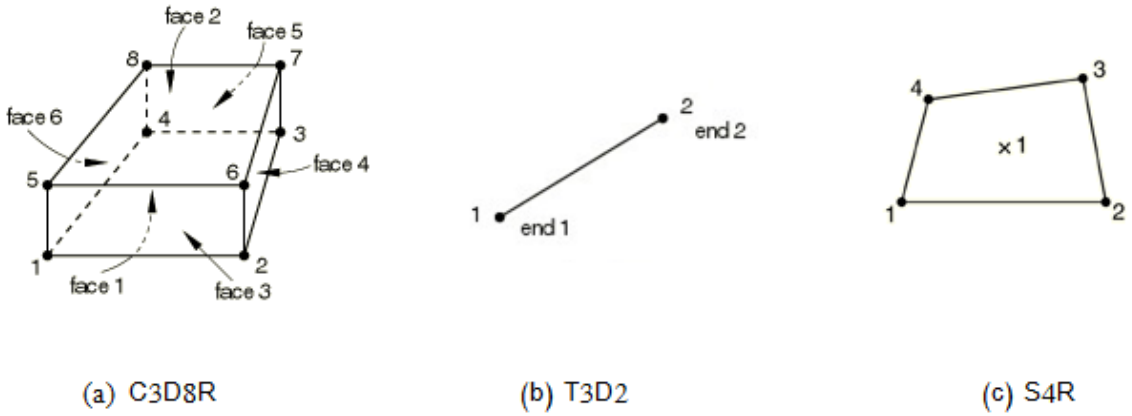

Figure 22 Finite Element Mesh Type

Chapter 4: Experimental Program

4.1 General

Data from experimental tests are used to validate the finite element model results. However, there are various experiments on R.C beams. Many of these experiments have not been reported in detail and are therefore difficult to model. A well-documented set of experiments is chosen to validate the results of the FE model. Many independent tests reported in the literature are used to determine the validation. One of them is an R.C beam subjected under four – point static load (displacement control) which was tested by (Karimipour and Edalati, 2020).

4.2 Beam geometry and reinforcement

According to the selected paper, the Reinforced Concrete beam has a cross-section that is 150 mm wide, 200 mm high, and a length of 1500 mm. This beam is reinforced with two phi10 compression bars on top, two phi20 tension bars on the bottom, and with phi8/100mm stirrups in the beam we intended to strengthen against flexure. There are no stirrups in the beam, which we intended to strengthen against shear.

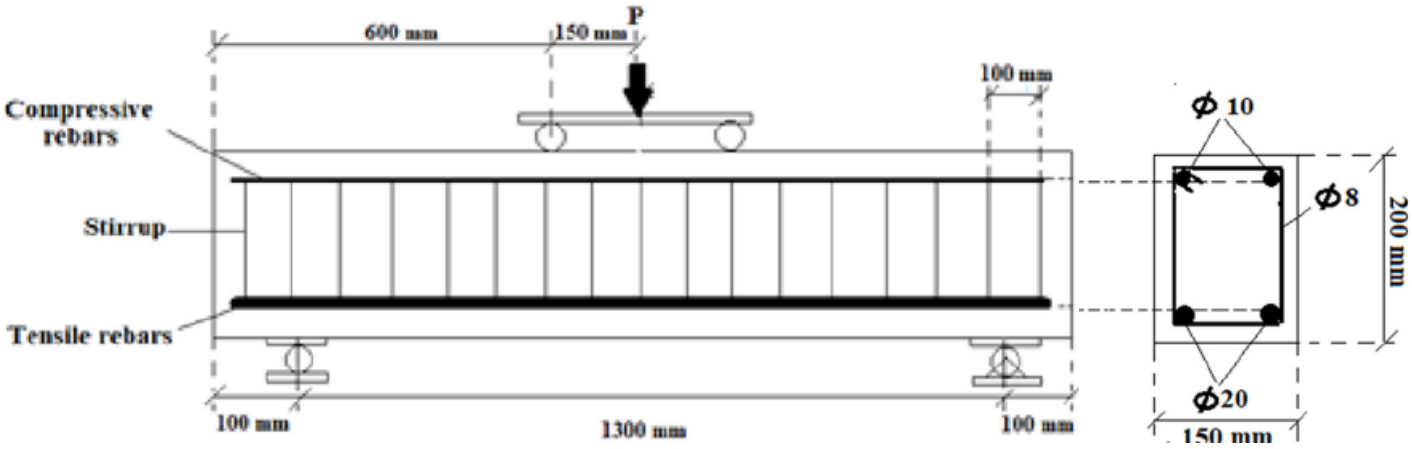

Figure 23: Studied Beam

4.3 Specifications of materials used

Steel bars have a modulus of elasticity of 200,000 MPa and a Poisson's Ration of 0.3. For the GFRPs, the modulus of elasticity and Poisson's Ratio were set to 105,000 MPa and 0.2 respectively. The paper provide the following information about the properties of rebars used:

Table 8: Rebar Properties

Rebar diameter	Yield strength	Ultimate strength	Yield strain	Ultimate strain	Modulus of elasticity
mm	MPa	MPa	%	%	GPa
8	371	545	0.1294	24.93	209.28
10	371	571	0.1304	24.82	210.10
20	558	694	0.1527	25.51	213.17

The concrete compressive strength was determined by performing a compressive test during the experiment and was determined to be 38 MPa. Because The curves were not provided so Elkady's tool (Elkady, 2023) will be used in order to obtain data based on the Chinese Code (GB 50010-2010) as follows:

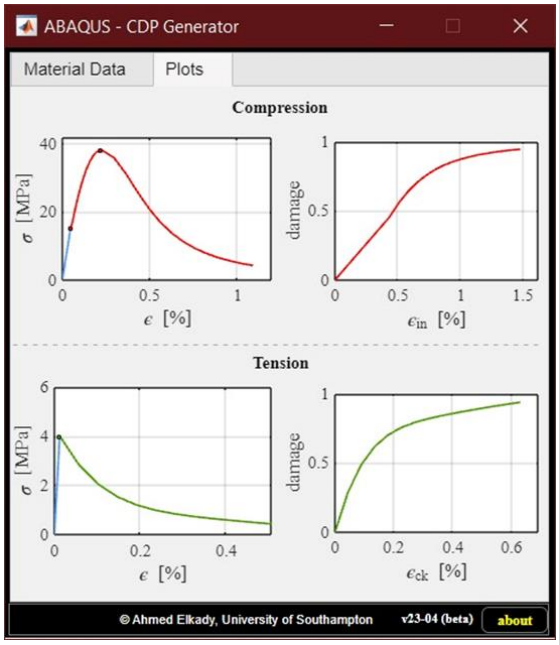

Figure 24: Elkady's Tool Data for 38 MPa Concrete

Table 4.2: Parameters of concrete used in test of Karimipour and Edalati (2020)

E_0(MPa)	ν	ψ	e	f_{b0}/f_{c0}	K
27806	0.2	36°	0.1	1.16	0.67

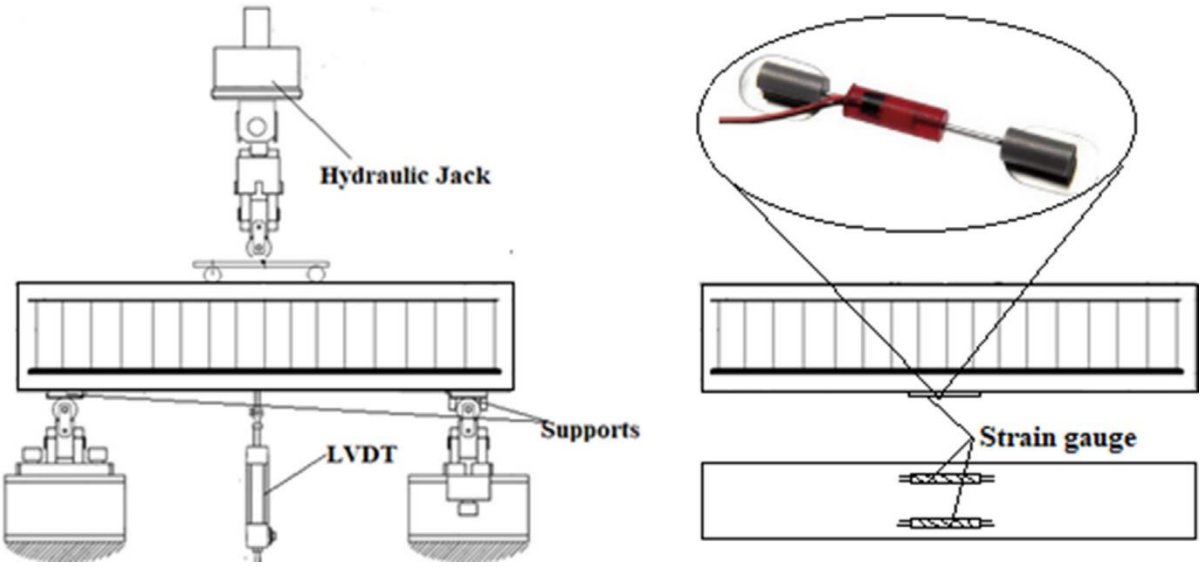

Figure 25: Experimental test setup

4.4 Building and verification of model data

Abaqus was used by creating parts with the predefined dimensions and added materials' definitions, then by assigning each part creating and the corresponding material to new sections. To apply the load on and support the beam, a new part called "Steel Plate" has been added. To ensure that this component has no effect on the results, the modulus of elasticity defined as 10 times the normal steel's modulus (2,000,000 MPa) with relatively small dimensions. Then the parts assembled together to complete with the model shaped as the experiment. There were two load points separated by 300 mm, each with two supports, a roller and a pin.

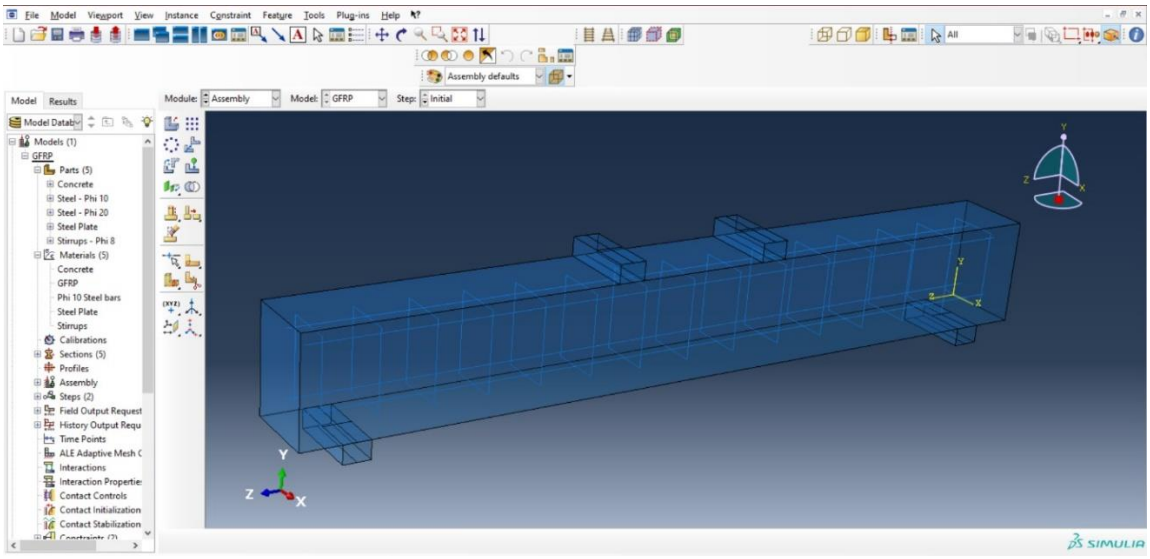

Picture 1: Parts menu and showing Reinforced Concrete Beam

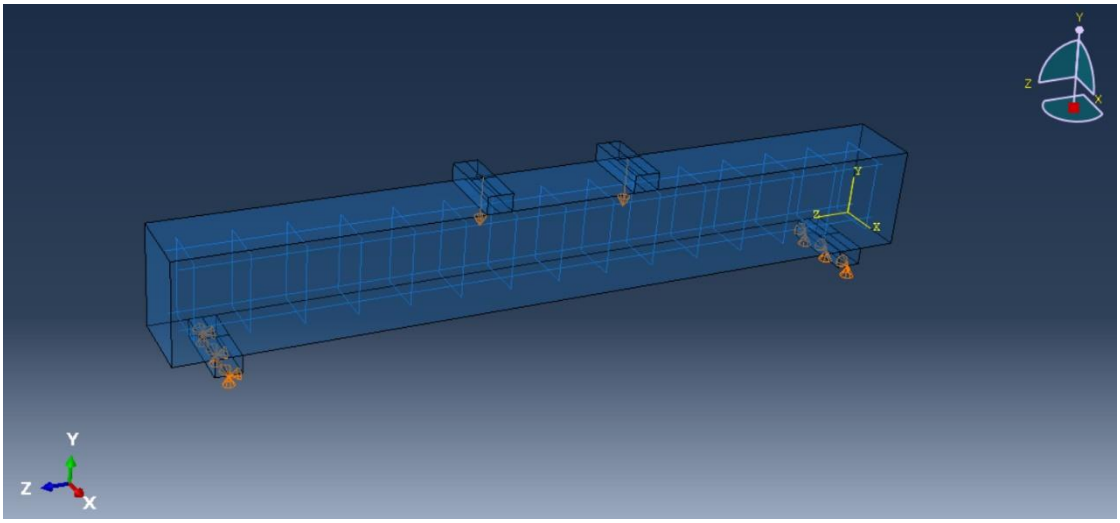

Picture 2: Original Model Load and supports' locations

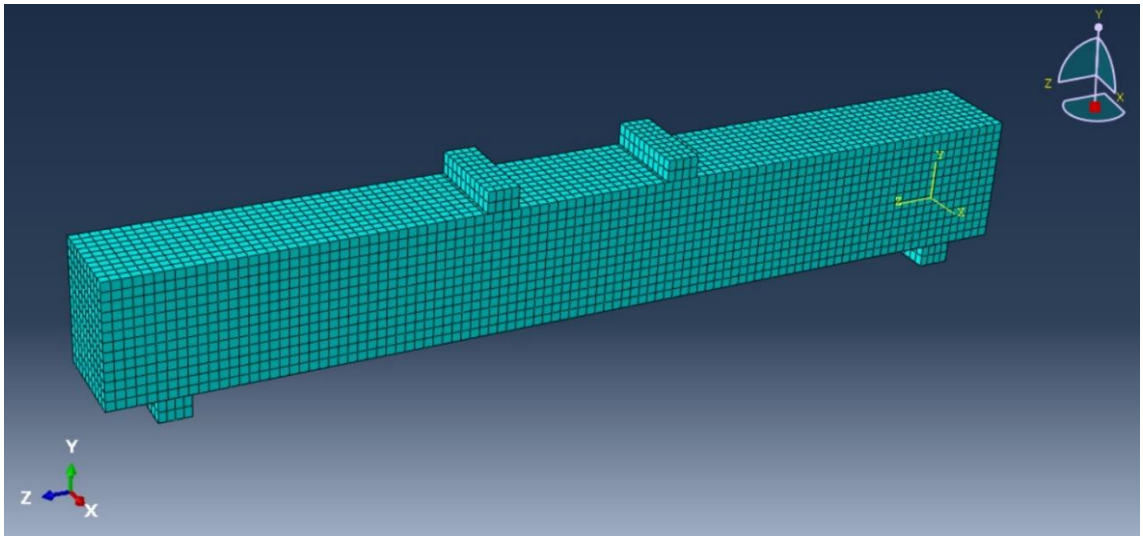

Picture 3: Meshing the whole model

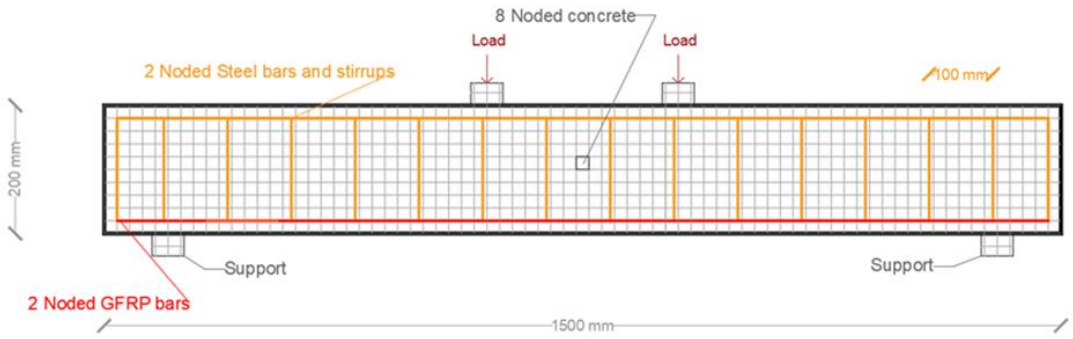

Figure 26: Meshing standards

A sensitivity study was carried out to ignore the effect of mesh size on the results. The parameters of materials are assumed to have been given by Karimipour and Edalati. (2020). various global mesh sizes were studied (10 mm to 45 mm). The results show that the obtained curves are approximately stable for meshes ranging from 15mm to 35 mm as shown in Figure 4.1. However, a mesh size of 15 mm was used in all later samples to avoid the divergence error in ABAQUS that occurs in many 35/25 mesh size samples.

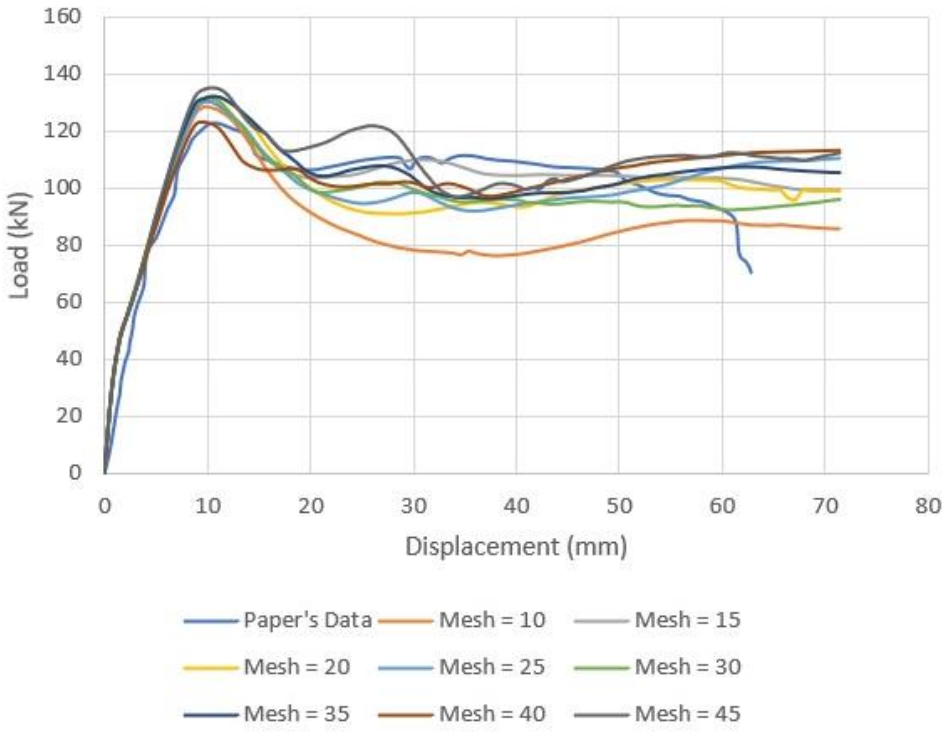

Figure 27: Load - Displacement Curve for different mesh sizes

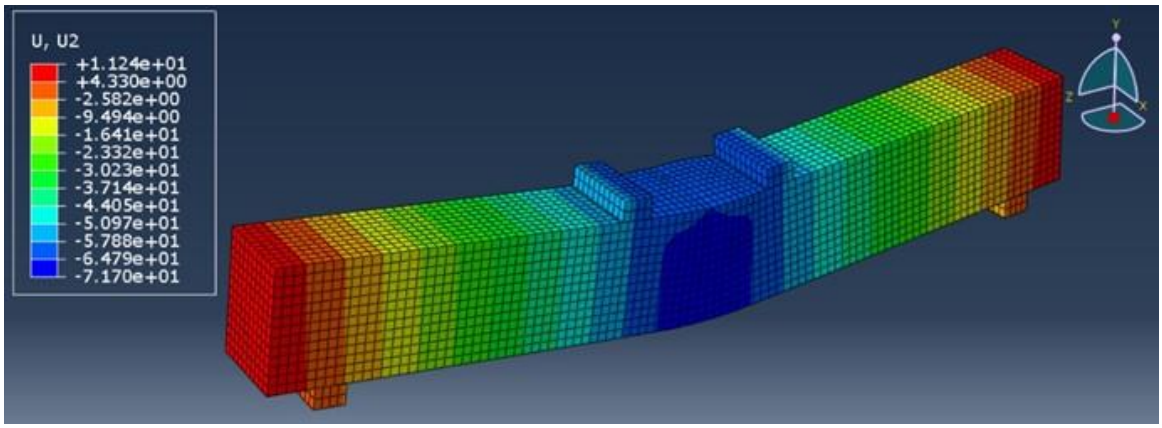

Picture 4: With GFRP - U2 (Vertical Displacement)

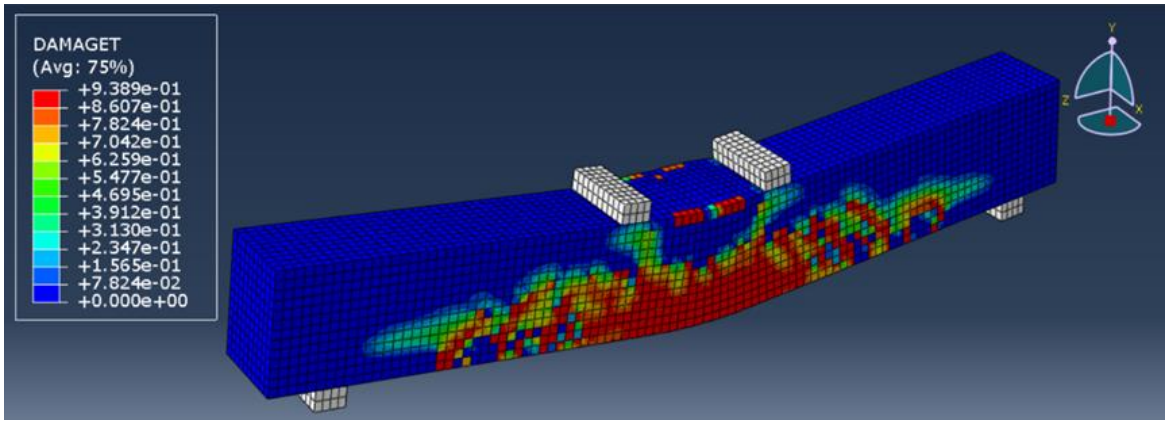

Picture 5: With GFRP - Damage Tension

Picture 6: Experimental sample damage

As shown in the two above pictures, the damage in the concrete due tension is approximately the same. The cracks start from the middle of the beam and moved on to the sides (toward the supports).

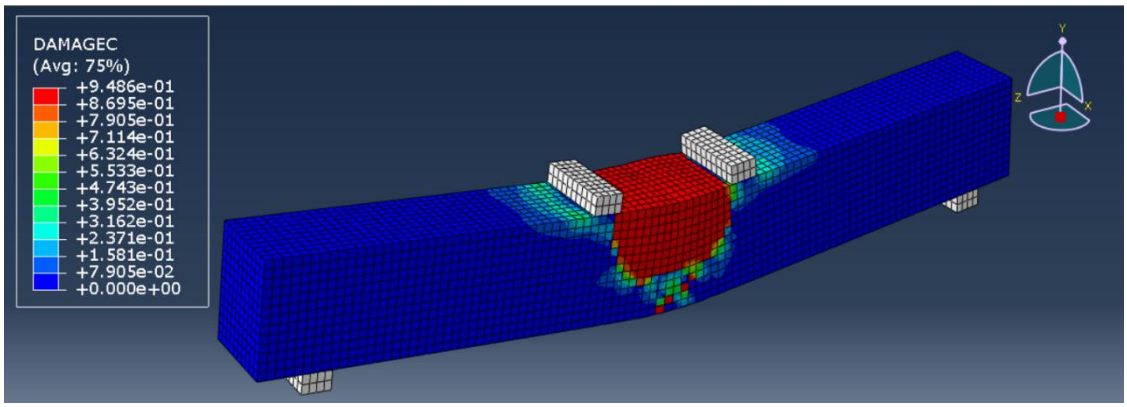

Picture 7: With GFRP – Compression Damage

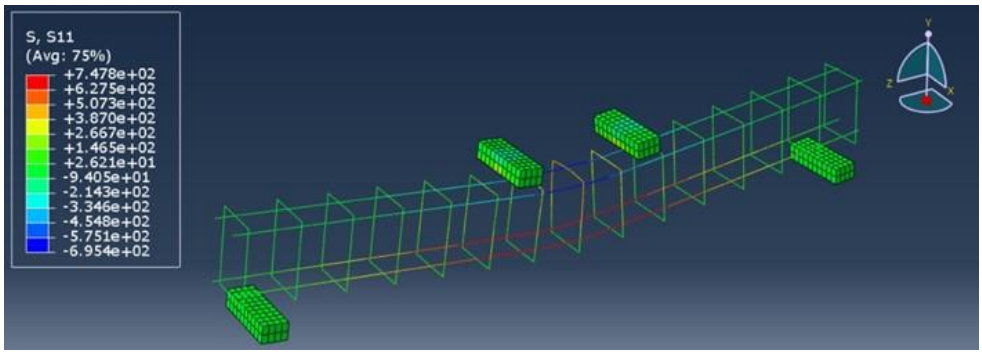

Picture 8: With GFRP – Steel and GFRP Normal Stress

The figure below presents the relationship between load and displacement both as shows in the paper and as derived using the Abaqus software. The experimental beam's behavior and reaction were quite comparable to the Abaqus model. At a midspan displacement of 10mm, the maximum load capacities in the Abaqus model and experiment were roughly 131 kN and 123 kN, respectively. The variation in maximum load capacity determined by Abaqus is around 6.5%, which is an acceptable amount

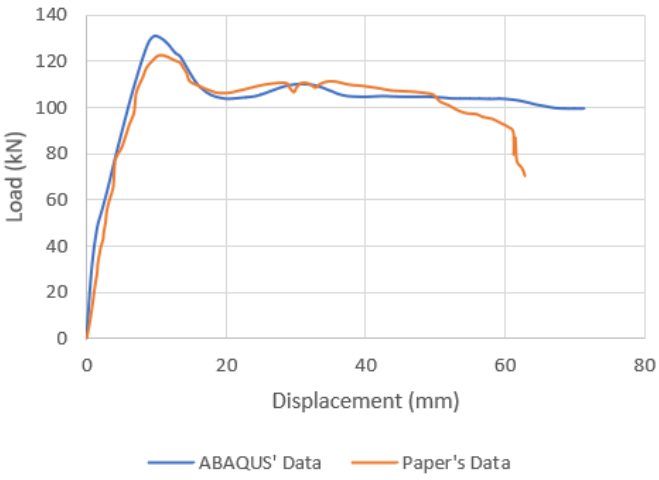

Figure 28: Load - Displacement Curve for original model

4.5 Parametric study

Parametric study is carried out to investigate the behavior of R.C beam reinforced by GFRP in various cases. The behavior influence will be studied by various parameters. These parameters are:

4.5.1 Changing the area of GFRP bars

The GFRP bars applied for resisting tension force were having different sizes as following:

4.5.1.1 Phi 16 GFRP bars

Two phi 16 bars have the total area of 401.92 mm^2 will give us the following deflection:

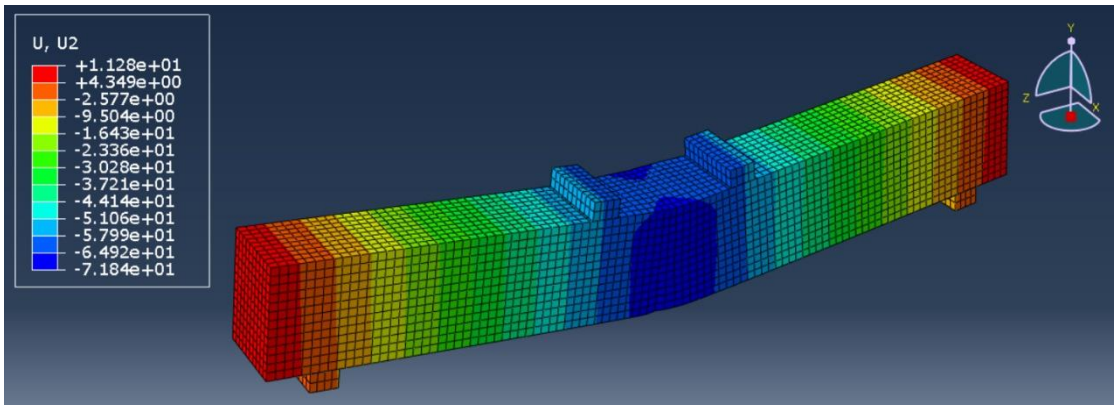

Picture 9: GFRP-Phi16 Model - U2 (Vertical Displacement)

4.5.1.2 Phi 18 GFRP bars

Two phi 18 bars have the total area of 508.68 mm^2 will give us the following deflection:

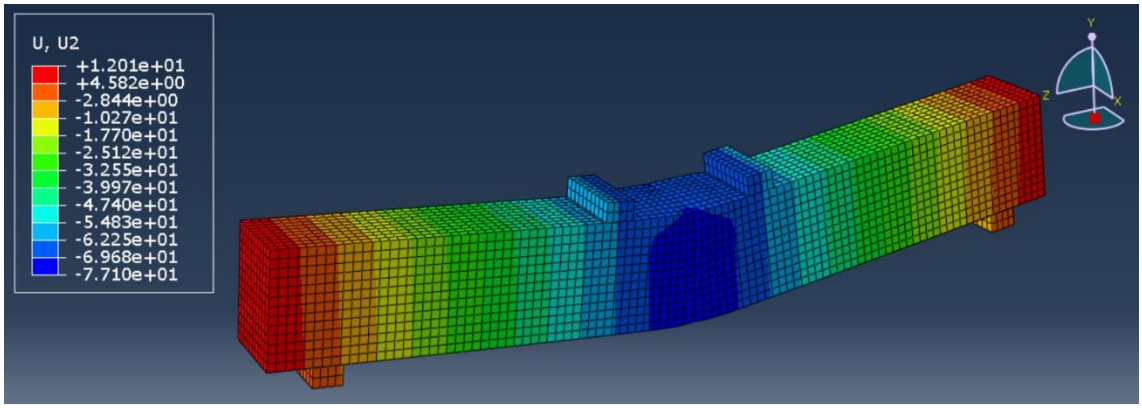

Picture 10: GFRP-Phi18 Model - U2 (Vertical Displacement)

4.5.1.3 Phi 20 GFRP bars

This study is exactly the same of the original model.

4.5.1.4 Phi 22 GFRP bars

Two phi 22 bars have the total area of 759.88 mm^2 will give us the following deflection:

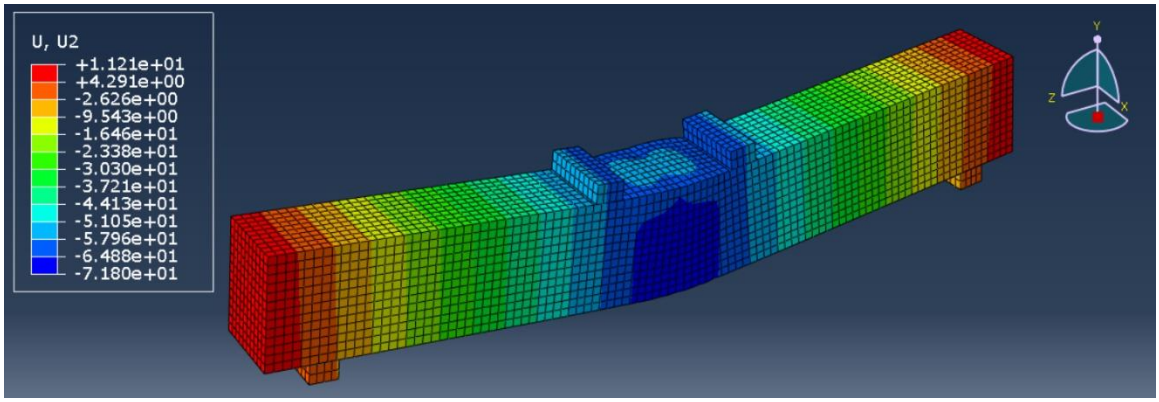

Picture 11: GFRP-Phi22 Model - U2 (Vertical Displacement)

4.5.1.5 Phi 24 GFRP bars

Two phi 24 bars have the total area of 904.32 mm^2 will give us the following deflection:

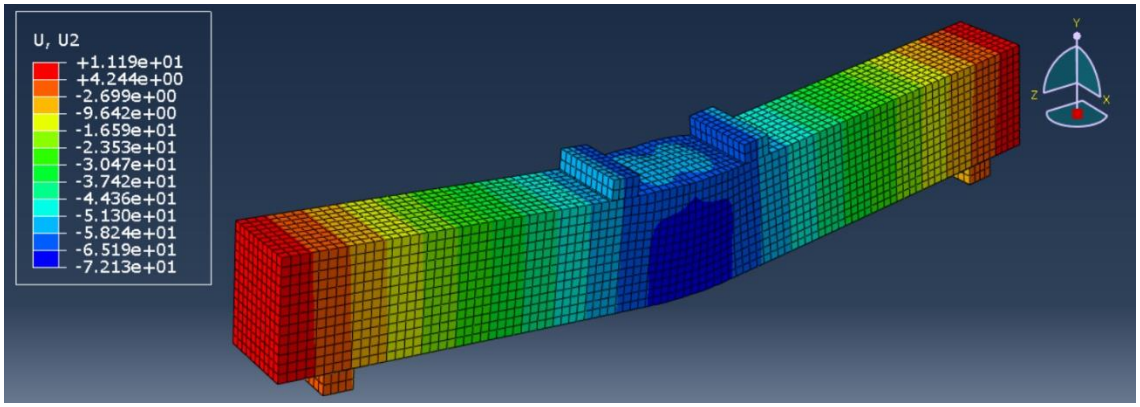

Picture 12: GFRP-Phi24 Model - U2 (Vertical Displacement)

4.5.2 Changing distances between Loads

The load applied on the beam on two-upper points, the distance between these two points is changed. There are 5 models developed in this area:

4.5.2.1 Distance = 0 mm

Two phi 20 bars have the total area of 628 mm^2 will be used with no distance between the load points (only one point load in the middle of the beam) will give us the following data:

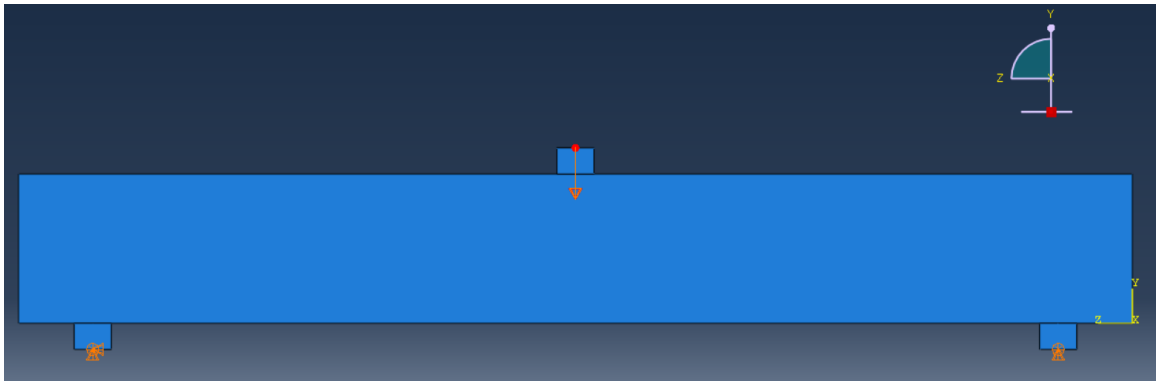

Picture 13: GFRP-0 Model - Load and supports' locations

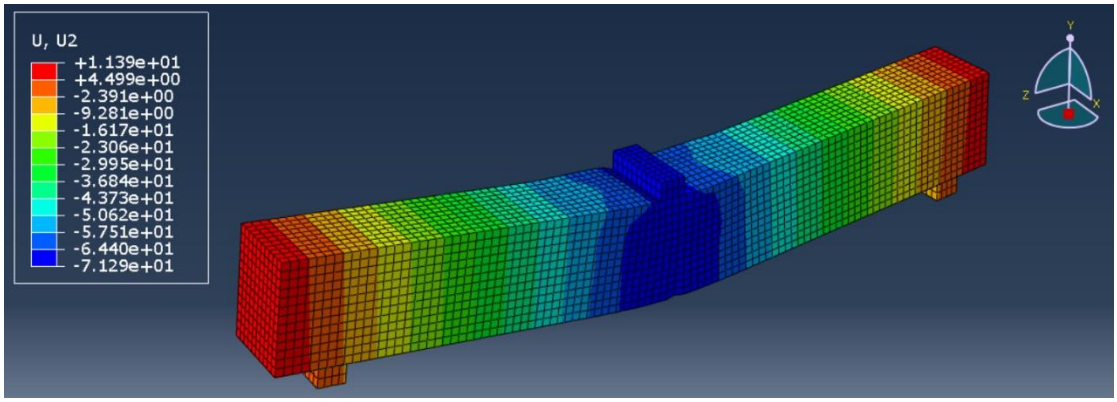

Picture 14: GFRP-0 Model - U2 (Vertical Displacement)

4.5.2.2 Distance = 150 mm

Two phi 20 bars have the total area of 628 mm^2 will be used with distance between the load points equal to 150 mm will give us the following data:

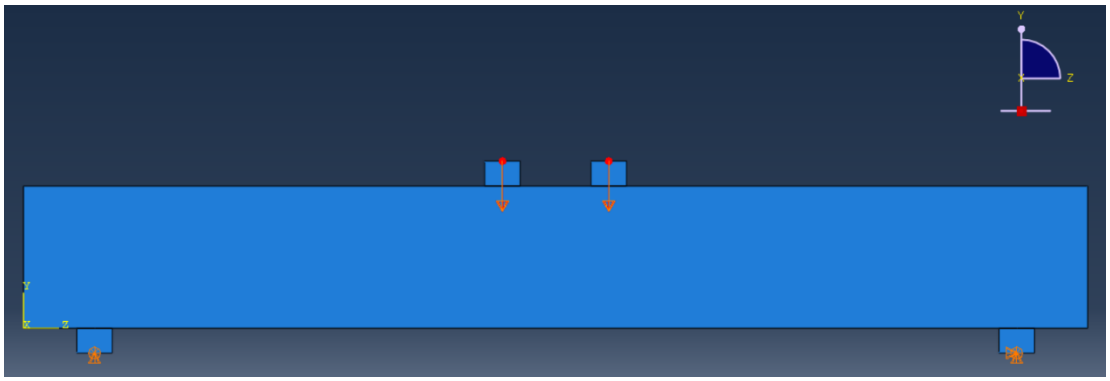

Picture 15: GFRP-150 Model - Load and supports' locations

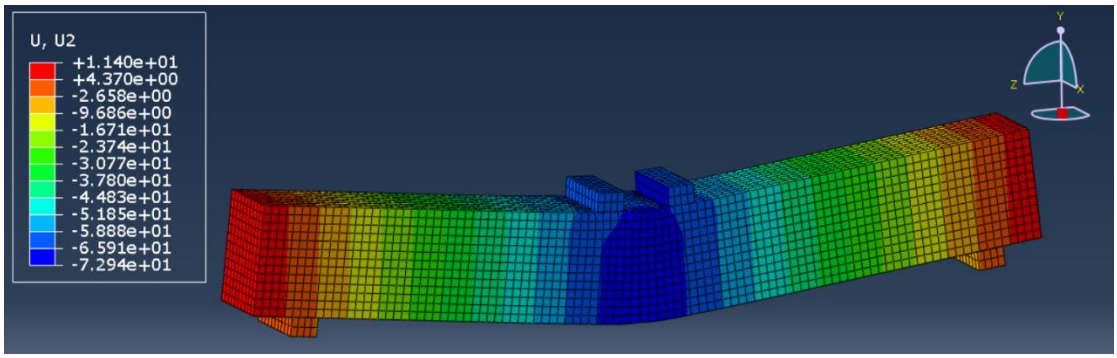

Picture 16: GFRP-150 Model - U2 (Vertical Displacement)

4.5.2.3 Distance = 300 mm

This study is also exactly the same of the original model.

4.5.2.4 Distance = 450 mm

Two phi 20 bars have the total area of 628 mm^2 will be used with distance between the load points equal to 450 mm will give us the following data:

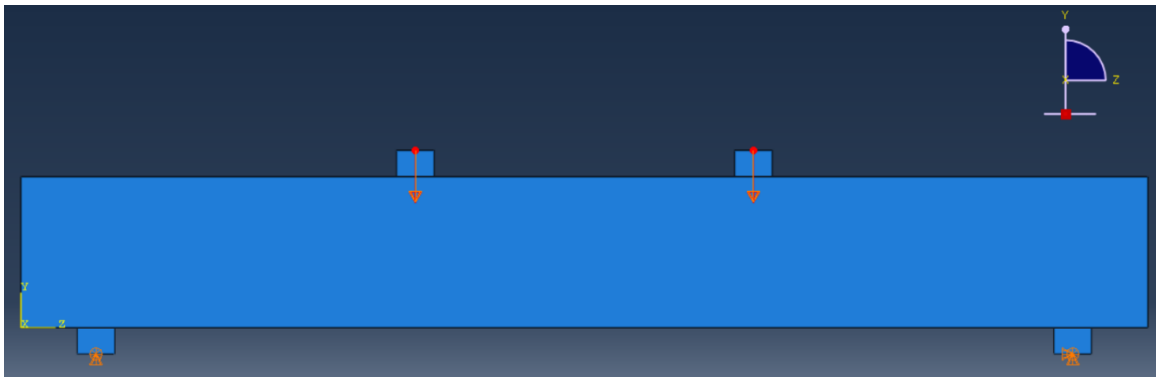

Picture 17: GFRP-450 Model - Load and supports' locations

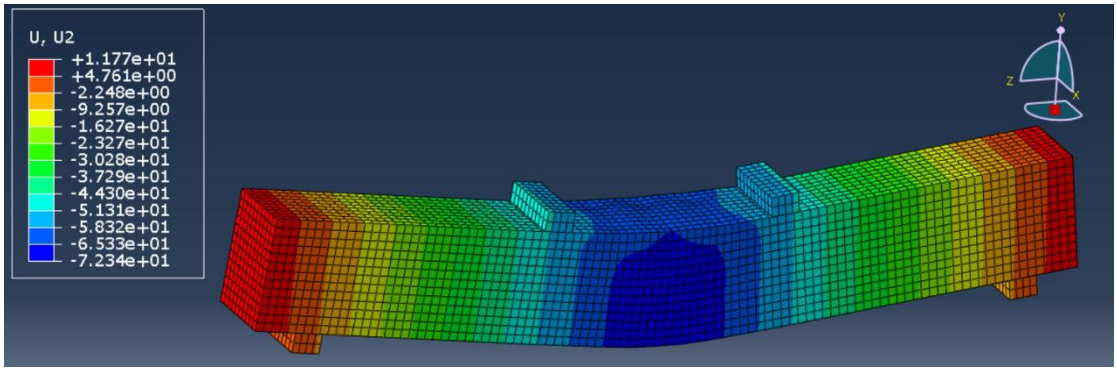

Picture 18: GFRP-450 Model - U2 (Vertical Displacement)

4.5.2.5 Distance = 600 mm

Two phi 20 bars have the total area of 628 mm^2 will be used with distance between the load points equal to 600 mm will give us the following data:

Picture 19: GFRP-600 Model - Load and supports' locations

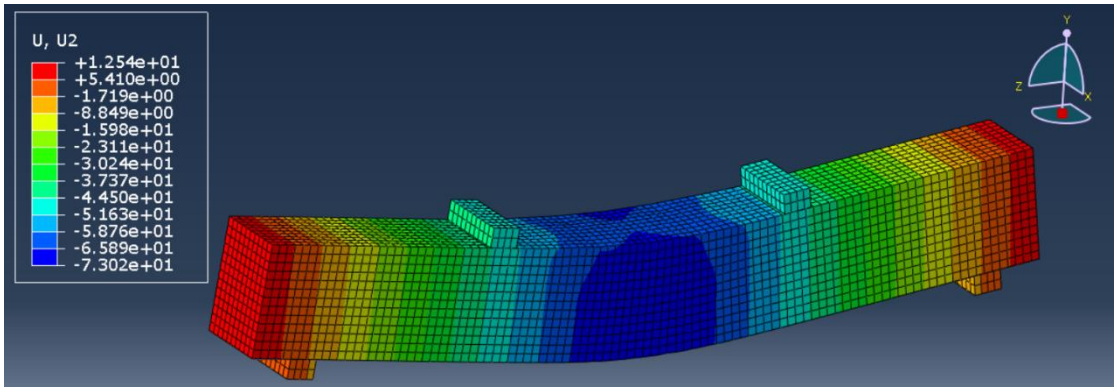

Picture 20: GFRP-600 Model - U2 (Vertical Displacement)

4.5.3 Changing concrete compressive strength (f_c`)

The concrete strength was changed to examine the effect on the whole model strength as follows:

4.5.3.1 Concrete have the compressive strength of 22 MPa

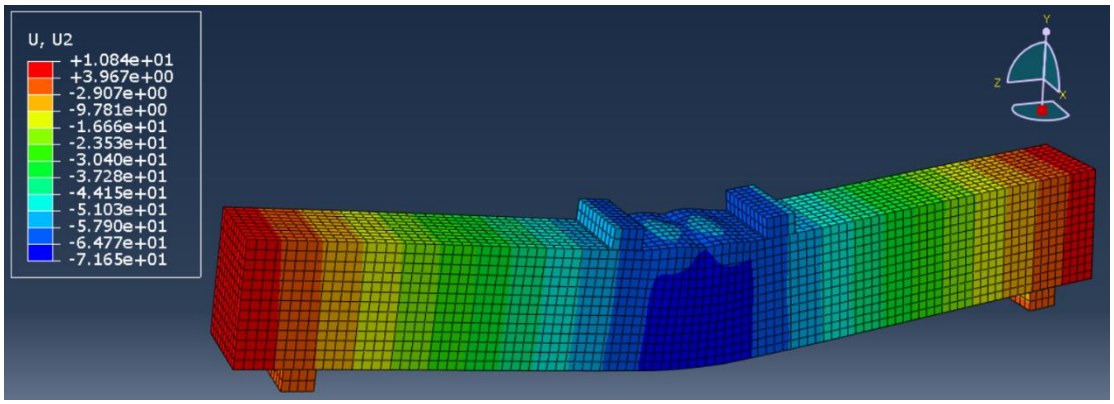

Picture 21: 22MPa-Concrete Model - U2 (Vertical Displacement)

4.5.3.2 Concrete have the compressive strength of 30 MPa

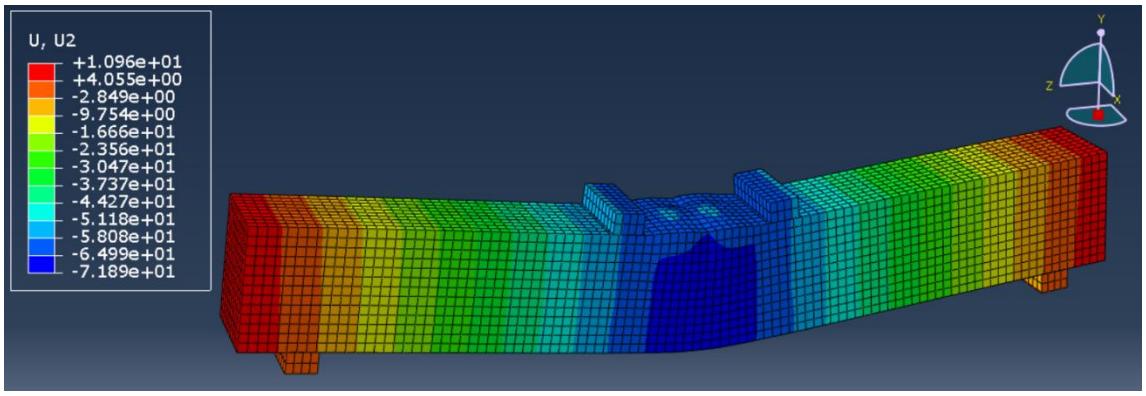

Picture 22: 30MPa-Concrete Model - U2 (Vertical Displacement)

4.5.3.3 Concrete have the compressive strength of 38 MPa

This study is also exactly the same of the original model.

4.5.3.4 Concrete have the compressive strength of 46 MPa

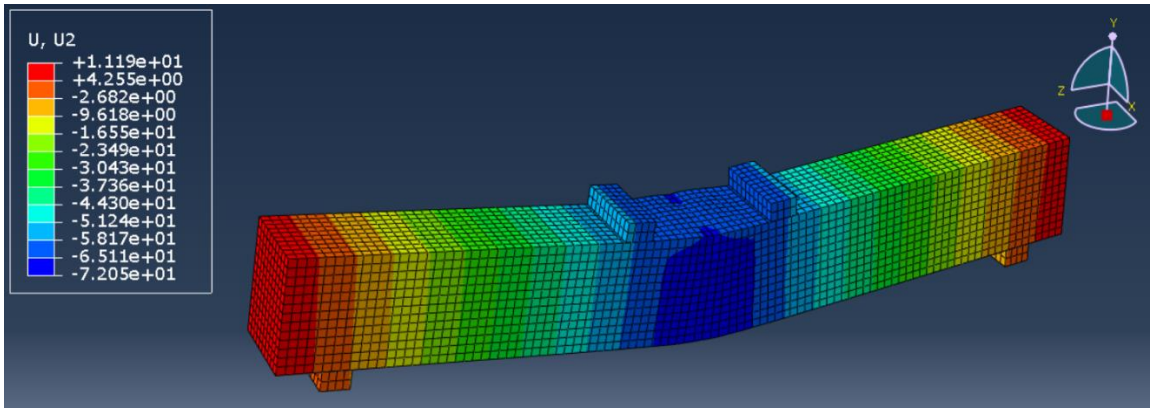

Picture 23: 46MPa-Concrete Model - U2 (Vertical Displacement)

4.5.3.5 Concrete have the compressive strength of 54 MPa

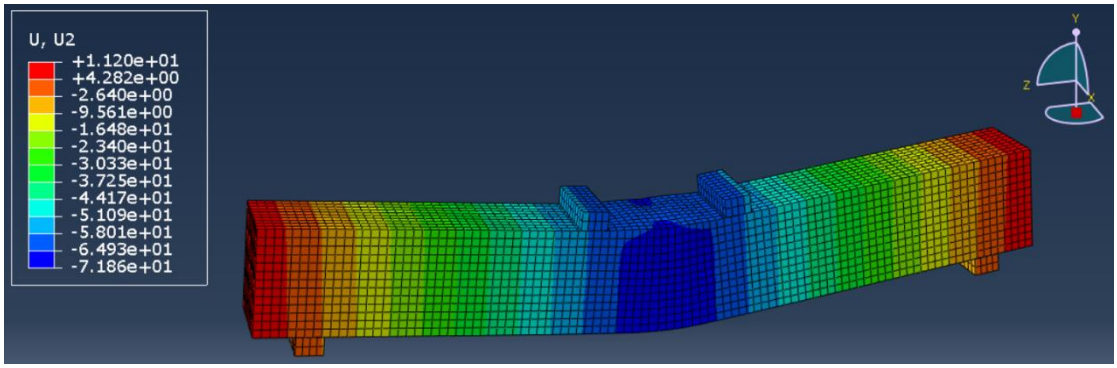

Picture 24: 54MPa-Concrete Model - U2 (Vertical Displacement)

Chapter 5: Results

5.1 Damage in tension

In this section, damaget (Tension Damage) will be shown for all models studied.

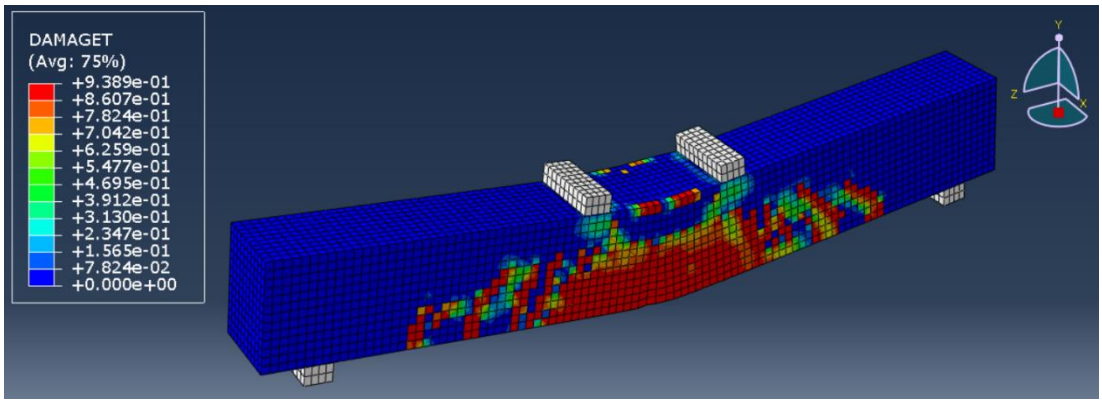

Picture 25: GFRP-Phi16 Model - Tension Damage

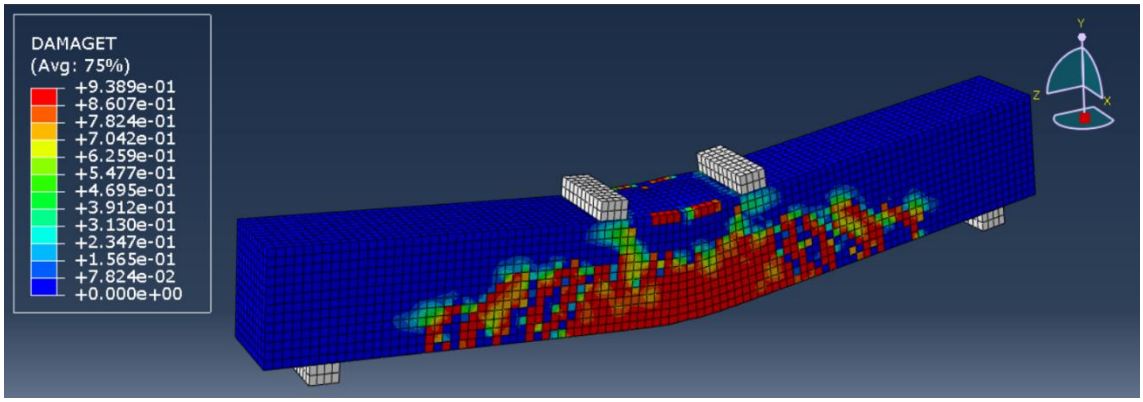

Picture 26: GFRP-Phi18 Model - Tension Damage

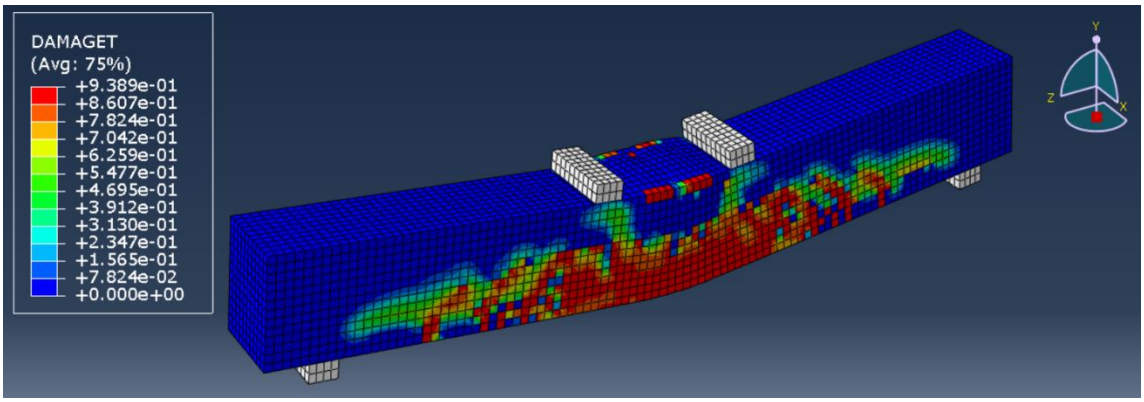

Picture 27: GFRP-Phi22 Model - Tension Damage

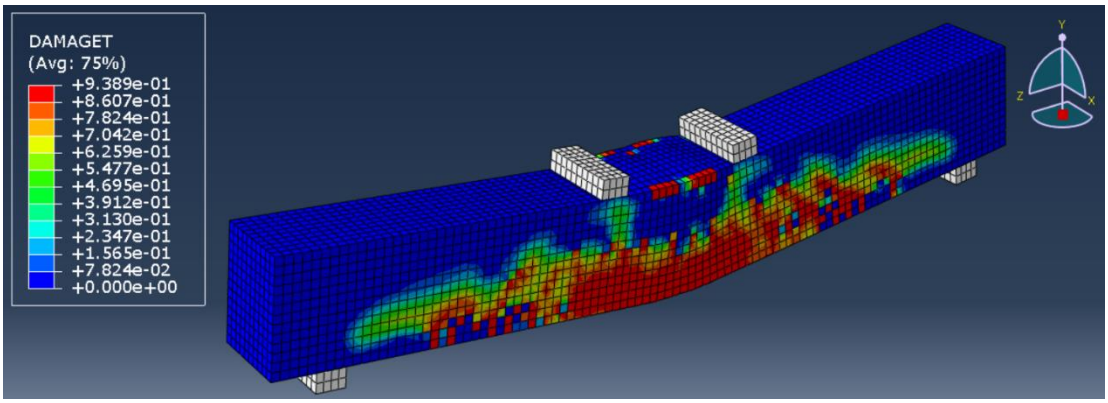

Picture 28: GFRP-Phi24 Model - Tension Damage

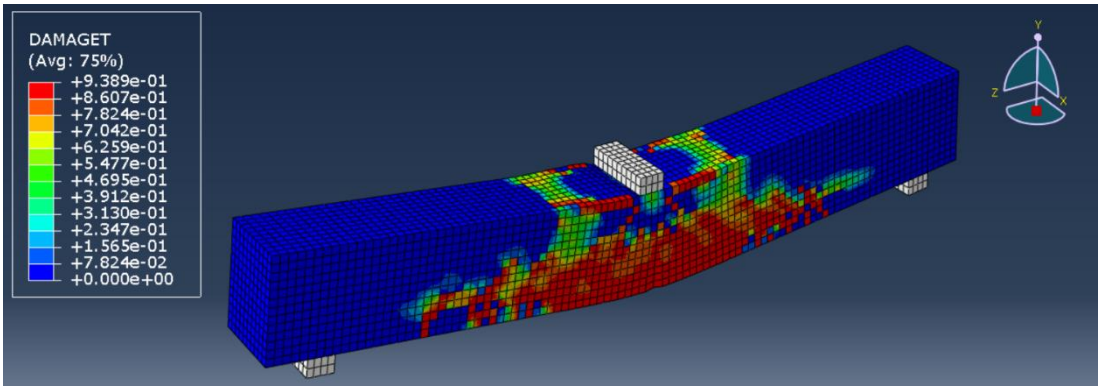

Picture 29: GFRP-0 Model - Tension Damage

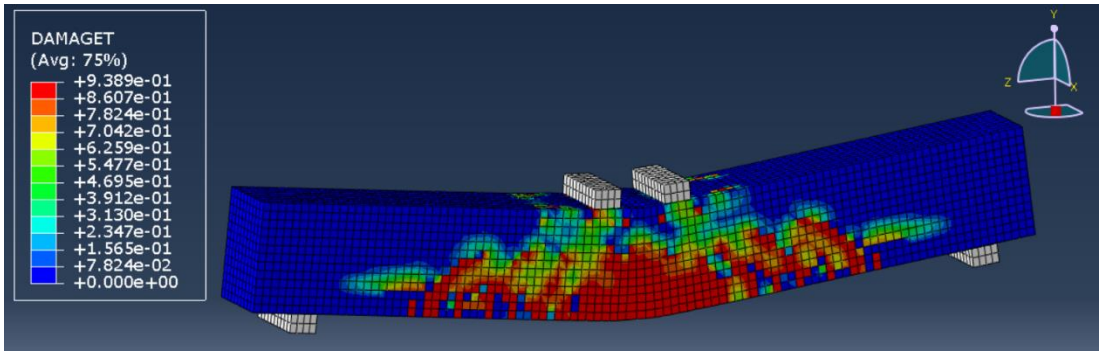

Picture 30: GFRP-150 Model - Tension Damage

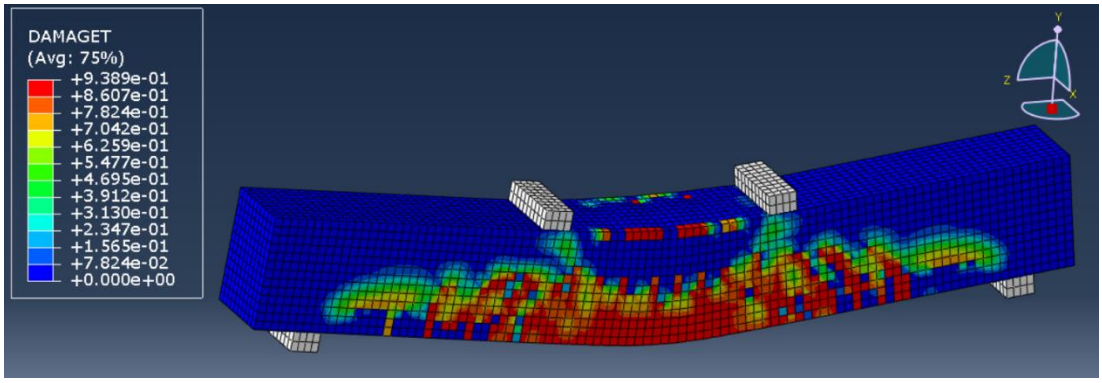

Picture 31: GFRP-450 Model - Tension Damage

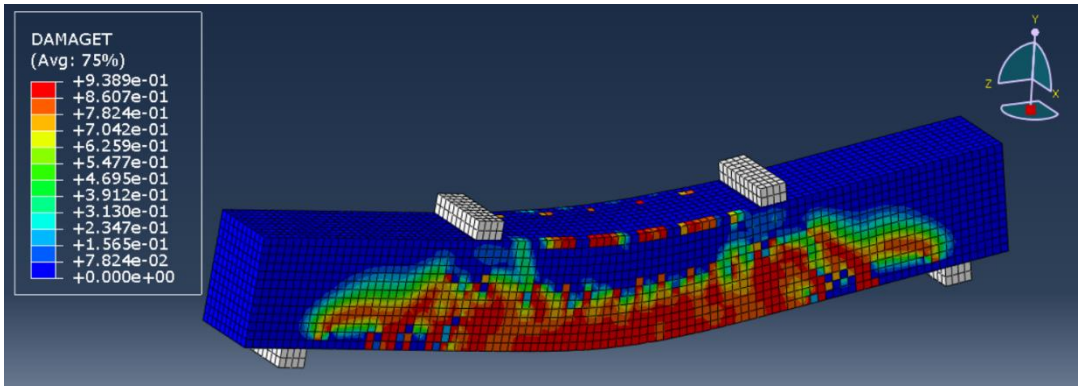

Picture 32: GFRP-600 Model - Tension Damage

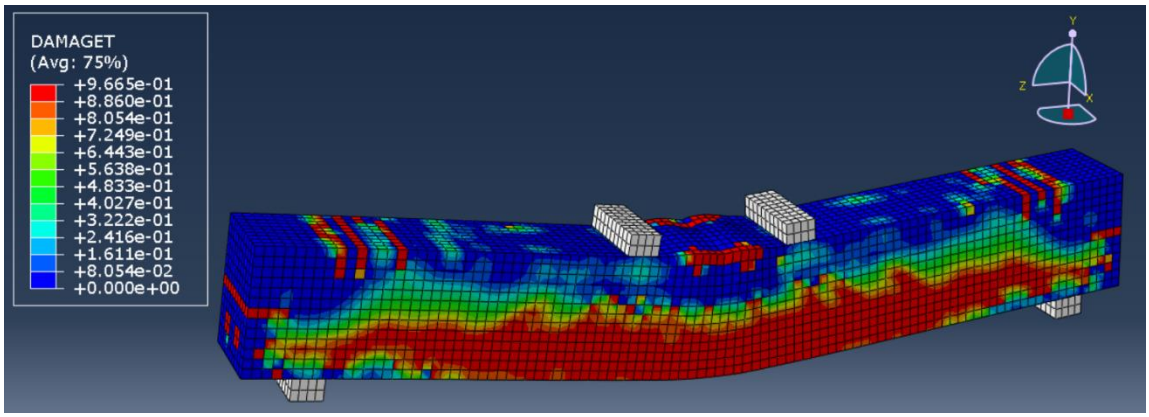

Picture 33: 22MPa-Concrete Model - Tension Damage

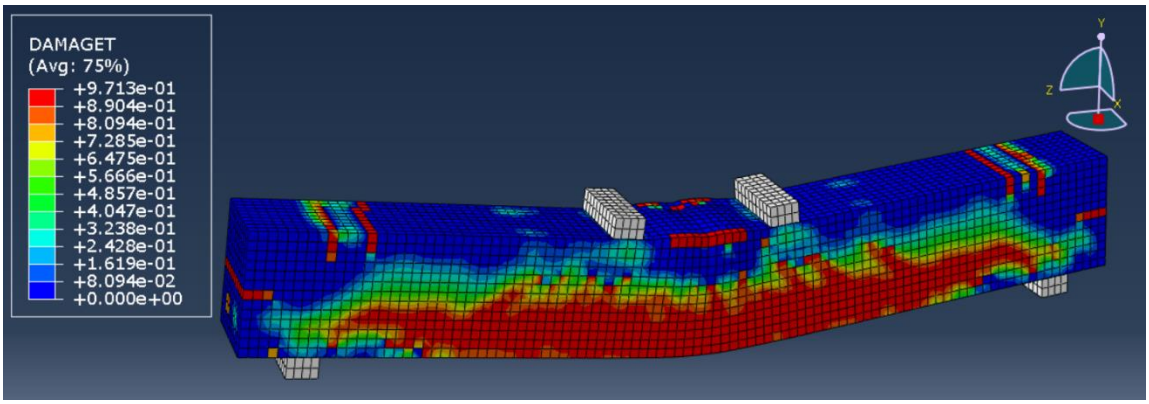

Picture 34: 30MPa-Concrete Model - Tension Damage

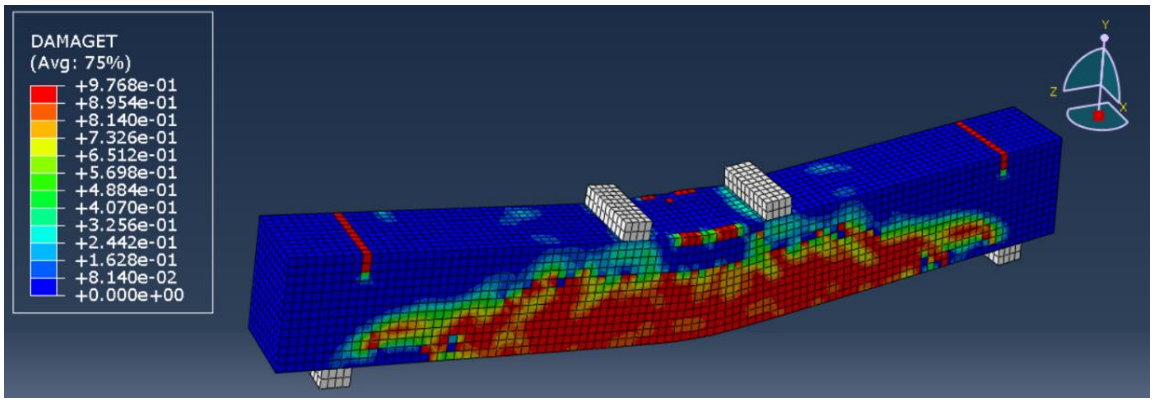

Picture 35: 46MPa-Concrete Model - Tension Damage

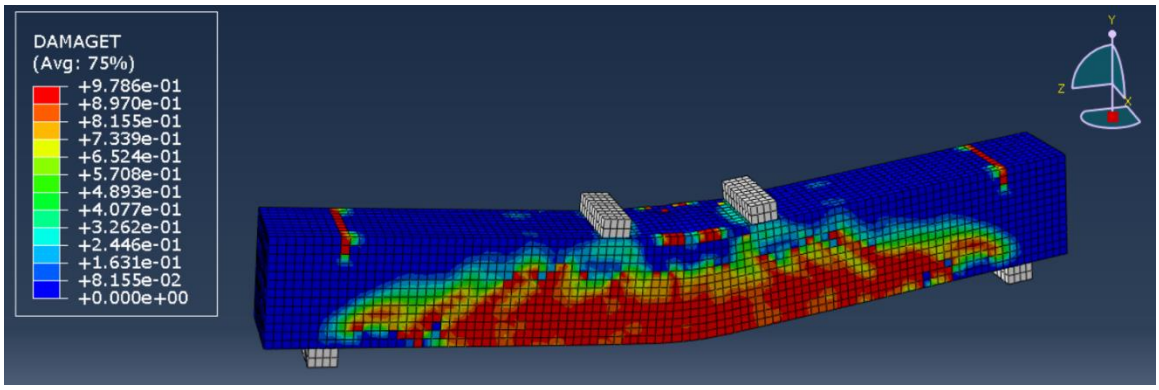

Picture 36: 54MPa-Concrete Model - Tension Damage

5.2 Damage in compression

In this section, damage c (Compression Damage) will be shown for all models studied.

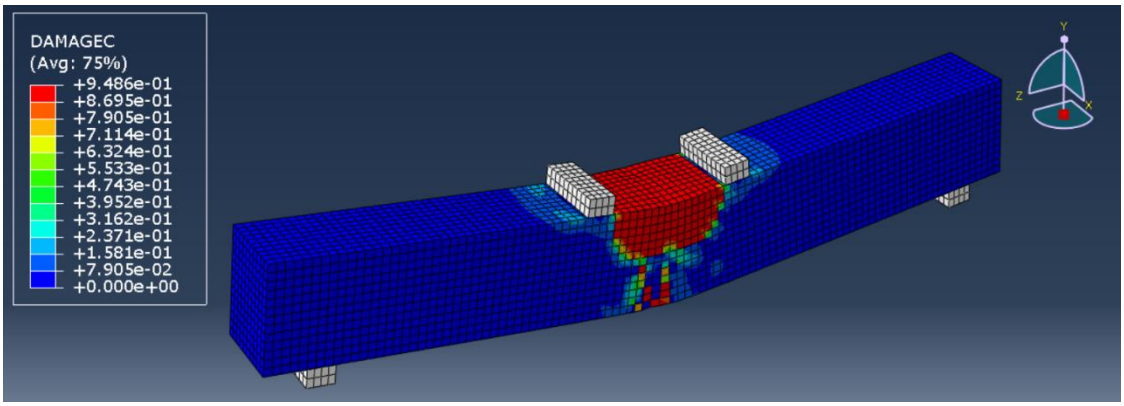

Picture 37: GFRP-Phi16 Model - Compression Damage

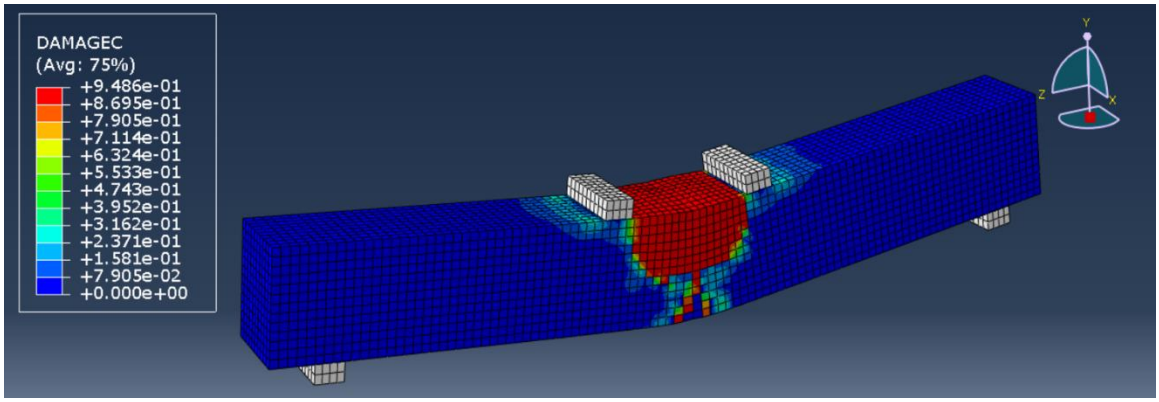

Picture 38: GFRP-Phi18 Model - Compression Damage

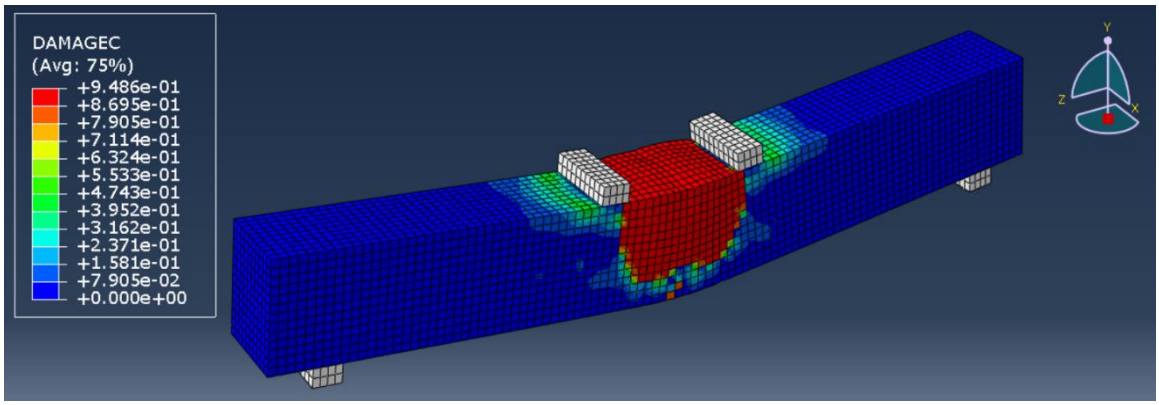

Picture 39: GFRP-Phi22 Model - Compression Damage

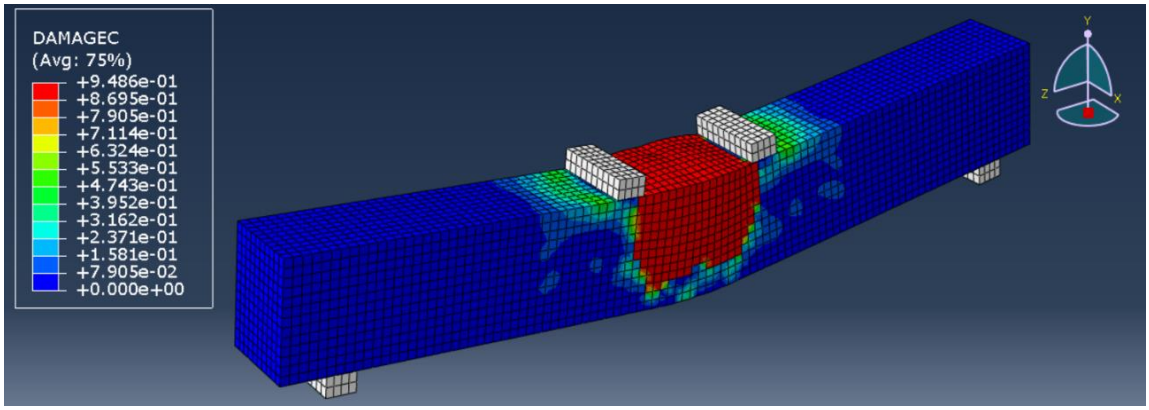

Picture 40: GFRP-Phi24 Model - Compression Damage

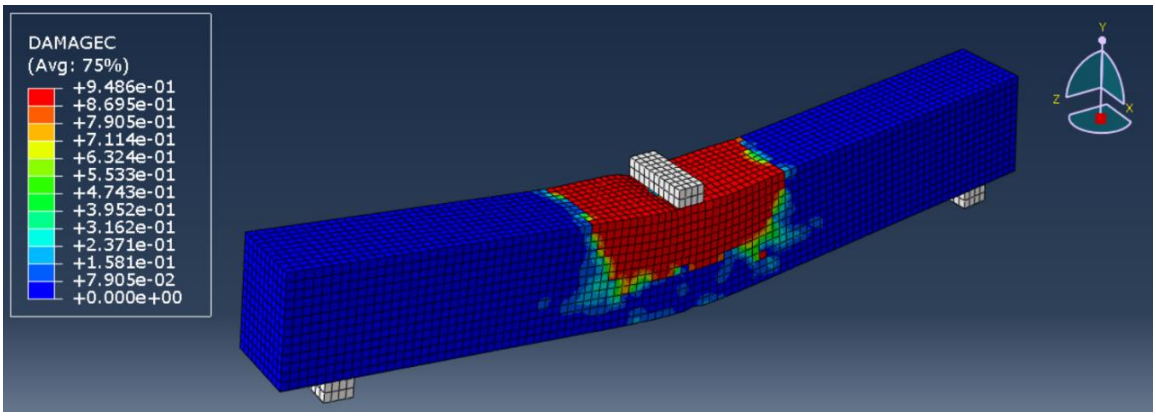

Picture 41: GFRP-0 Model - Compression Damage

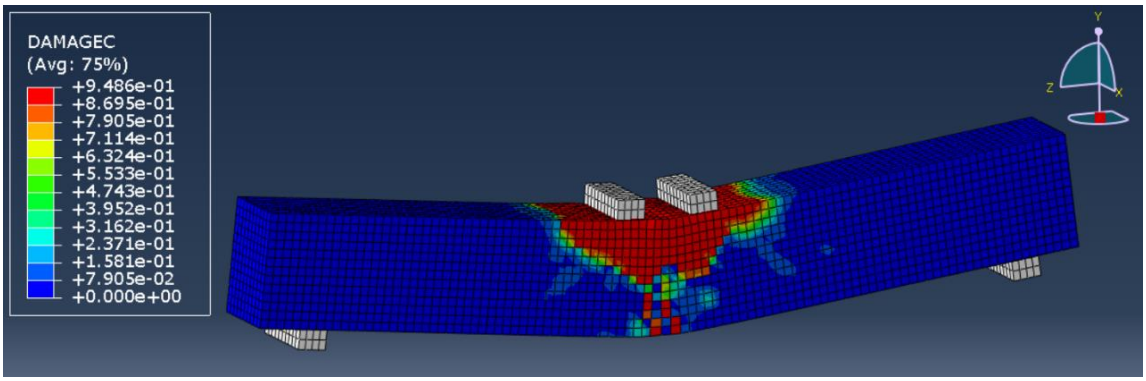

Picture 42: GFRP-150 Model - Compression Damage

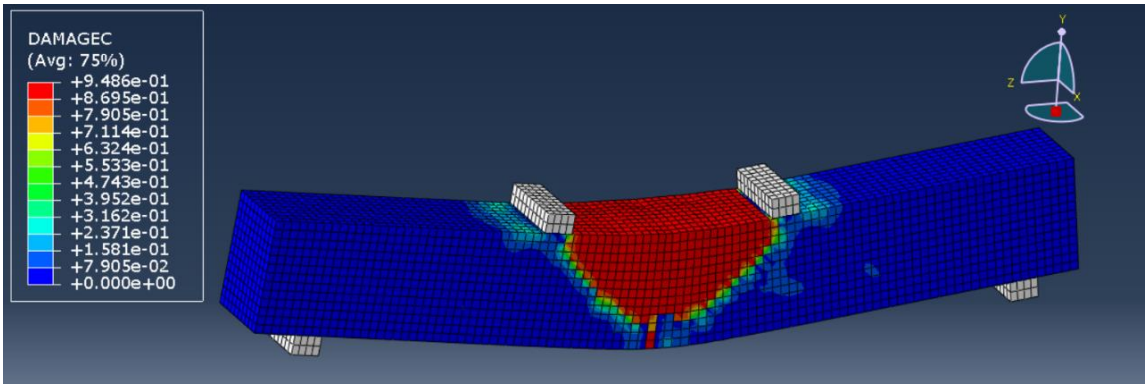

Picture 43: GFRP-450 Model - Compression Damage

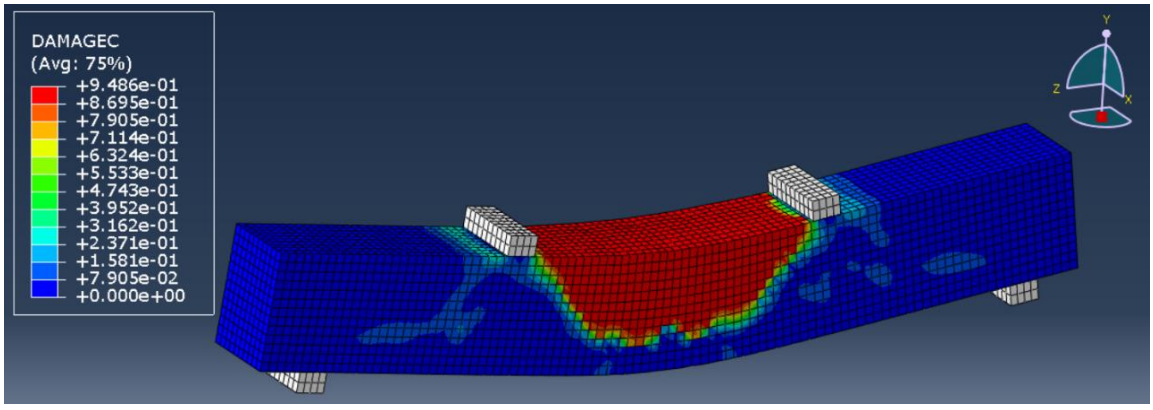

Picture 44: GFRP-600 Model - Compression Damage

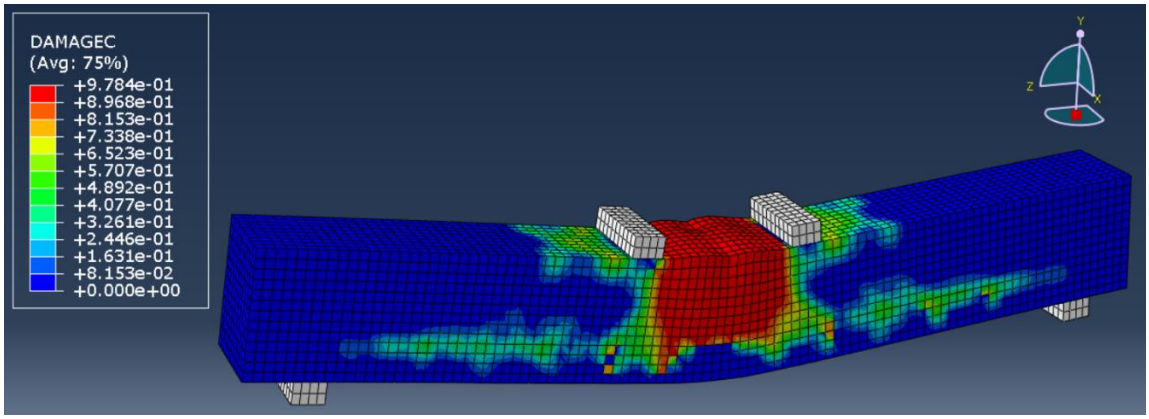

Picture 45: 22MPa-Concrete Model - Compression Damage

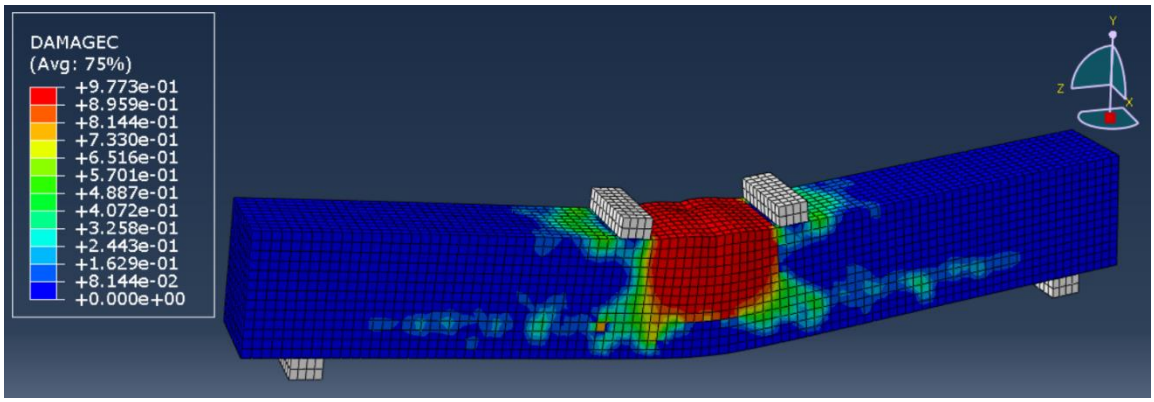

Picture 46: 30MPa-Concrete Model - Compression Damage

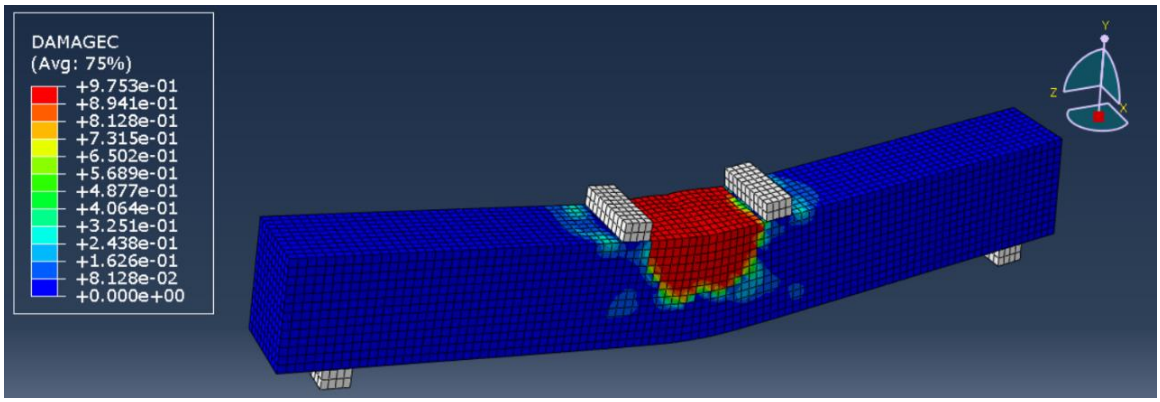

Picture 47: 46MPa-Concrete Model - Compression Damage

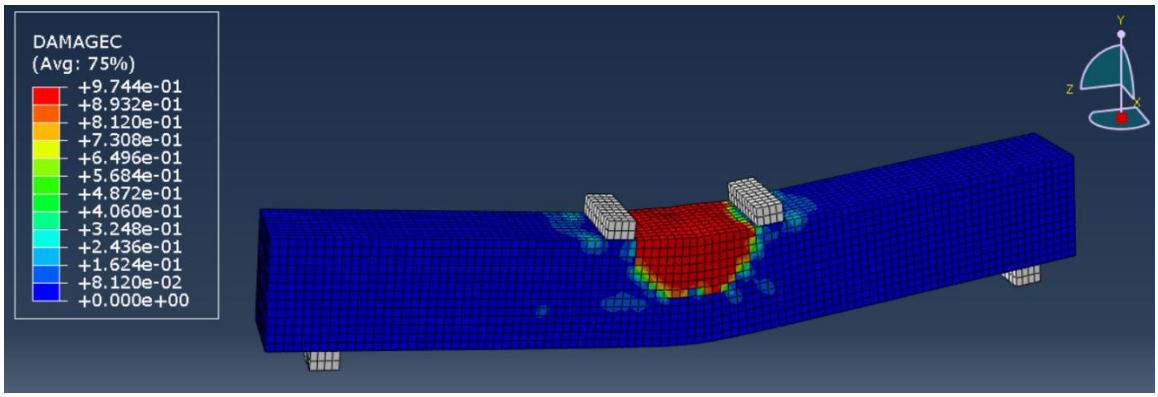

Picture 48: 54MPa-Concrete Model - Compression Damage

5.3 Reinforcement normal stress

In this section, reinforcement normal stresses will be shown for all models studied.

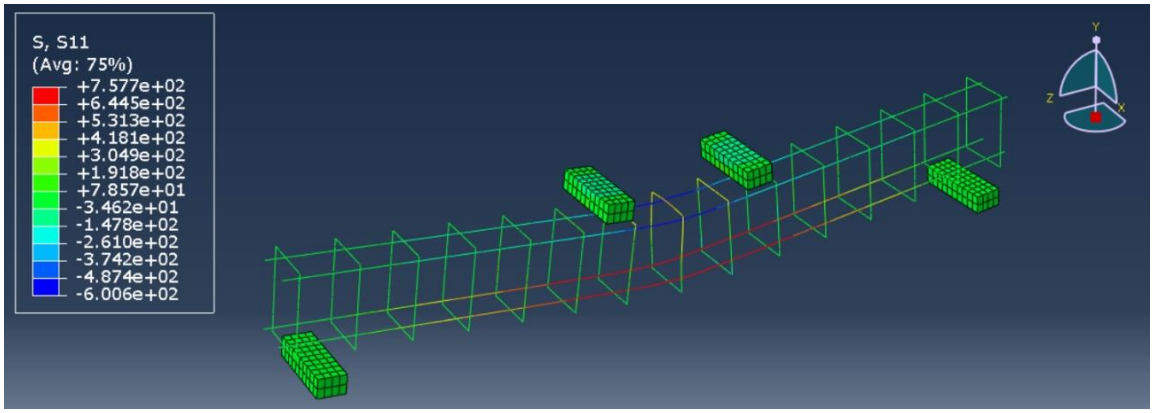

Picture 49: GFRP-Phi16 Model - Reinforcement Normal Stress

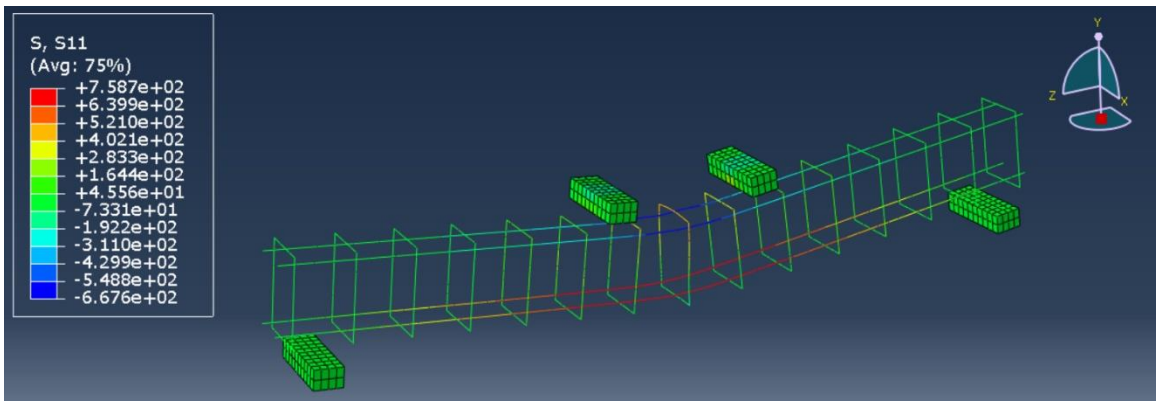

Picture 50: GFRP-Phi18 Model - Reinforcement Normal Stress

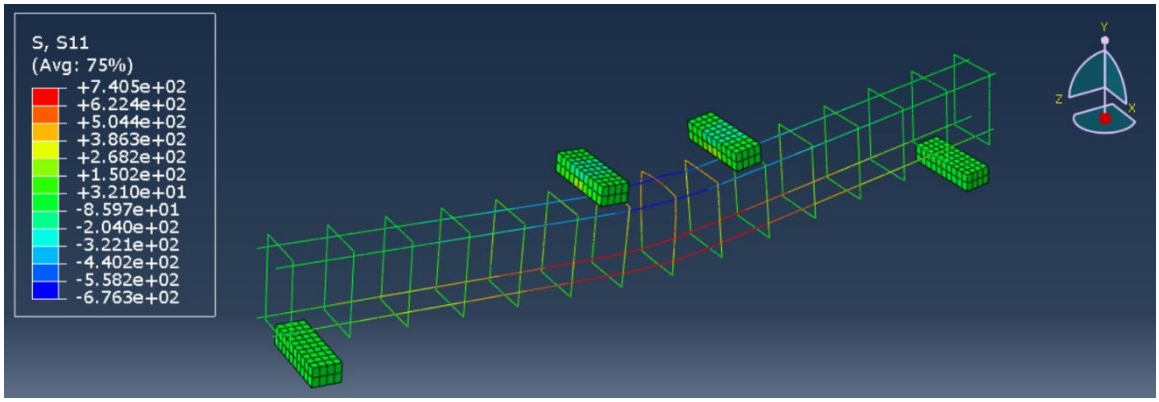

Picture 51: GFRP-Phi22 Model - Reinforcement Normal Stress

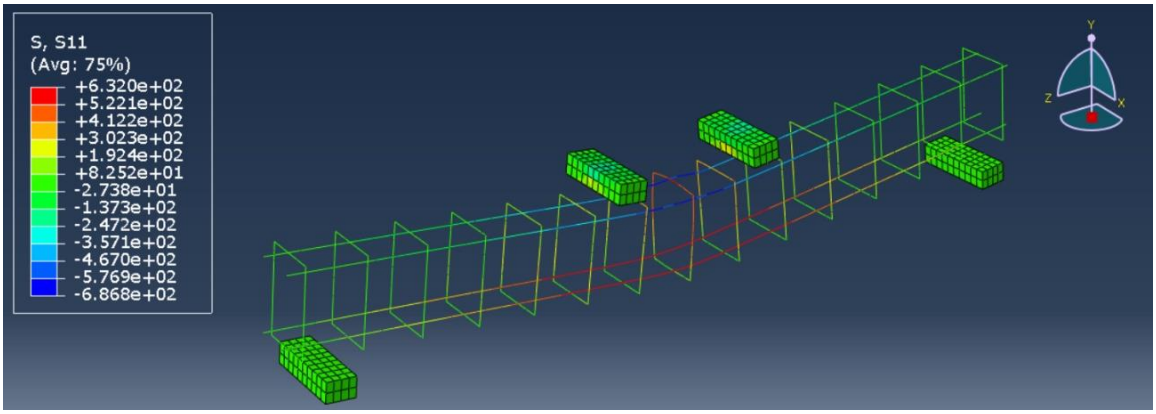

Picture 52: GFRP-Phi24 Model - Reinforcement Normal Stress

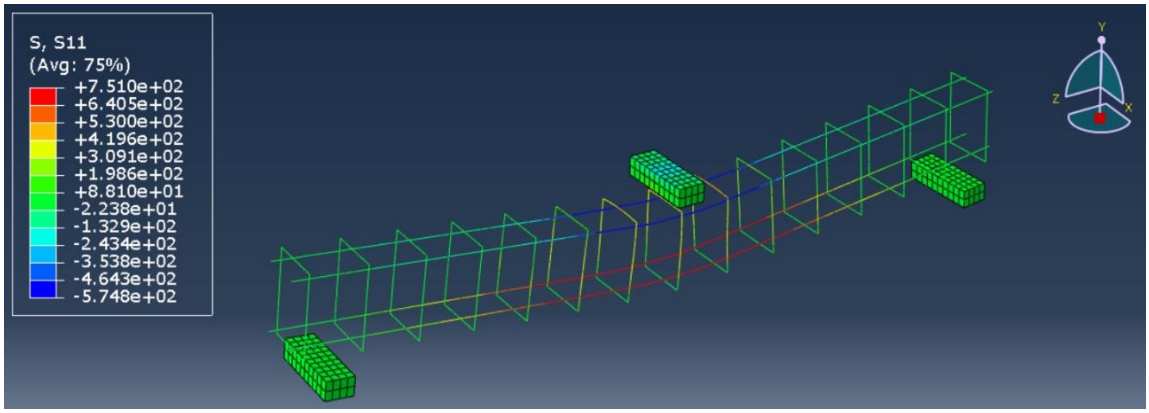

Picture 53: GFRP-0 Model - Reinforcement Normal Stress

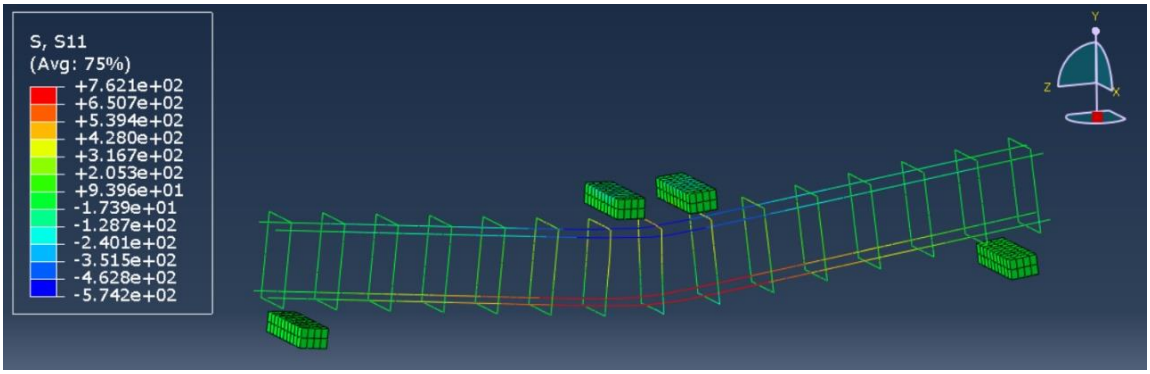

Picture 54: GFRP-150 Model - Reinforcement Normal Stress

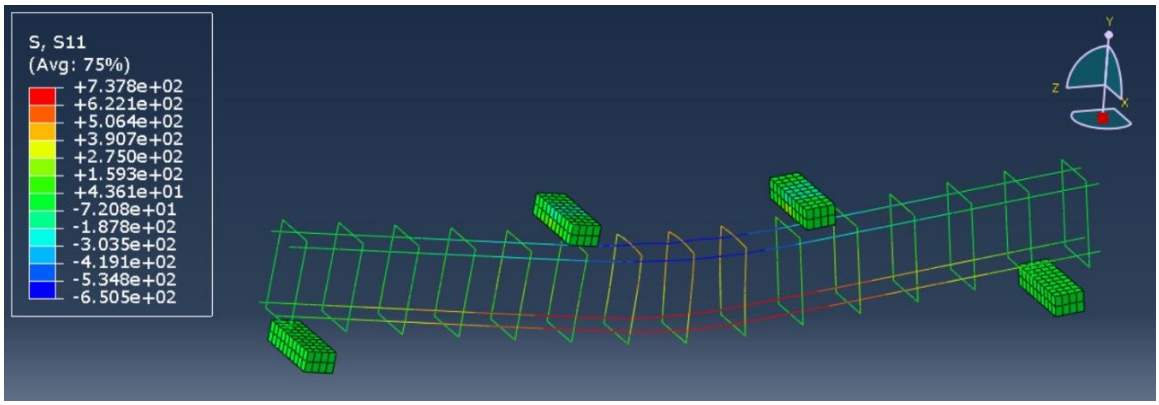

Picture 55: GFRP-450 Model - Reinforcement Normal Stress

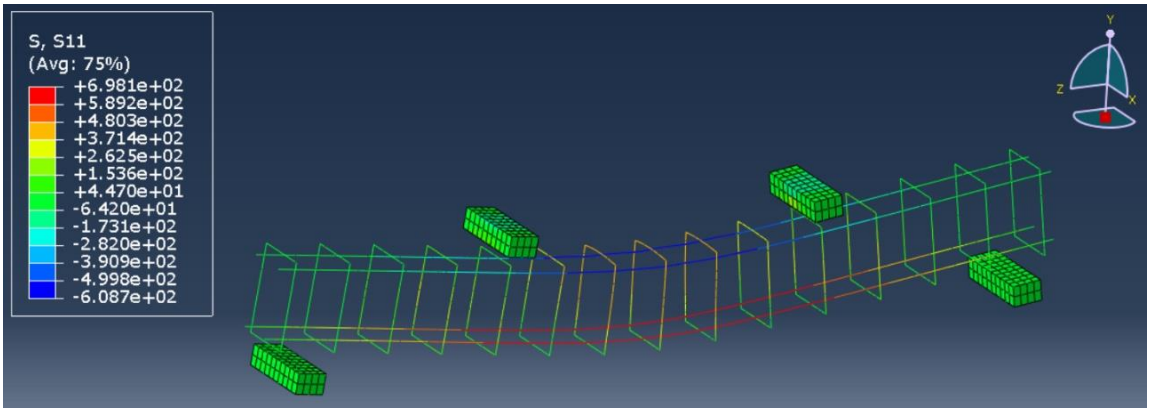

Picture 56: GFRP-600 Model - Reinforcement Normal Stress

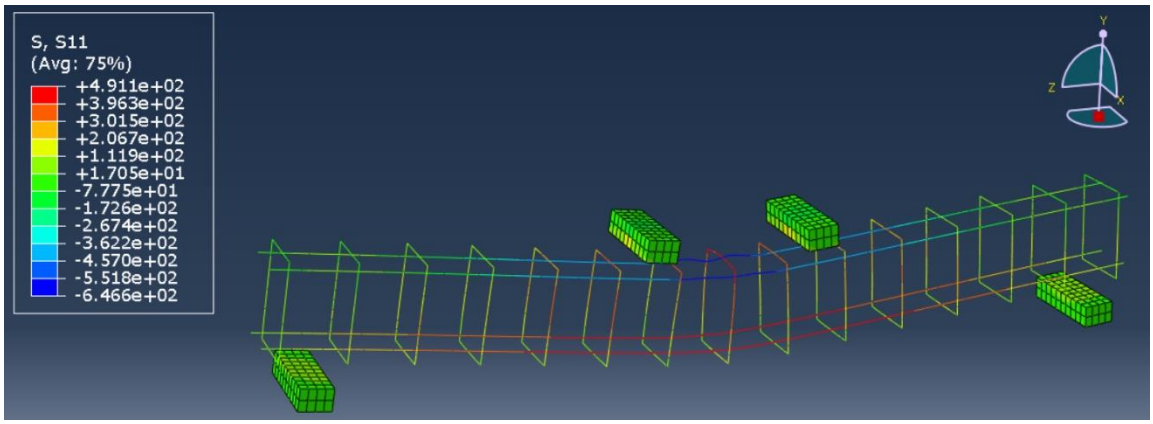

Picture 57: 22MPa-Concrete Model - Reinforcement Normal Stress

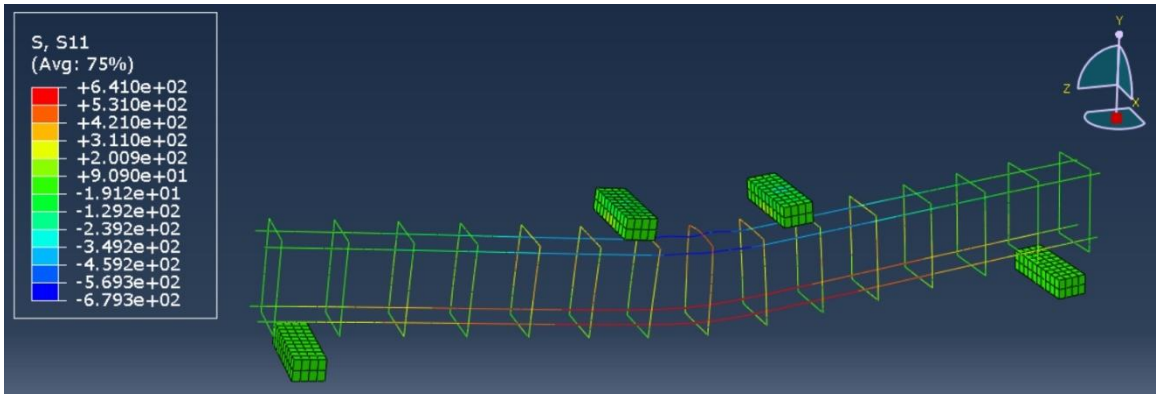

Picture 58: 30MPa-Concrete Model - Reinforcement Normal Stress

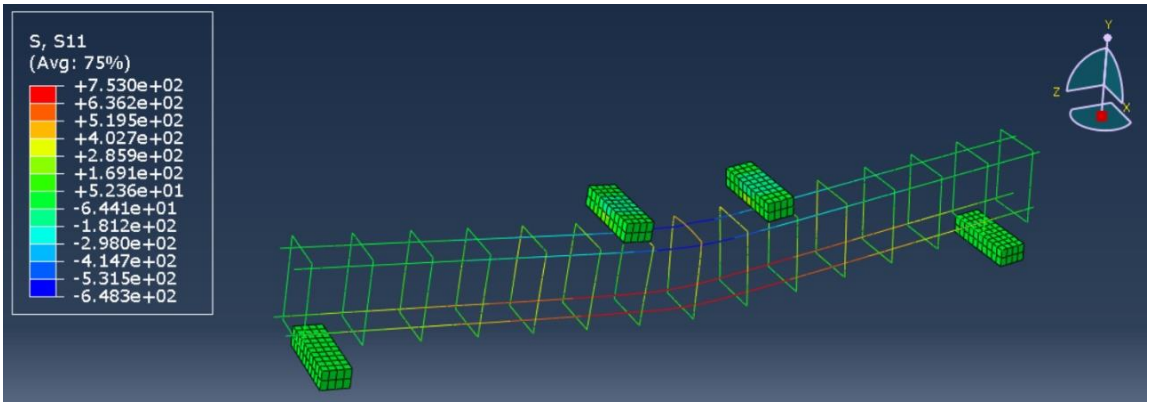

Picture 59: 46MPa-Concrete Model - Reinforcement Normal Stress

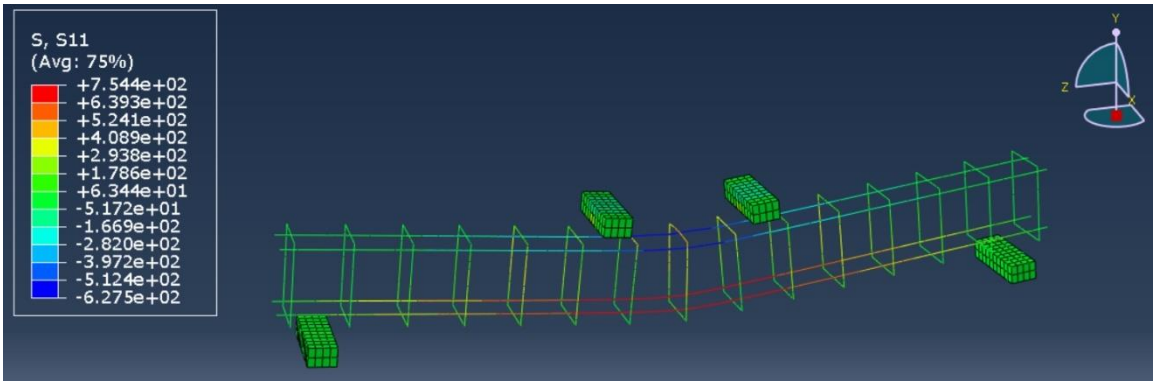

Picture 60: 54MPa-Concrete Model - Reinforcement Normal Stress

5.4 Load-Displacement curve

In this section, load-displacement curves will be shown for all models studied.

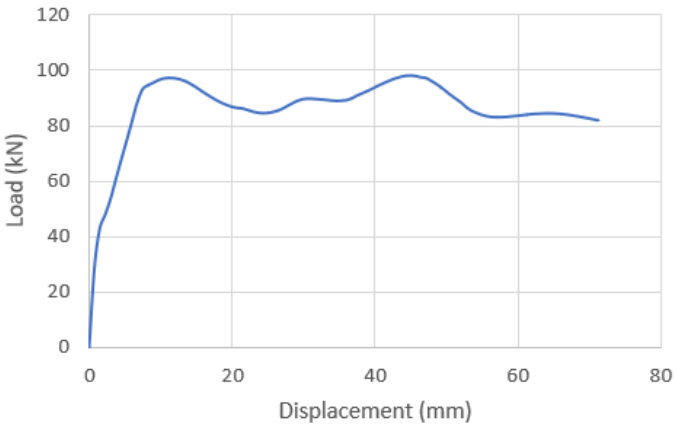

Figure 29: Load-Displacement curve for GFRP-Phi16 Model

As can be seen in the figure above, the local maximum load capacity was 97 kN at a midspan displacement of 11.2 mm. And an absolute maximum load capacity of 97.85 kN at a midspan displacement of 45 mm.

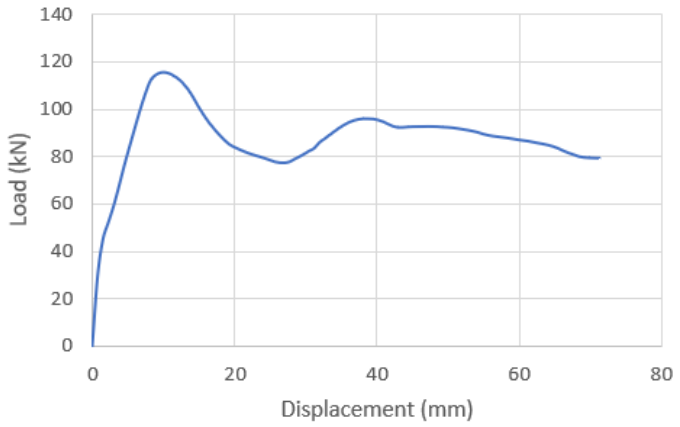

Figure 30: Load-Displacement curve for GFRP-Phi18 Model

As can be seen in the figure above, the absolute maximum load capacity was 115.3 kN at a midspan displacement of 9.7 mm. And a local maximum load capacity of 95.83 kN at a midspan displacement of 38.1 mm.

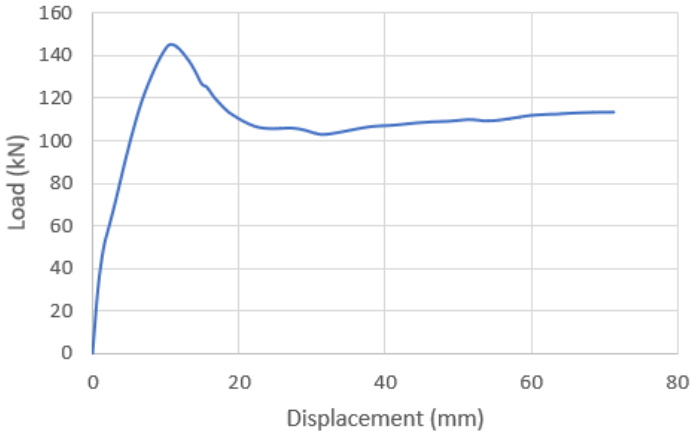

Figure 31: Load-Displacement curve for GFRP-Phi22 Model

Based on the figure above, the maximum load capacity was 144.75 kN at a midspan displacement of 10.4 mm.

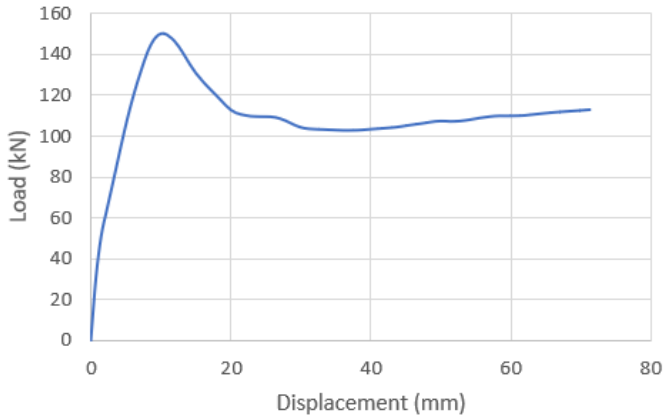

Figure 32: Load-Displacement curve for GFRP-Phi24 Model

The figure above shows the maximum load capacity was 150.3 kN at a midspan displacement of 10.4 mm.

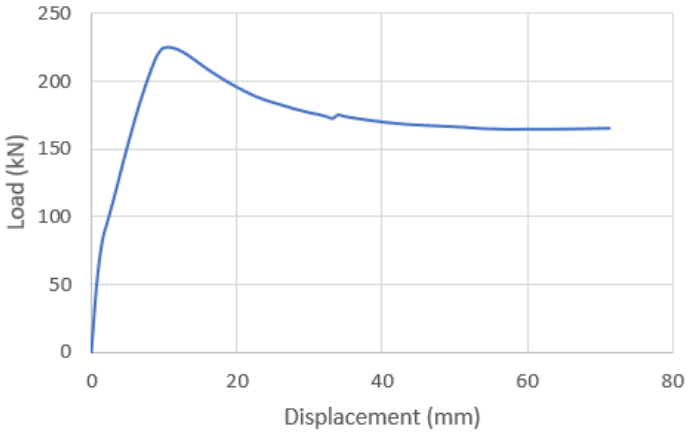

Figure 33: Load-Displacement curve for GFRP-0 Model

As can be seen in the figure above, the maximum load capacity was 225 kN at a midspan displacement of 10.4 mm.

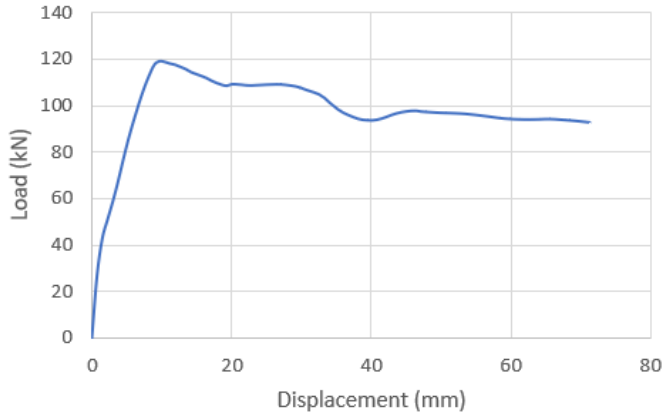

Figure 34: Load-Displacement curve for GFRP-150 Model

In the figure above, the maximum load capacity was 119.375 kN at a midspan displacement of 9.7 mm.

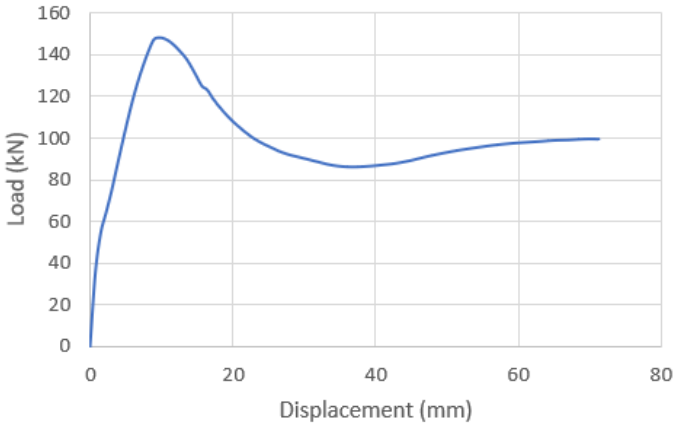

Figure 35: Load-Displacement curve for GFRP-450 Model

As shown in the figure above, the maximum load capacity was 148.3 kN at a midspan displacement of 9.7 mm.

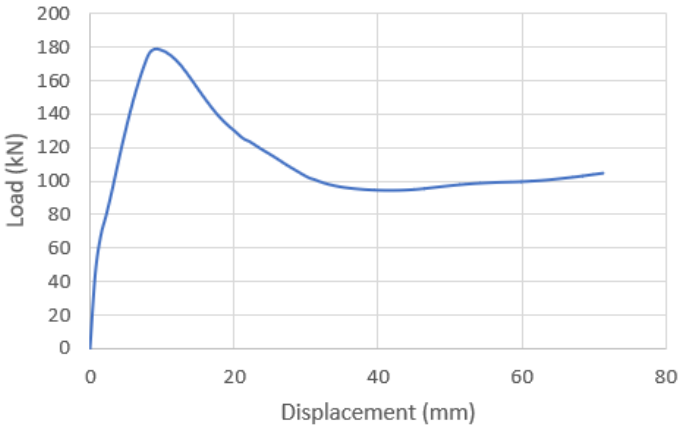

Figure 36: Load-Displacement curve for GFRP-600 Model

As presented in the figure above, the maximum load capacity was 178.65 kN at a midspan displacement of 10.4 mm.

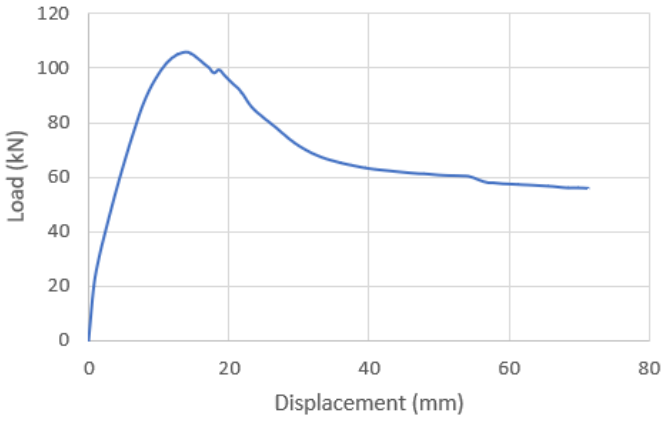

Figure 37: Load-Displacement curve for 22MPa-Concrete Model

As presented in the figure above, the maximum load capacity was 105.95 kN at a midspan displacement of 14.2 mm.

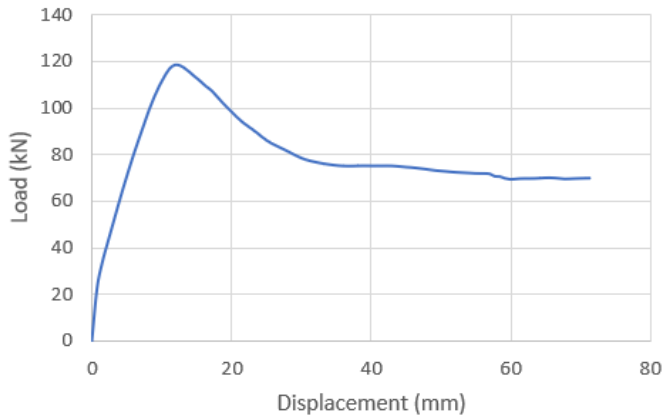

Figure 38: Load-Displacement curve for 30MPa-Concrete Model

As presented in the figure above, the maximum load capacity was 118.83 kN at a midspan displacement of 11.9 mm.

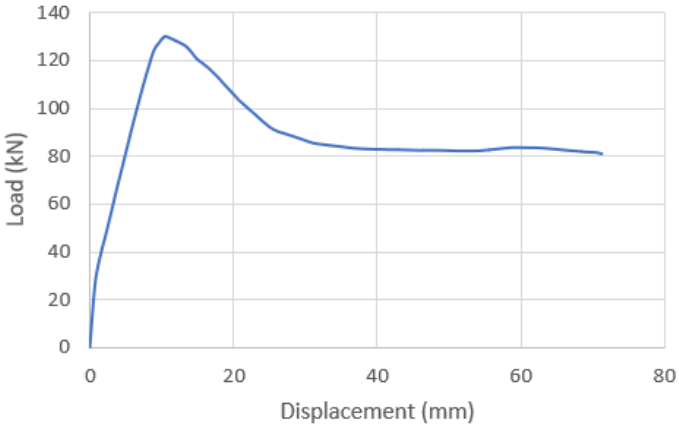

Figure 39: Load-Displacement curve for 46MPa-Concrete Model

As presented in the figure above, the maximum load capacity was 130.24 kN at a midspan displacement of 10.4 mm.

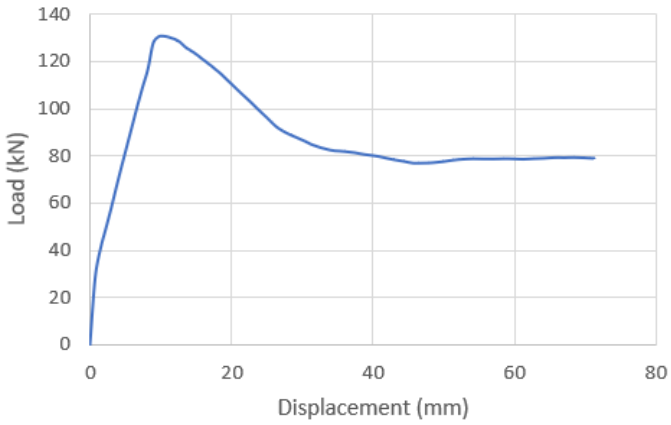

Figure 40: Load-Displacement curve for 54MPa-Concrete Model

As presented in the figure above, the maximum load capacity was 130.63 kN at a midspan displacement of 10.4 mm.

5.5 Groups Load-Displacement curves

5.5.1 Changing the area of GFRP bars

The GFRP bars applied for resisting tension force were having different sizes as following:

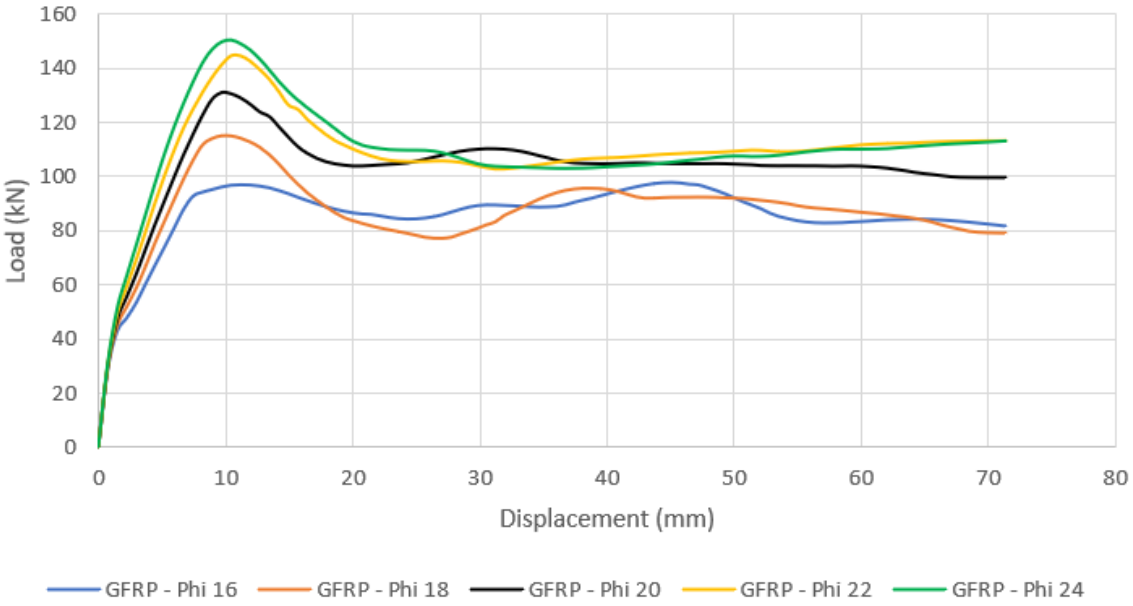

Figure 41: Load-Displacement Curves for Different GFRP Bars' sizes

As can be noticed in the figure above, when increasing the GFRP bar area, a higher value for the maximum load capacity is obtained while maintaining this capacity at a displacement from 9.5 to 11 mm.

5.5.2 Changing distances between Loads

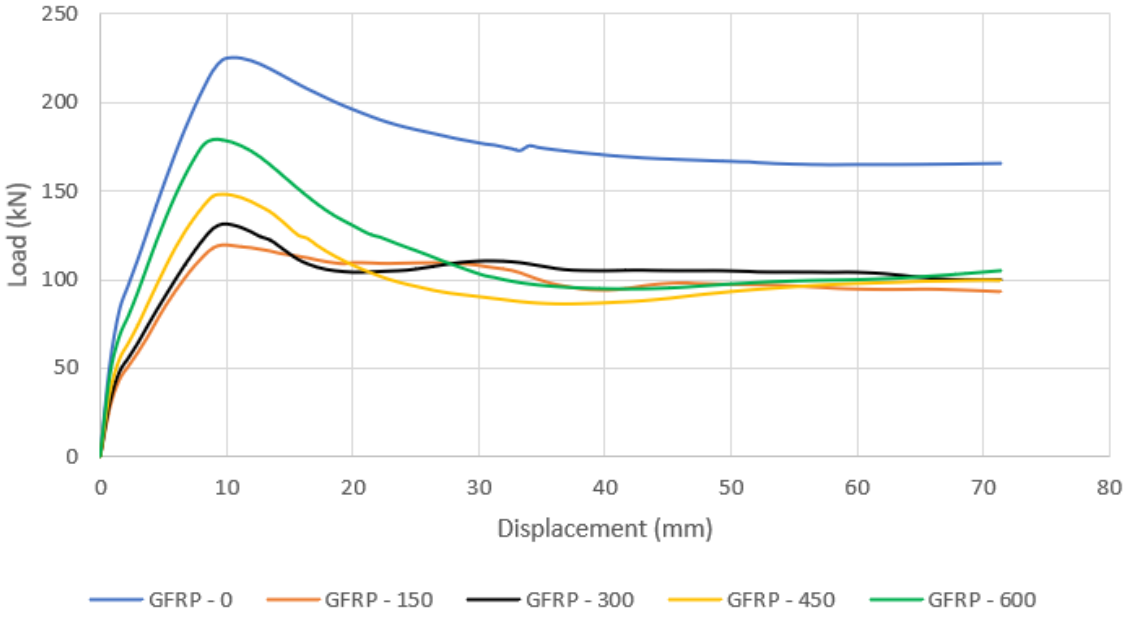

Figure 42: Load-Displacement Curves for Different Distances between Point Loads

As illustrated in the figure above, applying one load point on the beam will result in a noticeable high load capacity can be resisted. For the case of applying two-point loads, increasing the distance between these two points results in increasing the load capacity.

5.5.3 Changing concrete compressive strength (fc`)

The GFRP bars and loads applied on beams having different compressive strength as following:

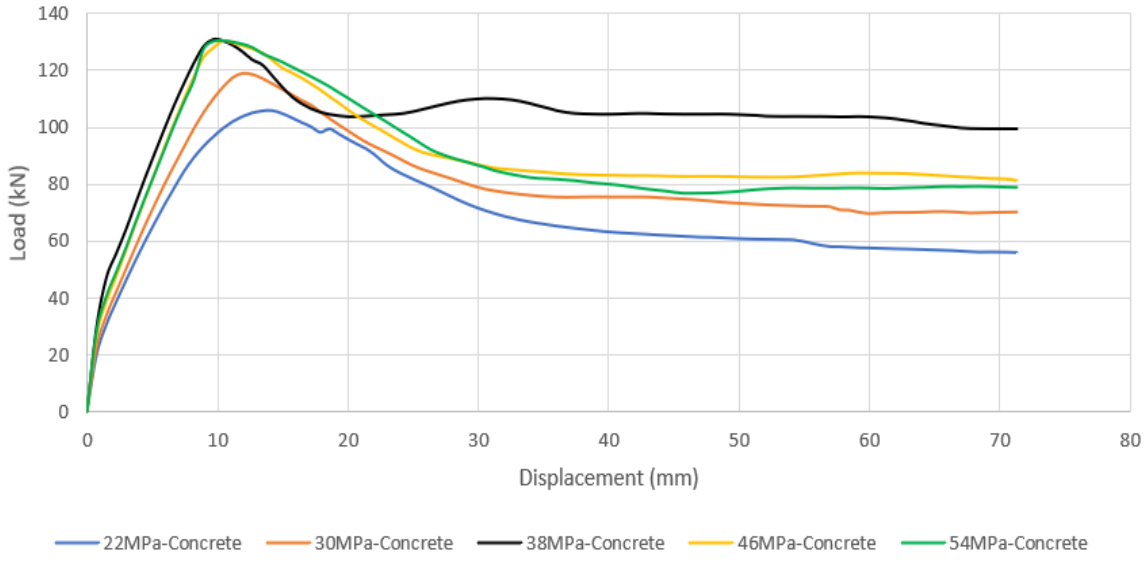

Figure 43: Load-Displacement Curves for Different Concrete Compressive Strength

As shown above, the maximum load strength is about 130 kN at the midspan displacement of 10 mm approximately as in 38, 46, and 54 MPa concrete. 22 and 30 MPa concrete were resulting in lower strength. It is so important to highlight that 38 MPa concrete results in a higher load strength when the midspan displacement exceeds 25 mm comparing with the other concrete strength.

5.5.4 Whole study

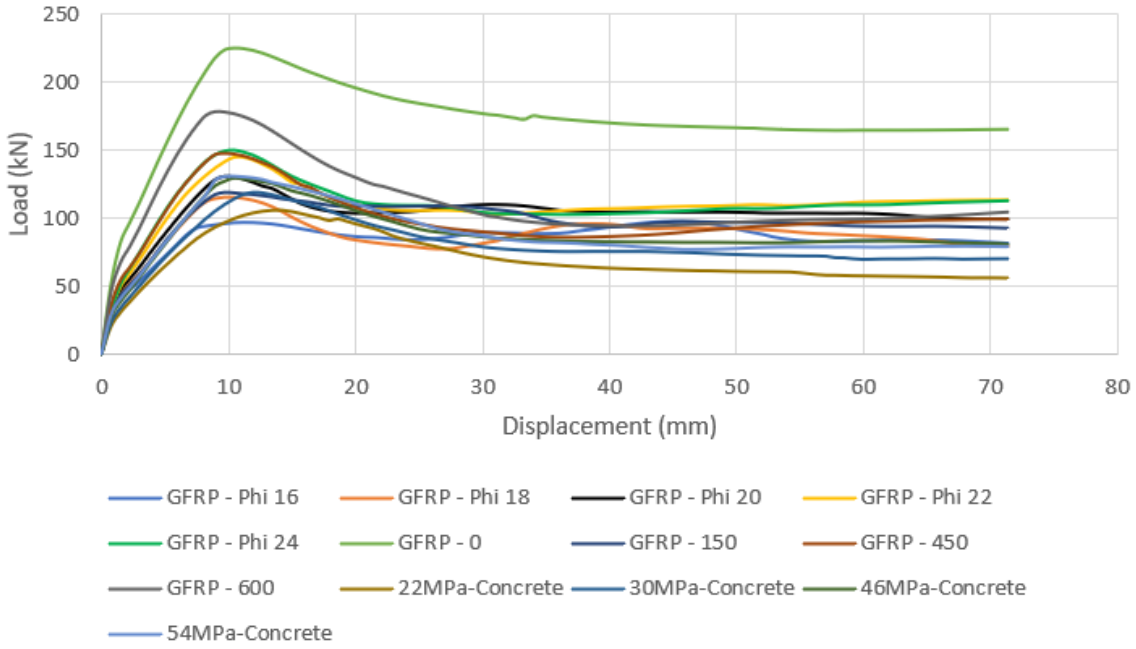

Figure 44: Load-Displacement Curves for all models

Comparing the results for fixing the GFRP bars to phi 16 and changing the distance between loads with the results got from fixing the distance between loads to 300 mm and changing the GFRP bars' areas, it can be concluded that the most two load capacities were obtained from fixing the GFRP area with changing the distance between loads to 0 mm - only one point load applied- and 600 mm respectively. Then, two near results, which are GFRP-Phi24 and GFRP-450, were obtained. The least load capacity obtained from fixing the distance between loads to 300 mm and changing the GFRP bars to Phi16.

Chapter 6: Conclusion

From models and figures in previous chapters, this study can be concluded in the following points:

- GFRP can be used instead of the steel tension reinforcement to gain higher strength while decreasing the whole structure's weight.
- GFRP reinforcement percentage (GFRP diameter) is directly proportional to the load capacity.
- Applying one point load on the middle of the beam results in increasing the load strength of the beam comparing to applying two-point load.
- Two-point load showed an increment in the load strength of the beam when increasing the distance between these two points.
- GFRP is better to be used when the concrete has higher compressive strength. Low compressive strength of the concrete can vanish the advantages of using GFRP.

Chapter 7: References

Abdalla, H.A., 2002. Evaluation of deflection in concrete members reinforced with fibre reinforced polymer (FRP) bars. Composite Structures 56, 63–71. https://doi.org/10.1016/S0263-8223(01)00188-X

Abdelkarim, O.I., Ahmed, E.A., Mohamed, H.M., Benmokrane, B., 2019. Flexural strength and serviceability evaluation of concrete beams reinforced with deformed GFRP bars. Engineering Structures 186, 282–296. https://doi.org/10.1016/j.engstruct.2019.02.024

Adhikari, S., 2009. Mechanical properties and flexural applications of basalt fiber reinforced polymer (BFRP) bars.

Ahmed, E.A., Benmokrane, B., Sansfaçon, M., 2017. Case Study: Design, Construction, and Performance of the La Chancelière Parking Garage's Concrete Flat Slabs Reinforced with GFRP Bars. J. Compos. Constr. 21, 05016001. https://doi.org/10.1061/(ASCE)CC.1943-5614.0000656

Aiello, M.A., Ombres, L., 2000. Load-Deflection Analysis of FRP Reinforced Concrete Flexural Members. J. Compos. Constr. 4, 164–171. https://doi.org/10.1061/(ASCE)1090-0268(2000)4:4(164)

Alsalihi, M.A.J., 2014. Mechanical Properties of Glass Fiber Reinforced Polymer Bars After Exposure to Elevated Temperatures 177.

Al-Sunna, R.A.S., 2006. Deflection behaviour of FRP reinforced concrete flexural members.

American Concrete Institute, 2015. Guide for the design and construction of structural concrete reinforced with fiber-reinforced polymer (FRP) bars, 1st printing. ed, ACI report. American Concrete Institute, Farmington Hills, MI.

Ascione, L., Mancusi, G., Spadea, S., 2010. Flexural Behaviour of Concrete Beams Reinforced With GFRP Bars: Flexural Behaviour of GFRP RC Members. Strain 46, 460–469. https://doi.org/10.1111/j.1475-1305.2009.00662.x

Ashour, A.F., 2006. Flexural and shear capacities of concrete beams reinforced with GFRP bars. Construction and Building Materials 20, 1005–1015. https://doi.org/10.1016/j.conbuildmat.2005.06.023

Bakis, C.E., Bank, L.C., Brown, V.L., Cosenza, E., Davalos, J.F., Lesko, J.J., Machida, A., Rizkalla, S.H., Triantafillou, T.C., 2002. Fiber-Reinforced Polymer Composites for Construction—State-of-the-Art Review. J. Compos. Constr. 6, 73–87. https://doi.org/10.1061/(ASCE)1090-0268(2002)6:2(73)

Bank, L.C., 2006. Composites for construction: structural design with FRP materials. John Wiley & Sons.

Barris, C., Torres, L., Baena, M., Pilakoutas, K., Guadagnini, M., 2012. Serviceability Limit State of FRP RC Beams. Advances in Structural Engineering 15, 653–663. https://doi.org/10.1260/1369-4332.15.4.653

Benmokrane, B., Chaallal, O., Masmoudi, R., 1995. Glass fibre reinforced plastic (GFRP) rebars for concrete structures. Construction and Building Materials 9, 353–364. https://doi.org/10.1016/0950-0618(95)00048-8

Bhatnagar, N., Asija, N., 2016. Durability of high-performance ballistic composites, in: Lightweight Ballistic Composites. Elsevier, pp. 231–283. https://doi.org/10.1016/B978-0-08-100406-7.00008-8

Bischoff, P.H., 2007. Deflection Calculation of FRP Reinforced Concrete Beams Based on Modifications to the Existing Branson Equation. J. Compos. Constr. 11, 4–14. https://doi.org/10.1061/(ASCE)1090-0268(2007)11:1(4)

Bischoff, P.H., Paixao, R., 2004. Tension stiffening and cracking of concrete reinforced with glass fiber reinforced polymer (GFRP) bars. Can. J. Civ. Eng. 31, 579–588. https://doi.org/10.1139/l04-025

Branson, D.E., 1963. Instantaneous and time-dependent deflections of simple and continuous reinforced concrete beams. Alabama. State Highway Department.

Brown, J., 2015. Glass fibre reinforced polymer bars in concrete compression members, in: Proceedings of the Second International Conference on Performance-Based and Life-Cycle Structural Engineering (PLSE 2015). Presented at the International Conference on Performance-based and Life-cycle Structural Engineering, School of Civil Engineering, The University of Queensland, Brisbane, QLD, Australia, pp. 1590–1599. https://doi.org/10.14264/uql.2016.767

Byars, E.A., Waldron, P., Dejke, V., Demis, S., Heddadin, S., 2003. Durability of FRP in concrete ? current specifications and a new approach. IJMPT 19, 40. https://doi.org/10.1504/IJMPT.2003.003553

Cheung, M.S., 2001. DESIGN AND CONSTRUCTION OF BUILDING COMPONENTS WITH FIBRE REINFORCED POLYMERS: A NEW CANADIAN STANDARD. Presented at the FRP Composites in Civil Engineering. Proceedings of the International Conference on FRP composites in Civil EngineeringHong Kong Institution of Engineers, Hong Kong Institution of Steel Construction.

Chidan, a S.H., 2017. Flexural Behaviour of Concrete Beams Reinforced With GFRP Rebars 10.

Darwin, D., Dolan, C.W., Nilson, A.H., 2016. Design of concrete structures, Fifteenth edition. ed. McGraw-Hill Education, New York, NY.

Dupuis, M.R., Best, T.D., Elwood, K.J., Anderson, D.L., 2014. Seismic performance of shear wall buildings with gravity-induced lateral demands. Canadian Journal of Civil Engineering 41, 323–332.

El-Nemr, A., Ahmed, E.A., El-Safty, A., Benmokrane, B., 2018. Evaluation of the flexural strength and serviceability of concrete beams reinforced with different types of GFRP bars. Engineering Structures 173, 606–619. https://doi.org/10.1016/j.engstruct.2018.06.089

Fico, R., 2008. Limit States Design of Concrete Structures Reinforced with FRP Bars 167.

GangaRao, H.,1993. Flexural Behavior and Design of RC Members Using FRP Reinforcement 2.

Ghobarah, A., Said, A., 2002. Shear strengthening of beam-column joints. Engineering structures 24, 881–888.

Goldston, M., Remennikov, A., Sheikh, M.N., 2016. Experimental investigation of the behaviour of concrete beams reinforced with GFRP bars under static and impact loading. Engineering Structures 113, 220–232.

Hollaway, L.C., 2010. A review of the present and future utilisation of FRP composites in the civil infrastructure with reference to their important in-service properties. Construction and Building Materials 24, 2419–2445. https://doi.org/10.1016/j.conbuildmat.2010.04.062

International Federation for Structural Concrete (Ed.), 2007. FRP reinforcement in RC structures, Bulletin / International Federation for Structural Concrete Technical report. International Federation for Structural Concrete, Lausanne.

Jumaat, M.Z., Alam, M.A., 2007. PLATE BONDED STRENGTHENED R.C. BEAMS WITH END AND INTERMEDIATE ANCHORS. International Journal of Engineering and Technology 4, 9.

Kheni, H.L., Satasiya, A.P., Balar, K.P., Khokhar, P.R., 2019. GFRP Bars as a Substitution in Structure 4.

Kocaoz, S., Samaranayake, V.A., Nanni, A., 2005. Tensile characterization of glass FRP bars. Composites Part B: Engineering 36, 127–134. https://doi.org/10.1016/j.compositesb.2004.05.004

Krall, M., Polak, M., 2019. Concrete beams with different arrangements of GFRP flexural and shear reinforcement. Engineering Structures 198, 109333.

Machida, A., Uomoto, T., 1999. Recommendation for design and construction of concrete structures using continuous fiber reinforcing material. https://doi.org/10.5169/SEALS-61419

Maranan, G., Manalo, A., Benmokrane, B., Karunasena, W., Mendis, P., 2015. Evaluation of the flexural strength and serviceability of geopolymer concrete beams reinforced with glass-fibre-reinforced polymer (GFRP) bars. Engineering Structures 101, 529–541.

Masmoudi, R., Zaidi, A., Gérard, P., 2005. Transverse Thermal Expansion of FRP Bars Embedded in Concrete. J. Compos. Constr. 9, 377–387. https://doi.org/10.1061/(ASCE)1090-0268(2005)9:5(377)

Micelli, F., Nanni, A., 2004. Durability of FRP rods for concrete structures. Construction and Building Materials 18, 491–503. https://doi.org/10.1016/j.conbuildmat.2004.04.012

Modi, M., 2017. Comparative Study of GFRP Rebar and Steel Rebar used in Concrete Sections 2, 6.

Mondal, O.A., 2019. Rehabilitation and Flexural Strengthening of Reinforced Concrete Beams using External Steel Reinforcement 127.

Muhammad, M.S., 2019. COMPARATIVE STUDY OF GLASS FIBER REINFORCED POLYMER (GFRP) AND STEEL BARS IN REINFORCED CONCRETE (RC) MEMBERS. Civil Engineering 109.

Nanni, A., 2005. Guide for the design and construction of concrete reinforced with FRP bars (ACI 440.1 R-03). Presented at the Structures Congress 2005: Metropolis and Beyond, pp. 1–6.

Nanni, A., 2000. FRP REINFORCEMENT FOR BRIDGE STRUCTURES 5.

Pilakoutas, K., Neocleous, K., Guadagnini, M., 2002. Design Philosophy Issues of Fiber Reinfored Polymer Reinforced Concrete Structures. J. Compos. Constr. 6, 154–161. https://doi.org/10.1061/(ASCE)1090-0268(2002)6:3(154)

Rafi, M.M., Nadjai, A., Ali, F., 2007. Experimental Testing of Concrete Beams Reinforced with Carbon FRP Bars. Journal of Composite Materials 41, 2657–2673. https://doi.org/10.1177/0021998307078727

Rahmatian, A., 2014. Static and Fatigue Behaviour of FRP-Reinforced Concrete Beams and a SHM 225.

Ruan, X., Lu, C., Xu, K., Xuan, G., Ni, M., 2020. Flexural behavior and serviceability of concrete beams hybrid-reinforced with GFRP bars and steel bars. Composite structures 235, 111772.

Saafi, M., 2002. Effect of fire on FRP reinforced concrete members. Composite Structures 58, 11–20. https://doi.org/10.1016/S0263-8223(02)00045-4

Said, M.N., 2022. NEAR EAST UNIVERSITY 119.

Saikia, B., 2005. Performance of hybrid rebars as longitudinal reinforcement in normal strength concrete. Mater. Struct. 38, 857–864. https://doi.org/10.1617/14229

Salh, L., 2014. Analysis and Behaviour of Structural Concrete Reinforced with Sustainable Materials 108.

Shanour, A.S., Mahmoud, A.A., Adam, M.A., Said, M., 2014. EXPERIMENTAL INVESTIGATION OF CONCRETE BEAMS REINFORCED WITH GFRP BARS 5, 11.

Shekar, V., Petro, S.H., GangaRao, H.V.S., 2003. Fiber-Reinforced Polymer Composite Bridges in West Virginia. Transportation Research Record 1819, 378–384. https://doi.org/10.3141/1819b-48

Shin, S., Seo, D., Han, B., 2009. Performance of Concrete Beams Reinforced with GFRP Bars. Journal of Asian Architecture and Building Engineering 8, 197–204. https://doi.org/10.3130/jaabe.8.197

Standard, C., 2002. Design and construction of building components with fibre-reinforced polymers. S806-02, Canadial Standards Association.

Structural use of concrete, 2nd ed. ed, 1997. . BSI, London.

Theriault, M., Benmokrane, B., 1998. Effects of FRP reinforcement ratio and concrete strength on flexural behavior of concrete beams. Journal of composites for construction 2, 7–16.

Wang, H., Zha, X., Ye, J., 2009. Fire Resistance Performance of FRP Rebar Reinforced Concrete Columns. International Journal of Concrete Structures and Materials 3, 111–117. https://doi.org/10.4334/IJCSM.2009.3.2.111

Worner, V., Palermo, A., 2015. USE OF GLASS FIBRE REINFORCED POLYMER (GFRP) REINFORCING BARS FOR CONCRETE BRIDGE DECKS 11.

Worner, V.J., 2015 Use of Glass Fibre Reinforced Polymer (GFRP) reinforcing bars for concrete bridge decks 156.

Yasir, A., Effendi, M.K., Taveriyanto, A., Apriyatno, H., 2019. Analysis of Strengths of Reinforced Concrete Beam Structures with CFRP Sheet Using Abaqus Software 6.14. Jurnal Teknik Sipil dan Perencanaan 21, 9–19.